Developing a Remote Sensing Framework for Myrtle Rust (*Austropuccina psidii*) Detection on Lemon Myrtle (*Backhousia citriodora*)

DISSERTATION

for the degree of Doctor of Natural Sciences (Dr. rer. nat)

Disputed: 2019/02/08

at the Faculty of Mathematics, Informatics and Natural Science

Department of Biology

of Universität Hamburg

&

at the Faculty of Science and Engineering

Department of Biological Sciences

of Macquarie University

submitted by

René Hans-Jürgen Heim

(B.Sc. Bioengineering, M.Sc. Biology)

Hamburg, 2018

This page is intentionally left blank.

1st Supervisor: Dr Jens Oldeland (Universität Hamburg)

2nd Supervisor: Prof Ian J Wright (Macquarie University)

Dissertation (Submitted: 06.12.2018)

1st Reviewer: Prof. Dr. Kathrin Dausmann (Universität Hamburg)

2nd Reviewer: Prof. Dr. Kai Jensen (Universität Hamburg)

3rd Reviewer: Prof. Dr. Pablo J. Zarco-Tejada (University of Melbourne)

4th Reviewer: Assoc. Prof. Dr. Adam Sparks (University of Southern Queensland)

Disputation (Passed: 2019/02/08)

1st Reviewer: PD Dr. Cornelia Heinze (Universität Hamburg)

2nd Reviewer: Prof. Dr. Kai Jensen (Universität Hamburg)

3rd Reviewer: Dr Jens Oldeland (Universität Hamburg)

4th Reviewer: Prof. Dr. Jens Gunter Rohwer (Universität Hamburg)

This page is intentionally left blank.

Acknowledgements

Foremost, I would like to express my great appreciation to my humble, energetic and knowledgeable doctoral supervisors Ian J. Wright and Jens Oldeland for their tremendous support throughout my joint-PhD candidature. I am most grateful for them granting me the independency to freely plan, organize and conduct my research while being available at any time when I felt lost or overwhelmed by unexpected situations. They both offered me insight into their experience and abilities and provided excellent guidance in my professional, but also personal, development. I couldn´t have wished for more.

Also, I want to thank Michelle Leishman, Angus J. Carnegie and Michael Chang for their support as secondary supervisors. They provided ideas and feedback without hesitation and greatly influenced the overall outcome of my thesis. Especially, Angus Carnegie relentlessly read manuscripts and was never too tired to respond to my questions about the realm of plant pathology. Thanks for the warm welcome and support in your research world, Angus.

I deeply appreciate the financial support given by Macquarie University in Australia and by the German Academic Scholarship Foundation, without which this thesis could not have been realised.

Moreover, I am indebted to Gary Mazzorana and Emily K. Lancaster. Gary granted me access to his lemon myrtle plantation and Emily to her experimental setup on which much of my work was based on. I also would like to express my gratitude to Geoff S. Pegg who put a lot work in inoculating plants and assessing them for some of my projects.

My appreciation extends to Pablo Zarco-Tejada, Anne-Katrin Mahlein, Andrew P. Allen, Arko Lucieer, Peter Scarth and Darren Turner who all considerably contributed to my thesis by kindly offering advice and guidance.

I owe special thanks to Daniel Falster who offered mentoring and guidance on my R programming and strongly influenced my understanding of open and transparent science.

My sincere thanks go to my incredible friends and colleagues at Macquarie University in Australia. I loved my everyday life especially because of them. Thank you so much James, Laura, Maria, Sas, Vashi, Sarah, Jennifer, Tarun, Kath, Gustavo and Martyna!

Last, but by no means least, I would like to pay special thankfulness to my family who are (always) willing to listen to my thoughts and doubts. Thanks, Dad, for your ongoing support and reminding me that everything starts and ends with family. Thank you, Birgit, Patrick and Peter, for accepting me as a part of your family.

Finally, I express my deep gratitude and love for you Ina. Frankly, when you met me in 2008, you started to make me a better person. I cannot imagine what my life would look like without you. Your kindness, great-heartedness, and your (curiously odd) wisdom is not just affecting my world in a positive way but the world of everyone close to us.

P.S.: Welcome Frida. I am so excited to see how you will explore the world and impact our lives.

This page is intentionally left blank.

Table of Contents

Summary (English Version) 1

Summary (German Version).. 3

CHAPTER I 8

General Introduction

RHJ Heim

CHAPTER II 42

Detecting myrtle rust (*Austropuccinia psidii*) on lemon myrtle trees using spectral signatures and machine learning

RHJ Heim • IJ Wright • HC Chang • AJ Carnegie • GS Pegg • EK Lancaster • DS Falster • J Oldeland

Published in*: Plant Pathology* doi: 10.1111/ppa.12830

CHAPTER III 66

Developing a spectral disease index for myrtle rust (*Austropuccinia psidii*)

RHJ Heim • IJ Wright • AP Allen • I Geedicke • J Oldeland

Accepted in: *Plant Pathology* doi: pending

CHAPTER IV.. 90

Multispectral, aerial disease detection for myrtle rust (*Austropuccinia psidii*) on a lemon myrtle plantation

RHJ Heim • IJ Wright • P Scarth • AJ Carnegie • D Taylor • J Oldeland

In review

CHAPTER V 122

General Discussion

RHJ Heim

DECLARATION... 138

Summary (English Version)

As global population is expected to double by 2050, the need for securing adequate food production is becoming an urgent problem to be solved. At the same time agriculture's environmental footprint needs to be decreased drastically. As pathogens and pests are responsible for the loss of one third of global crop production, optimizing their management is of utmost importance. By combining information systems, sensors and enhanced machinery, the field of 'precision agriculture' promises to be a smart solution to fulfil the demands of modern agriculture. The site- and crop-specific adaption of precision agriculture can account for the variability and uncertainty in a managed landscape and thus allows for an improved use of resources, such as water, fertilizer or even pesticides and fungicides which in turn can help maintain environmental integrity. Remote sensing technologies, such as spectral sensors and spectral vegetation indices, are now routinely incorporated into precision agriculture strategies to monitor crop needs such as fertilizer, water and pathogen deterring agrochemicals across large areas.

In this thesis, the pathogen myrtle rust (*Austropuccinia psidii*) on lemon myrtle (*Backhousia citriodora*) is studied to explore whether it is possible to establish a remote sensing approach for the detection – and management – of myrtle rust in managed landscapes. Hyperspectral and multispectral sensors were utilized at leaf- and canopy-scale to collect spectral signatures of fungicide treated and untreated lemon myrtle trees. These reflectance signatures were used to build random forest classification models which were evaluated for their accuracy to discriminate treated and untreated trees at both scales. Further, relevant wavebands for both classification problems were selected to reduce redundancy and data load. We developed an innovative method to design a new form of spectral vegetation indices, a disease-specific spectral vegetation index (SDI). We tested the classification accuracy of our new SDI and compared it to common spectral vegetation indices.

Overall, results indicate that sensor-guided disease detection is possible at leaf- and canopy-scale. High classification accuracies were found based on data collected on a single lemon myrtle plantation and from a botanical garden. If more spectral data can be collected from the investigated pathosystem it would be possible to validate the findings of this thesis, and the integration of our developed methods into standardized management workflow seems feasible. However, there is still much research required to use remote sensing techniques commercially for plant disease detection. Until we are able to compare and harmonize spectral disease data from different geographical locations, pathosystems and abiotic stress sources, it will be difficult to generalize gained insights from this interdisciplinary field. More research is necessary to understand plant physiological responses to different sources of stress and then link these responses to specific spectral regions and signatures. Future research should be guided by questions addressing (i) the detection of pre-symptomatic phases of diseases of pathogenesis, (ii) the differentiation among different pathogens on identical and different hosts, (iii) the separation of biotic and abiotic stresses, and (iv) the quantification of disease severity.

Summary (German version)

Es wird erwartet, dass sich die Weltbevölkerung bis 2050 verdoppelt. Daher ist eine nachhaltige Versorgung mit Nahrung ein ernstzunehmendes Problem, das umgehend gelöst werden muss. Dies muss jedoch im Einklang mit der Reduzierung des immensen, ökologischen Fußabdruckes der Landwirtschaft geschehen. Da Krankheitserreger und Schädlinge von Pflanzen für den Verlust von einem Drittel der weltweiten landwirtschaftlichen Produktion verantwortlich sind, ist die Optimierung ihrer derzeitigen Behandlungsmethoden von größter Bedeutung. Durch die Kombination von Sensoren, Informationssystemen und modernen, Nutzmaschinen bietet das Forschungsfeld der Präzisionslandwirtschaft Lösungen für die Ansprüche des modernen Agrarwesens. Das Prinzip der Präzisionslandwirtschaft ist die gezielte und systemspezifische Anwendung von Maßnahmen, die zu einer optimierten Verwaltung aller Produktionsbereiche führen. Dies beinhaltet unter anderem die gezielte Applikation von Wasser, Nährstoffen und Chemikalien. Im Gegensatz zu der systemischen Verwendung von Resourcen, kann durch gezielte Maßnahmen nicht nur die Produktionseffizienz gesteigert werden, sondern auch eine, an der natürlichen Umwelt angepasste Landwirtschaft gewährleistet werden. Die Umsetzung von Strategien in der Präzisionslandwirtschaft wird heutzutage durch Methodiken aus der Fernerkundung unterstützt. Optische Sensoren und spektrale Vegetationsindizes können zur Überwachung von relevanten Produktionsparametern routinemäßig in den landwirtschaftlichen Arbeitsablauf integriert werden.

Die vorgelegte Dissertation erbringt einen Nachweis zur sensorgesteuerten Erkennung des pathogenen Rostpilzes *Austropuccinia psidii* auf einer industriell relevanten Wirtspflanze, der Zitronenmyrte (*Backhousia citriodora*). Hyperspektrale und multispektrale Sensoren kamen auf Blatt- und Baumkronenebene zum Einsatz um spektrale Signaturen von fungizid-behandelten und unbehandelten Zitronenmyrtebäumen aufzuzeichnen. Diese Signaturen wurden daraufhin verwendet, um mehrere Random Forest Klassifikationsmodelle zu trainieren, welche wiederum nach ihrer Genauigkeit evaluiert wurden, um die

behandelten und unbehandelten Zitronenmyrtebäume zu unterscheiden. Auf Blatt- und Baumkronenebene wurden klassifkationsrelevante Prädiktoren (Bänder) selektiert, um Informationsredundanz und Datenmenge zu reduzieren. Darauf basierend, wurde ein innovativer spektraler Index entwickelt, der spezifisch für das untersuchte Pathosystem ist (LMMR Index = Lemon Myrtle/ Myrtle Rust). Letztendlich wurde die Klassifikationsgenauigkeit des LMMR Index getested und mit herkömmlichen spektralen Indizes verglichen.

Die gefundenen Ergebnisse deuten darauf hin, dass optische Sensoren für die Detektion des Rostpilzes *A. psidii* sowohl auf Blatt- als auch auf Baumkronenebene geeignet sind. Hohe Klassifikationsgenauigkeiten konnten anhand von spektralen Signaturen, die auf einer Zitronenmyrtenplantage und in einem botanischen Garten aufgezeicnet wurden, ermittelt werden. Weitere spektrale Daten des untersuchten Pathosystems müssen in Zukunft aufgezeichnet werden, um die Ergebnisse dieser Dissertation zu validieren. Es lässt sich schlussfolgern, dass eine Integration und Erweiterung der hier entwickelten Methoden in standartisierte Arbeitsabläufe möglich und lohnenswert sind. Um eine routinemäßige und kommerziell nutzbare Anwendung basierend auf unseren Ergebissen zu etablieren, ist jedoch weitere Forschung notwenig. Das Harmonisieren und Vergleichen von kontinentübergreifenden spektralen Daten unterschiedlichster Pathosysteme und auch von abiotischen Stressquellen ist notwendig, um generalisierbare Ergebnisse in diesem interdisziplinären Feld zu erzielen. Weitere Forschung sollte versuchen eine sinnvolle Beziehung zwischen spektralen Signaturen und physiologischen Veränderungen von Pflanzen unter biotischem und abiotischem Stress herzustellen. Hier könnten sich zukünftige Forschungsprojekte durch folgende Fragen bezüglich der Erkennung von Pflanzenkrankheiten leiten lassen: Ist die spektrale Übersetzung von Symptomen an unterschiedlichen Zeitpunkten des Krankheitsverlaufes umsetzbar? Können unterschiedliche Krankheiten spektral voneinander unterschieden werden? Können abiotische und biotische Signale ebenfalls voneinander unterschieden werden und kann die Anfälligkeit von Pflanzen gegenüber Krankheiten quantifiziert werden? Auch die Erkennung von Pflanzenkrankheiten bevor Symptome mit dem bloßen Auge erkennbar werden ist von großer Bedeutung.

This page is intentionally left blank.

This page is intentionally left blank.

CHAPTER I

General introduction into developing a remote sensing framework for myrtle rust (*Austropuccina psidii*) detection on lemon myrtle (*Backhousia citriodora*)

RHJ Heim

General Introduction

The importance of plants

Based on biomass, plants are the most dominant organism of the earth's living environment and provide all the food, directly or indirectly, on which humans and all other animals depend (Agrios *et al.*, 2005). Current estimates report 452 vascular plant families, while 80% of the food derived from plants comes from only 17 plant families (Willis, 2017). Over 30,000 species have been documented as being "useful", meaning that they fulfil a specific need for the wider environment, humans and other animals. The largest number of plants with a documented use are those that have been utilised as medicines or building/textile materials (Willis, 2017). Probably one of the most important "use" of plants is that they enable our survival by providing oxygen, shaping our environment and providing indirect benefits by restricting erosion and allow for fertile soil in agronomy. That is, plants provide essential "ecosystem services" to humanity (Reid *et al.*, 2005).

The provision of food is an essential service. Securing future food supplies requires basic quality standards and the production of sufficient quantities. At the same time, agricultural production must be intensive, sustainable and yet environmentally safe (Gebbers & Adamchuk, 2010). However, over the last 10,000 years, we developed agricultural practices that now seem unsustainable to support human population beyond 2050 (Palmgren *et al.*, 2015). One reason for this projection is that genetic diversity of many species has decreased as the selection of traits that provide higher yields and quality are desired (Warschefsky *et al.*, 2014). As a consequence, such species now suffer severely depleted gene pools (Van De Wouw *et al.*, 2010). Often, traits that result in higher yields cannot be harmonized with those that enable resilience to changing climates or to pests and diseases, leaving them vulnerable to these threats (Palmgren *et al.*, 2015).

Plants that show reduced resilience to pests, diseases and environmental factors are more easily stressed and cannot perform to their full genetic potential. By conservative estimates, stress is causing the reduction or destruction of one third of the global production of all crops (Agrios *et al.*, 2005). Increased globalization and connectedness via world trade allow pests and pathogens to invade new habitats and their impact on native and managed landscapes can be drastic. An analysis of 1,300 currently known invasive pests and pathogens projected potential cost to global agriculture at over US$540 billion annually (Willis, 2017). In the United States alone, agricultural and forestry losses from invasive pests have been estimated at US$40 billion annually (Paini *et al.*, 2016). Losses caused by environmental and abiotic factors such as droughts and nutrient deficiencies are not included in those estimates. To secure food availability and increase its production efficiency, plant pathologists strive to understand causes of disease (i.e. aetiology), disease mechanisms (i.e. pathogenesis) and disease cycles (i.e. epidemiology). This allows them to manage diseases and focus on mitigating the environmental impact caused by control measures such as agrochemicals. However, it is now acknowledged that unilateral research enterprises might be too inefficient to solve problems of this extent (Rhoten & Parker, 2004). A discipline that might be able to support the efforts of plant pathologists is precision agriculture.

Precision Agriculture

The concept of ‘precision agriculture’ emerged approximately 30 years ago and has been commercially applied since the 1990´s (Mulla, 2013). Precision agriculture shows great potential to optimize agricultural production by reducing the expansion of arable land and closing ‘yield gaps’ through increased production efficiency (Foley *et al.*, 2011). Agricultural expansion into natural ecosystems is detrimental to biodiversity, carbon storage and environmental services (Foley, 2005; Vogel, 2017). Yield gaps are created – and should be avoided – by management methods that result in differences between average and potential yields (Foley *et al.*, 2011). Traditional agriculture assumes that crops demand homogenous management strategies which is one of the driving factors of the above-mentioned shortcomings. This leads to the application of fertilizer, pesticides and other agrochemicals in a holistic and inefficient manner (Mahlein, 2016). By contrast, management strategies in precision agriculture aim at managing a crop in a targeted and timely fashion by dividing arable land into management zones that each receives customised management inputs based on their specific needs (Gebbers & Adamchuk, 2010; Mulla, 2013). Tools for such site-specific management are available for most tasks, including tillage, sewing, mechanical weeding, and the distribution of agrochemicals. Adoption rates of precision agricultural management are most notable in the European Union, North America and Australia (Mulla, 2013).

To obtain reliable and objective diagnosis of stressed and underperforming crops, adopters of precision agriculture have to rely on state-of-the-art sensor systems and data analysis techniques (Mahlein, 2016). Typically applied sensors measure either spectral reflectance, temperature or fluorescence (West *et al.*, 2003; Sankaran *et al.*, 2010). To choose the optimal sensor and platform for the task at hand, the required temporal and spatial resolution must be considered. The smallest ground area that can be resolved by a sensor, the spatial resolution, strongly depends on the distance between the sensor and the object (Figure 1). It also has a strong influence at what level stress can be detected (West *et al.*, 2003; Mahlein, 2016). For stress causing agents at leaf-level, proximal sensors with high spatial (< 5 cm) resolution could be mounted on ground-based autonomous robots, tractors or even unmanned aerial platforms. Such platforms also offer the advantage of high temporal resolutions, the time it takes to revise a certain area, as the sensor can be deployed in short intervals (<0.5 days). High temporal resolution might be required when disease progression or the phases of other stresses are monitored. To monitor vegetation at larger scales (e.g. forests), it would be possible to use airplane- and satellite-mounted sensors with lower spatial (>1 m) and temporal (> 1 week) resolution (Mahlein, 2016). As it is projected that future farms are likely to be managed with tools allowing for high spatial and temporal resolution there is considerable interest in collecting remote sensing data across temporal, spatial and spectral scales to conduct near real time soil, crop and pest management (Mulla, 2013).

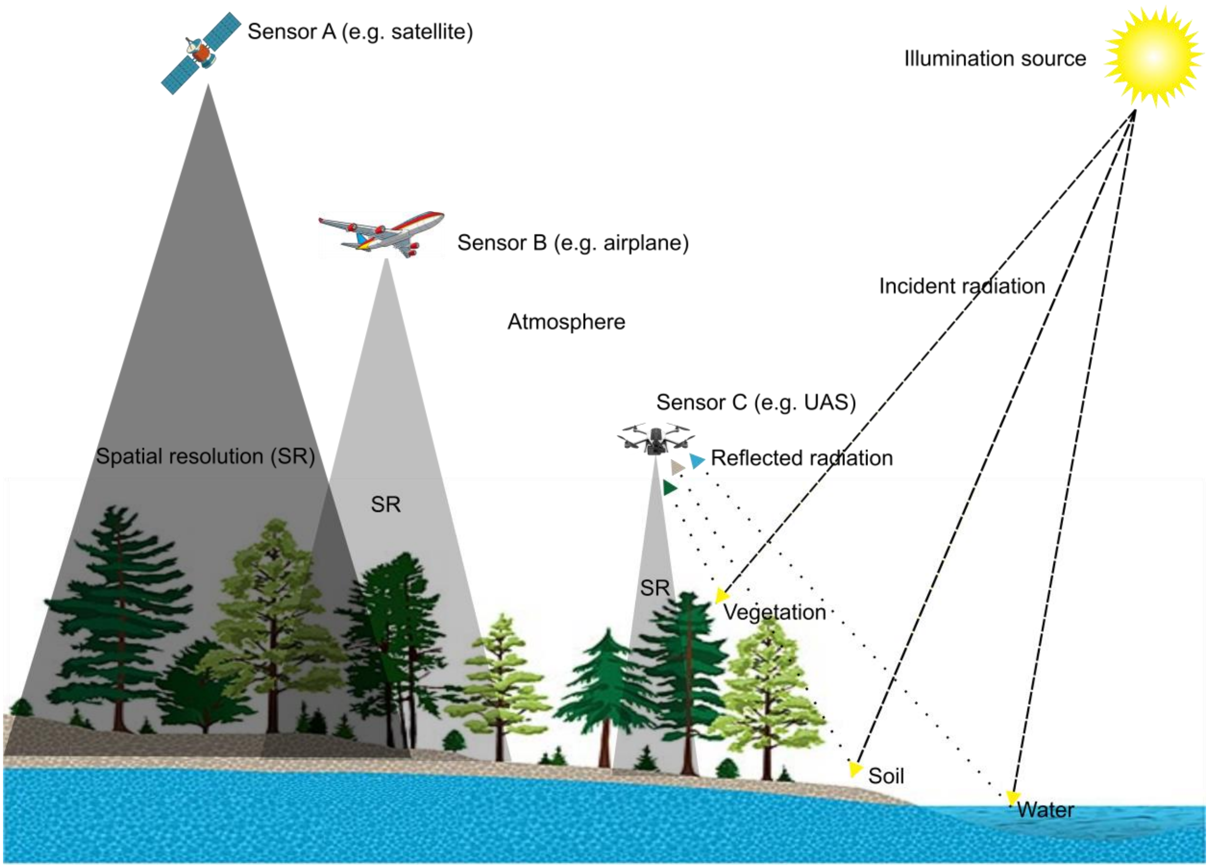

Figure 1 | Remote sensing platforms and sensors can be deployed at various scales depending on the required temporal and spatial resolution. Satellite-mounted sensors (Sensor A) can have a temporal resolution of more than 14 days and a spatial resolution of more than 50 m. Unmanned aircraft systems (Sensor C) can be deployed more frequently (temporal resolution < 30 min) and, depending on the flight altitude resolve incident, reflected radiation below 5 cm. Figure adapted from Groundwater-Illustration (2012)

Remote Sensing for Stress Detection in Precision Agriculture

Multispectral or hyperspectral sensors are commonly integrated as a remote sensing tool into precision agriculture (Moshou *et al.*, 2004; Devadas *et al.*, 2009; Mahlein *et al.*, 2010; Calderón *et al.*, 2015; Candiago *et al.*, 2015). These types of sensors mainly differ in their number and width of measured wavebands (i.e. spectral resolution) and whether they produce an image (imaging sensor) or record single reflectance signatures (non-imaging sensor). The first routinely applied multispectral sensor was mounted on the Landsat 1 satellite in 1972 (Campbell & Wynne, 2011). The Landsat Multispectral Scanner (MSS) spectrally resolved four broad bands between 500 and 1100 nm, each wider than 100 nm. Then, during the 1980s, scientists at the Jet Propulsion Laboratory (Pasadena, California) developed the first hyperspectral sensors (Campbell & Wynne, 2011). Instead of four wavebands, these sensors were able to resolve more than 200 spectral bands within similar spectral ranges as earlier multispectral sensors. By contrast, our standard mobile phone cameras can detect radiation in three relatively broad bands, the red, green and blue band. Today, hyperspectral sensors provide spectral data with tremendous complexity: typically, within a spectral range between 400 and 2,500 nm, and a spectral resolution below 1 nm (Mahlein, 2016). The spectral range between 400 and 2500 nm has become standard because incident solar radiation in this region is not blocked by the atmosphere. Whereas most other radiation emitted from the sun is blocked by the atmosphere (e.g. X-rays and ultraviolet radiation). The range of 400 and 2500 nm is traditionally subdivided into the visible region (VIS, 400 to 700 nm), the red-edge (RE, ~700±30 nm), the near-infrared (NIR, 700 to 1400 nm) and the shortwave-infrared region (SWIR, 1400 to 2500 nm).

Both multi- and hyperspectral sensors rely on either an active (light bulb) or passive (sun) source of electromagnetic energy and on the physical principle that this energy is either reflected, absorbed or transmitted by the complex assemblage of biological, geological and hydrological features of the earth's surface (Figure 1). For vegetation studies, either single leaves or entire canopies are diagnosed. The interpretation of leaf reflectance signatures is relatively simple because incident energy is emitted from an active illumination source and therefore not scattered through the atmosphere. However, the interpretation of plant canopy signatures is often difficult because the reflected electromagnetic radiation contains complex information of leaves and stems mixed with soil and plant litter (Knipling, 1970). Patterns across entire plant reflectance signatures are usually analysed to form conclusions about plant properties. For instance, healthy vegetation (Figure 2A – green signature) at leaf-level usually reflects 10% of the total reflectance in the VIS region. Around 550 nm, where roughly 20% of the light is reflected, the “green peak” can be found. It is this spectral feature that causes human vision to perceive plants as being green. In the NIR, total reflectance increases to approximately 50% but gradually decreases to a low value at about 2500 nm (SWIR). The typical VIS reflectance pattern is evoked by much absorbed radiation through leaf pigments, primarily the chlorophylls. Also, the carotenoids, xanthophylls, and anthocyanins have an effect (Gates *et al.*, 1965). The high NIR reflectivity is caused by internal leaf cellular structures (Knipling, 1970). The radiation is diffused and scattered through the cuticle and epidermis to the mesophyll cells and air cavities in the interior of the leaf (Figure 2B). Here the radiation undergoes multiple reflections and refractions caused by refractive index differences between air (1.0) and hydrated cellulose walls (1.4). Finally, spectral reflectance variation in the SWIR is mainly caused by water and parts of the vegetation that is photosynthetically not active, such as litter, senesced leaves, bark and other lignin-cellulose dominated parts (Jacquemoud & Ustin, 2001; Thenkabail *et al.*, 2011). The reflectance properties of single leaves are fundamental for understanding plant-light interactions. However, these leaf-scale principles cannot be applied to canopies without modifications (Knipling, 1970). Hence, the physics of radiation, the underlying physiology of stressed vegetation and the timing of assessments must be considered to extract useful information.

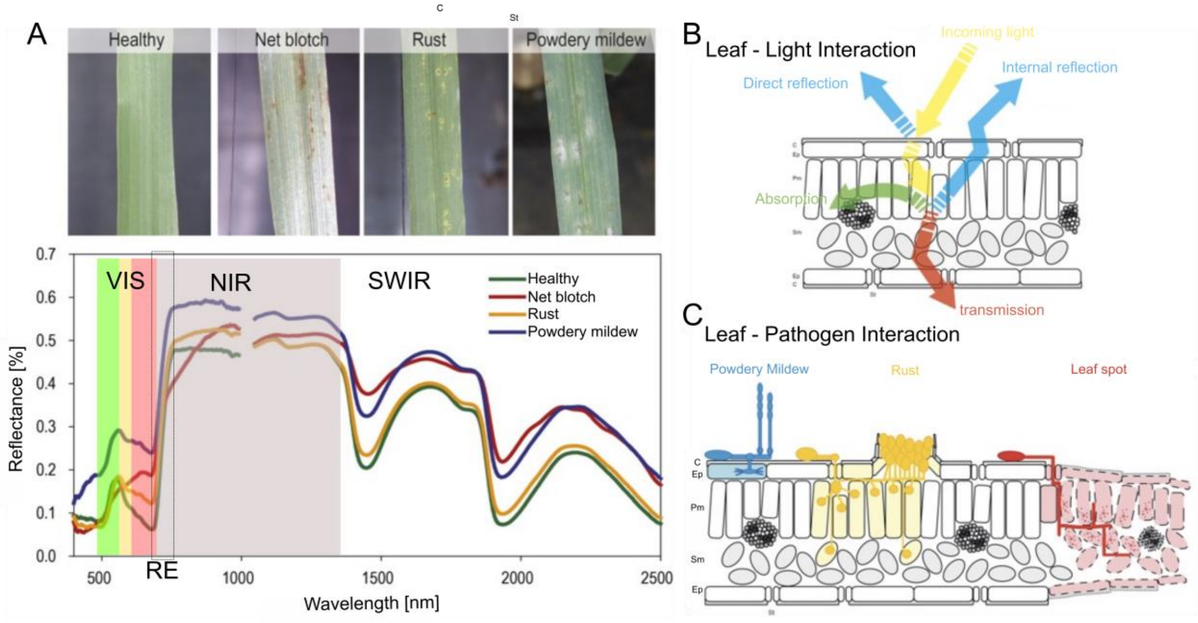

Figure 2 | A) Simplified principle of radiation energy (light) interacting with plant leaves. B) Simplified principle of the interaction between fungal pathogens and plant leaves. C) General spectral response of diseased and healthy leaves across the typical proportions of the electromagnetic spectrum. Figure adapted from Figure 3 and 5 in Mahlein, 2016.

This leaf-light interaction principle can be extended to study the interaction of plant pathogens and their hosts. During pathogenesis variation in light reflectance is caused by changes in surface structure, chemical composition and physiology (Figure 2C). Each pathogen can provoke a specific pattern and sequence of symptoms that can be detected by optical sensors. For instance, biotrophic fungi such as powdery mildews or rusts are less aggressive and therefore do not destroy leaf structures and plant pigment processes at early stages of infection. For stripe rust, it has been found that vegetative growth of the pathogen may extend around an infection site (Sharp *et al.*, 1985; Jackson, 1986). Symptoms of stem rust are initially restricted to the immediate area of individual rust pustules; later the fungus forms secondary and tertiary colonized areas and further pustule development can be observed. These variation in fungal structures on the leaf surface may be detected in the VIS region of the electromagnetic spectrum (Figure 2B and 2C). By contrast, perthotrophic pathogens are more aggressive and often degrade tissue due to toxins or enzymes that swiftly result in membrane damage and cell death after the fungus has penetrated the leaf

(Knogge, 1996; Mahlein *et al.*, 2010). While there has been no attempt to spectrally quantify pathogen-related enzymes and toxins, specific chemical substances, such as phenolic compounds (Kokaly & Skidmore, 2015), can be quantified in the SWIR region. Variation in structure and chemical composition of pathosystems are often reflected in very specific regions of the electromagnetic spectrum. Therefore, hyperspectral sensors are preferred to detect plant diseases. Their high spectral resolution allows them to mirror these complex and spectrally confined processes and to pinpoint singular relevant wavebands related to specific pathosystem. Detailed pathosystem exploration turns out to be difficult with multispectral sensors as they do not offer enough spectral resolution and range (Mahlein *et al.,* 2018).

Spectral Vegetation Indices

Spectral vegetation indices (SVIs) only require a few relevant wavebands to highlight changes in physiological, structural and chemical plants instead of evaluating entire spectral signatures. They have been developed for over 40 years and are especially useful to reduce computational processing time and redundant information of the high-dimensional output of hyperspectral sensors (Carter, 1993; Huete *et al.*, 2002). Relevant wavebands can be selected by using a “feature selection” techniques which are usually integrated in machine learning algorithms (Kuhn & Johnson, 2013). The most well-known SVI is probably the normalized difference vegetation index (NDVI, Rouse *et al.*, 1973). The NDVI is calculated based on the VIS and NIR proportion reflected by vegetation. Healthy vegetation absorbs most of the energy in the VIS for photosynthesis and reflects a large portion of the incident NIR energy. Stressed or sparse vegetation reflects more VIS and less NIR energy. Other indices, such as the anthocyanin reflectance index (ARI) pick up the concentrations of anthocyanins and suppress the impact of variable chlorophyll (Gitelson *et al.*, 2007). Most of these SVIs have been developed to explore physiological changes in plants without considering the influence of pathogens. Therefore, it could be useful to design a new suite of indices that take the influence of specific pathogens into account.

Spectral disease indices (SDIs) appeared just recently in the literature. Mahlein et al. (2013) were the first to develop SDIs and selected relevant spectral bands for three fungal pathogens of sugar-beet. Mahlein *et al*. (2013) were able to successfully discriminate *Cercospora beticola*, *Erysiphe betae*, and *Uromyces betae* causing Cercospora leaf spot, powdery mildew and rust, respectively. Initially, Mahlein et al. (2010) tested whether it would be possible to differentiate those three pathogens using multiple SVIs (e.g. NDVI and ARI) and a hyperspectral sensor at leaf-level. As they also assessed spectral changes during pathogenesis, they could monitor disease severity. Because reflectance spectra were recorded under constant light and temperature conditions, pre-processing to smooth the spectrum and reduce signal noise was not necessary. To select relevant features, they subtracted the mean reflectance of diseased sugar beet plants from the mean reflectance of healthy sugar beet plants at each wavelength and used standard analysis of variance (ANOVA) to compare them. They concluded that SVIs are useful for the differentiation between healthy and diseased plants, and some are also useful for disease quantification. However, they also found that single SVIs lack the potential to differentiate among diseases. They suggested the use of SVI combinations to improve disease detection and differentiation of biotic and abiotic plant stress and started to work on the development of SDIs (Mahlein et al., 2013). Various other studies, mentioned in the following, successfully discriminated healthy and diseased plants at leaf-level using field spectrometry.

Studies on Disease Detection using Remote Sensing

Most of these studies used pure spectral signatures for classification and additionally tested multiple SVIs to discriminate healthy and diseased vegetation. Ashourloo et al. (2014) tested whether a set of SVIs (e.g. NBNDVI, NDVI, PRI) would be effective to reflect the disease severity of wheat leaf rust (*Puccinia triticina*) infected hosts. They encountered difficulties when attempting to detect early symptoms as only minor reflectance changes were observed, and with increasing disease severity the symptoms became too scattered for specific classification of the pathogen. They concluded that SVIs are valuable due to the reduction of data dimensionality and data processing time, but it would be necessary to carefully choose suitable SVIs for disease detection depending on the pathosystem and symptoms. Another study used different apple cultivars to assess if leaves infected with apple scab (*Venturia inaequalis*) could be differentiated from non-infected leaves (Delalieux *et al.*, 2007). They also investigated at which developmental stage *V. inaequalis* infection could be detected, and they selected wavelengths that best differentiated between treatments. They collected hyperspectral data using a field spectrometer and compared classification results based on logistic regression, partial least squares logistic discriminant analysis, and tree-based models. Tree-based modelling suggested good predictability (c-index = 80%). It was concluded that the SWIR spectral domains between 1350–1750 nm and 2200–2500 nm were the most important regions for separating stressed from healthy leaves immediately after infection. The VIS wavelengths, especially around 650–700 nm, increased in importance three weeks after infection at a well-developed infection stage. Ultimately, they acknowledged the high potential of hyperspectral data in particular to detect diseases at early points in time but also when pathogenesis was already in an advanced stage.

Apart from studies that measured spectral reflectance directly at the leaf surface, there are studies that placed their spectral sensors further away but still close to the canopy.

Figure 3 | Research buggy used by Bravo et al (2003) to detect yellow rust on wheat.

Bravo et al. (2003) assessed the difference in spectral reflectance between healthy and diseased wheat plants infected with *Puccinia striiformis* (yellow rust). They used a custom-made buggy (Figure 3) to carry a visual monochromatic camera with a mounted spectrograph (460 nm – 900 nm). Their data could classify healthy and diseased wheat plants with an accuracy of 96%. However, measurements that are not recorded directly at the leaf surface show high variations in upward radiation as the light has to travel a certain distance to reach the sensor. To correct for these variations, Bravo et al. (2003) applied a sensor irradiance normalization. To select important wavebands, they used an Analysis of covariance (ANCOVA) F-test and to discriminate healthy and diseased plants they used a quadratic discriminant analysis model (QDA). Just recently, Herrmann et al. (2018) used a hyperspectral sensor mounted on a tractor and collected reflectance signatures from *Fusarium virguliforme* on soy plants (*Glycine max*) at leaf and canopy level to compare relevant wavebands at both levels. Partial least squares discriminant analysis revealed that canopy and leaf spectral data can be classified with accuracies of 82% and 92%, respectively. Interestingly, they found differences in relevant wavelengths between leaf and canopy measurements which confirms that upscaling experiments cannot be done without modification.

Increasing the distance to the canopy, Albetis et al. (2017) collected reference data on the ground and multispectral imagery in the VIS and NIR domain from the air using an unmanned aerial vehicle (UAV). Data were captured from red and white grape cultivars infected with Flavescence Dorée, a phytoplasma (wall-less bacterial pathogens)-borne grapevine disease. A set of eleven vegetation indices (e.g. NDVI and ARI) and four biophysical parameters (e.g. anthocyanin and carotenoid content) were calculated from five spectral bands (i.e. blue=B, green=G, red=R, red-edge=RE and near-infrared=NIR). Based on these parameters, both cultivars were classified, using generalized linear models, and important classification variables were selected. For red grape cultivars classification results were more successful (90-100%) than for white cultivars (68-80%). Important predictors were the RE and NIR region and four vegetation indices (GRVI, NDVI, RGI and ACI). Another study (Calderón *et al.*, 2014) acquired spectral leaf measurements (350–1 000 nm) and airborne thermal and multispectral imagery using an UAV. Their aim was to detect downy mildew (caused by *Peronospora arborescens*) on opium poppy (*Papaver somniferum*). The VIS and RE spectral region were useful to detect infections due to the necrotic and chlorotic lesions caused by chlorophyll degradation. Also, the NIR region due to changes in canopy density and leaf area, and the thermal-infrared region because of the changes in the transpiration rate that affect canopy temperature, were found to be relevant.

Sensors mounted on airplanes can capture spectral data from canopies while covering a greater spatial extent than UAVs. López-López *et al.* (2016) investigated the fungal disease red leaf blotch (*Polystigma amygdalinum*), a major foliar disease affecting almond (*Prunus amigdalus*) orchards. Their study entailed leaf-level measurements of chlorophyll fluorescence, stomatal conductance and hyperspectral reflectance measurements in the VIS and NIR regions to calculate multiple pigment indices (chlorophyll, carotenes, and xanthophyll), ratios of bands within the VIS region, and disease-related indices. By obtaining and comparing high-resolution thermal and hyperspectral airborne imagery in addition to their leaf-level measurements they added another level of information to evaluate disease incidence and severity. The use of airplanes as sensor platforms, and therefore increasing the distance to an object of interest, increases the complexity of data pre-processing. López-López et al. (2016) had to atmospherically correct and ortho-rectify their hyperspectral images to allow for the conversion of radiance values to reflectance. Their classification methods, linear discriminant analysis and support vector machine, using linear and radial basis kernels, revealed that chlorophyll and carotenoid indices and chlorophyll fluorescence were effective in detecting red leaf blotch at the early stages of disease development. Leaf-level measurements of stomatal conductance, chlorophyll content, chlorophyll fluorescence, photochemical reflectance index, and spectral reflectance showed no significant differences between healthy leaves and the green areas of symptomatic leaves. Remote sensing proved to be a useful tool for decision support in their study but also demonstrated the difficulty of the quantification of red leaf blotch in almond orchards due to the unreliably detectable temperature increase caused by *P. amygdalinum* infection. The necessity of high-resolution imagery for monitoring the disease was emphasized.

Probably the most advanced and complex study in this field was published by Zarco-Tejada et al. (2018). They showed that changes in plant functional traits retrieved from airborne imaging spectroscopy and thermography could be used to detect *Xylella fastidiosa* infection in olive trees (*Olea spp.*) before symptoms were visible. The bacterium *X. fastidiosa* is a plant pathogen of global importance as it is associated with a devastating olive tree disease epidemic in Italy (Sicard *et al.*, 2018). Zarco-Tejada et al. (2018) carried out intensive in situ inspections of thousands of olive trees across several years and obtained accuracies of disease detection exceeding 80%. These results were confirmed by quantitative polymerase chain reaction, high-resolution fluorescence imaging and thermal stress indicators that were coupled with photosynthetic traits sensitive to rapid pigment dynamics and degradation. They also found that the visually asymptomatic trees originally scored as affected by spectral plant-trait alterations developed *X. fastidiosa* symptoms at almost twice the rate of the asymptomatic trees classified as not affected by remote sensing. They demonstrated that spectral plant-trait alterations caused by *X. fastidiosa* infection are pre-visually detectable at the landscape scale, a critical requirement to help eradicate some of the most devastating plant diseases worldwide.

Finally, using the satellite mounted NASA's EO-1 Hyperion sensor, Apan et al. (2004) attempted to discriminate sugarcane areas affected by ‘orange rust’ (*Puccinia kuehnii*) disease. They calculated SVIs, related to leaf pigments, leaf internal structure, and leaf water content and confirmed that Hyperion imagery can be used to detect orange rust disease in sugarcane crops. They formulated a suite of ‘Disease–Water Stress Indices’ using only visible near-infrared (VNIR) bands (e.g. SIPI and R800/R680) and a moisture-sensitive band (1660 nm) which produced good correlations with orange rust infected plants. However, satellite-based disease detection might prove difficult to integrate into precision agriculture strategies as even Hyperion images are spatially resolved to 30 m. A targeted application of agrochemicals needs an even finer resolution.

Introduction to Myrtle Rust (*Austropuccinia psidii*)

Most of the above-mentioned studies investigated diseases where fungi were the causal agent. The division of Ascomycetes and Basidiomycetes are part of the subkingdom Dikarya and contain the highest number of known species in the kingdom of fungi (Raven *et al.*, 2006). Among the Basidiomycetes, the order Pucciniales (previously known as Uredinales and also known as Rusts) causes some of the most destructive plant diseases. They mostly threaten the production of grain crops such as wheat or barley. Infamous examples are the stem rust of wheat (*Puccinia graminis*), yellow or stripe rust of wheat, barley, and rye (*P. striiformis*), leaf or brown rust of wheat and rye (*P. triticina*) and leaf rust of barley (*P. hordei*). Just recently, *Puccinia graminis* destroyed tens of thousands of hectares of wheat crops in southern Europe (Bhattacharya, 2017). But rusts are not restricted to grain crops, they are also jeopardizing vegetables such as bean and asparagus, field crops such as cotton and soybeans, and ornamentals such as carnation, chrysanthemum, and snapdragon (Agrios *et al.*, 2005).

Symptoms of rust fungi often appear on leaves and stems as numerous rusty, orange, yellow, or even white-coloured spots (Agrios et al., 2005). Wang et al. (2018) explained that the yellow-orange colour of some rust species is due to four carotenoid pigments: phytoene, lycopene, g-carotene and b-carotene. The impact of rusts can escalate when host and pathogen did not co-evolve and pathogens become invasive (Helfer, 2014). For instance, host species of the coffee rust *Hemileia vastatrix* developed natural resistance in its natural range in Ethiopia. However, in the Americas, where coffee is highly cultivated and therefore lacks genetic diversity, the rust spread explosively and caused massive damage to yield and economic return (McCook & Vandermeer, 2015). Fortunately, most rust fungi are restricted to few host species. However, the fungus *Austropuccinia psidii*, the study species in this thesis, is different.

The causal agent of myrtle rust, formerly known as *Puccinia psidii*, has recently been assigned to a new genus as *Austropuccinia psidii* (G. Winter) Beenken, and placed in the family Sphaerophragmiaceae (Beenken, 2017). Currently, at least 513 host species from 78 genera, exclusively within the Myrtaceae plant family, are known (Giblin & Carnegie, 2014; Soewarto *et al.*, 2017; Berthon *et al.*, 2018). This pathogen was first reported from Brazil in 1884 infecting common guava (*Psidium guajava*) (Winter, 1884), from which the original name was gained, guava rust. It was believed to have undergone a host shift from native Myrtaceae to species of Eucalyptus and *Syzygium jambos* (De Castro *et al.*, 1983; McTaggart *et al.*, 2016). Today, it is established in numerous countries in South and Central America (Coutinho *et al.*, 1998), as well as in the USA in Hawaii (Killgore *et al.*, 2007), Florida (Marlatt & Kimbrough, 1980) and California (Zambino & Nolan, 2011). Other countries reporting incursions of *A. psidii* are Japan (Kawanishi *et al.*, 2009), China (Zhuang *et al.*, 2011), Australia (Carnegie *et al.*, 2010), New Caledonia (Giblin, 2013; Soewarto *et al.*, 2017), South Africa (Roux *et al.*, 2013), Indonesia (McTaggart *et al.*, 2016), Singapore (du Plessis *et al.*, 2017), and New Zealand (http://mpi.govt.nz/protection-and-response/responding/alerts/myrtle-rust/). Especially in Australia, the study area of this work, the occurrence of *A. psidii* is a major threat as the Myrtaceae are one of the most dominant plant families (Makinson, 2014) and probably the most iconic with widespread genera such as the eucalypts (*Eucalyptus*, *Angophora* and *Corymbia*), paperbarks and bottlebrushes (*Melaleuca* and formerly, *Callistemon*), and tea-trees (*Leptospermum*). Their ecological importance in Australia is without question (Myerscough, 1998). There are approximately 2,250 native species within 88 genera of Myrtaceae in Australia (Makinson, 2014), with half of these occurring in climatic zones identified as suitable for the establishment of myrtle rust (Berthon *et al.*, 2018; Carnegie & Pegg, 2018). Studies on the susceptibility to myrtle rust of species of Myrtaceae in Australia, including those from controlled screening (Potts *et al.*, 2016) and field-based assessments (Pegg *et al.*, 2014a; Carnegie *et al.*, 2016), show that more than 90% have been identified as being susceptible to *A. psidii* (Berthon et al. 2018). Further complicating the situation, the interspecific susceptibility of many host species can vary tremendously from fully resistant to extremely susceptible, while others show a great range of intraspecific variation in susceptibility (Morin *et al.*, 2012; Sandhu & Park, 2013; Lee *et al.*, 2014; Pegg et al., 2018). Unfortunately, the unusually wide host range and curious variability within and between species in Australia is not the only unanswered question on *A. psidii*.

Currently, several strains of *A. psidii* are known from native and introduced Myrtaceae in Brazil, Colombia, Jamaica and Uruguay (Graça *et al.*, 2013; Granados *et al.*, 2017; Carnegie & Pegg, 2018). Only one *A. psidii* strain, the 'pandemic' strain, is present in Australia (da S. Machado *et al.*, 2015; Stewart *et al.*, 2018). The pandemic strain has a yet unknown origin (Graça *et al.*, 2013; McTaggart *et al.*, 2016), and has spread across the globe where it is present now in Hawaii, China, New Caledonia, Indonesia, New Zealand (Carnegie & Pegg 2018) and Singapore (Stewart et al., 2018). However, a completely different strain occurs on several hosts in South Africa (Roux *et al.*, 2016).

Until recently, *A. psidii* was considered clonal (Morin *et al.*, 2014), and genetic diversity within a population has been attributed to mutations. Latest findings suggest that *A. psidii* produces basidiospores through recombination and therefore is not strictly clonal (McTaggart *et al.*, 2017). While life cycles of rust fungi are often macrocyclic and undergo all five spore stages (Agrios et al., 2005), *A. psidii* has three known life cycle stages (McTaggart *et al.*, 2017) and is considered a microcyclic fungus. The stages are (i) a mitotic, dikaryotic uredinial stage, which is used to distinguish it from other rusts on Myrtaceae (Maier *et al.*, 2016), (ii) a telial stage with diploid teliospores (Morin *et al.*, 2014), and (iii) basidiospores that develop on a basidium and have either one or two nuclei (Morin *et al*., 2014).

Infections occur on young, actively growing leaves, shoots, as well as on fruits and sepals (Coutinho *et al.*, 1998; Glen *et al.*, 2007). Juvenile and highly susceptible species may be defoliated and show signs of severe stem and foliage blight (Coutinho et al., 1998; Glen et al., 2007). Following infection, evidence of the rust becomes visible after two to four days and produces great amounts of yellow urediniospores that intensify in their visibility ten to twelve days after inoculation. This yellow-orange colour has been associated with carotenoid pigments for some other rust species (Wang *et al.*, 2018), but there is no information on spore chemical composition available for *A. psidii*. Infected areas subsequently increase in size in a circular manner due to the radial growth of the fungus while they are generally confined to areas between the veins. Leaves are often deformed. Secondary infections occur within a few days and are, again, confined to new plant tissues (Coutinho *et al.*, 1998). Coutinho et al. (1998) also reported that urediniospores are usually restricted to the lower leaf surfaces and that leaves show less intense sporulation when infected after reaching 50% of their full growth. However, for *Backhousia citriodora* leaves, we (Heim, 2018, chapter 2) observed yellow urediniospores on the upper leaf surface, an important feature for myrtle rust detection using remote sensing techniques. Sporulation of *A. psidii* on infected parts of seedlings ceases after 2 weeks. Plants recover by producing new growth that may become infected if the conditions are favourable. If the trees are continuously re-infected, they become stunted (Coutinho et al., 1998) and eventually die (Carnegie et al., 2016). The gross symptoms of disease caused by *A. psidii* are similar for all strains (Figure 4). This poses a great biosecurity risk in Australia as it aggravates the differentiation of the currently occurring pandemic strain, from newly arriving, more virulent strains at the Australian border. Hence, timely management responses are unlikely and a new strain could as well rapidly spread in Australia (Makinson, 2018).

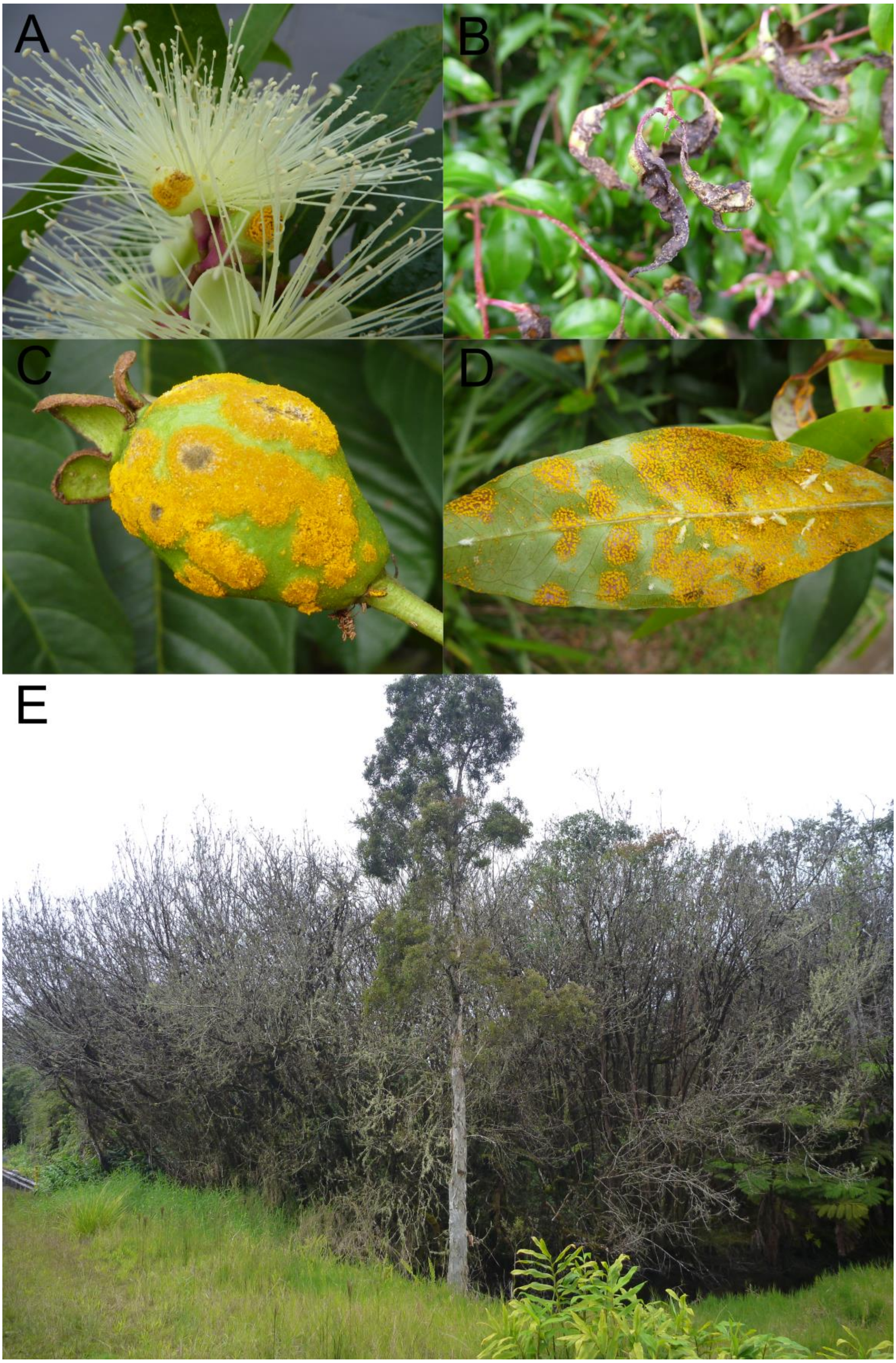

Figure 4* | *Austropuccinia psidii infection on species within the Myrtaceae. (A) Urediniospores on Syzygium jambos flower. (B) Necrotic Syzygium anisatum shoot. (C) Urediniospores on Psidium guajava fruit. (D) Urediniospores on Syzygium jambos leaf. (E) Dieback cause by A. psidii on Syzygium jambos. (Source: Angus Carnegie).

While the external disease pattern of *A. psidii* hosts is well described, little is known about the internal physiological symptoms. In general, physiological interactions between a fungal disease and its host vary depending on the pathogen (Knogge, 1996; Jones & Dangl, 2006). Often composition and content of leaf pigments (e.g. chlorophylls, carotenoids and anthocyanins), water content, functionality of tissue or the appearance of pathogen-specific structures change when the plant is exposed to phytopathogens. Leaf pigments are affected in particular when pathogens induce chlorotic- and necrotic-like symptoms (Gamon & Surfus, 1999; Carter & Knapp, 2001).

Environmental and Economic Impact of Myrtle Rust in Australia

The ecological consequences associated with the incursion of *A. psidii* are quick and serious decline in the extent and abundance of highly susceptible Australian native plant species (Makinson, 2018). Pegg (2014b) found 48 species to be highly susceptible in Queensland, Australia. Among these species were the keystone species *Melaleuca quinquenervia*, and the rare and endangered species *Backhousia oligantha*, *Gossia gonoclada* and *Rhodamnia angustifolia*. Especially at risk, because of their high susceptibility in some provenances, are three broad-leaved *Melaleuca* species (*M. leucadendra*, *M. quinquenervia* and *M. viridiflora*) and two understory rainforest species (*Rhodomyrtus psidioides*, *Rhodamnia rubescence*). All three *Melaleuca* species are a crucial component of the tropical and sub-tropical biota of Australia (Pegg & Carnegie, 2018). After *Eucalyptus*, *Melaleuca* is the most species-rich genus in Australia Myrtaceae containing approximately 259 species (Edwards *et al.*, 2010). They are of high conservation significance as they are an integral part of wetlands and occur in riverine gallery forests and the margins of rainforests (Barlow, 1986; Cook *et al.*, 2008). Regarding *R. rubescens* and *R. psidioides*, Carnegie et al. (2016) showed that repeated, severe infection by *A. psidii* resulted in a reduction in foliage production eventually leading to tree death in a native forest ecosystem in fewer than four years. Both species are now in decline, while the impact on *R.*

psidioides is particularly severe with deaths of more than half the trees in many stands, including mature trees up to 12-m tall (Pegg *et al.*, 2017). Pegg *et al*. (2017) also reported local extinction of *R. psidioides* in south-eastern Queensland, with no evidence of regeneration. After *A. psidii* was detected in 2010, the pathogen was so aggressive that it changed the ecological status in Australia for *R. rubescens* and *R. psidioides* from being considered common and widespread to being preliminarily listed as Critically Endangered in NSW (NSW Scientific Committee, 2017a,b).

Additionally, economic risks associated with the spread and impact of *A. psidii* have been reported. While the impact on tourism has been briefly touched by Booth (2000), the impact on horticulture, forestry and iconic native food products was discussed more widely. For the eucalyptus forestry industry, no current damage was reported in Australia (Carnegie, 2015) as Australia currently harbours only a single strain of *A. psidii*, the 'pandemic' strain (Stewart *et al.*, 2018). If any further strain of *A. psidii* would arrive in Australia, it could escalate the threats posed by this pathogen. Other strains of the pathogen are likely to have different host ranges with potentially different effects and environmental tolerances on current hosts (Makinson, 2018). Two strongly eucalypt-associated strains (C2, C3) are known from South America, where *A. psidii* has caused major economic damage to eucalypt species and hybrids (Makinson, 2018; Stewart et al., 2018; Carnegie & Pegg, 2018).

Myrtle rust first became a threat to the eucalyptus industry in South America in 1973 when large scale damage in nurseries was reported on *Eucalyptus grandis* (Ferreira, 1983; Furtado & Marino, 2002). Later, commercial plantations of *E. globulus* and *E. viminalis* have been found infected with *A. psidii*; disease severity was reported as being highly variable among plants of both species (Alfenas *et al.*, 2003). Usually, *Eucalyptus* species younger than 2 years old were most susceptible (Coutinho *et al.*, 1998). In Uruguay (Pérez *et al.*, 2011), pathogenicity tests showed that isolates from native Myrtaceae could infect *E. globulus* and *E. grandis*. Although the impact on *Eucalyptus* forestry has not been reported to be severe elsewhere than in Brazil, the potential impact of the spread of new strains should not be underestimated as the incursion of a more virulent strain of *A. psidii* into a not yet threatened region can become problematic (Cannon, 2011; Burgess & Wingfield, 2017; Carnegie & Pegg, 2018).

In Australia, where this study took place, *A. psidii* is reported along the eastern coast from Batemans Bay to northern Queensland, and around Darwin, with localised distribution in Victoria (Melbourne) and northern Tasmania (Makinson, 2018). Few data exist on the impact of myrtle rust on Australian horticultural production. However, it has been shown that Geraldton Wax (*Chamelaucium spp.*), which accounts for 40% of Australian cut-flower production (Makinson, 2018), is extremely susceptible to *A. psidii* and there is no known resistant genotype across the genus in the wild (Tobias *et al.*, 2015). A number of other industries rely on the Myrtaceae family for their products. Based on economic return, the largest product is tea-tree oil, followed by Lemon Myrtle, Aniseed Myrtle, and Riberry products (Makinson, 2018).

Lemon Myrtle (*Backhousia citriodora*) started its commercial trajectory in the 1990s, with a fresh weight leaf harvest of up to 1,000 tonnes p.a., compared with less than 15 tonnes for most other native food crops (AgriFutures, 2017). The expanding lemon myrtle industry has been particularly affected, as cultivars of *B. citriodora* currently in use are moderately to highly susceptible to myrtle rust (Doran *et al.*, 2012). Leaves of *B. citriodora* are commercially harvested to produce lemon-flavoured herbal teas, culinary herbs, and lemon-scented essential oils used for food flavouring and personal care products (Clarke, 2012). The farm gate value of this market has been estimated to be between AUD$ 7-23 million annually (Clarke, 2012). Rust-affected leaves of *B. citriodora* are unsuitable for use and cause yield losses up to 70%. The application of fungicides to control the disease is undesirable as the market demands a clean, organic product (Carnegie & Pegg, 2018). Therefore, the industries reliant on lemon myrtle are in urgent need of rust-resistant cultivars or measures to reduce the use of fungicides.

Rationale and Aims

As mentioned above, there is increasing interest in using remote sensing to detect and discriminate plant pathogens in precision agriculture (Mahlein, 2016). Because current field-based detection of myrtle rust and other plant pathogens are solely conducted by trained experts and rely on their experience, assessment performance may vary considerably, leading to issues with repeatability (Mahlein, 2016). Thus, disease assessment is subject to human bias. Automated, sensor-based disease detection can be performed with high reliability, sensitivity and specificity and improve the assessment of disease incidence and severity beyond the processes of visual disease detection (Mahlein, 2016). While efforts have been made to collect and interpret spectral information of various pathosystems, no one has explored remote sensing methods that could detect myrtle rust in a plant production system. Consequently, the aim of this doctoral thesis was to develop proof-of-concept for the sensor-guided detection of myrtle rust. The thesis is divided into three main data chapters (Chapters 2, 3, 4) that are formally introduced (Chapter 1) and discussed (Chapter 5). The data chapters consist of individual projects that explore the spectral reflectance signature of infected and fungicide treated lemon myrtle trees across multiple scales.

The initial study (Chapter 2) explored whether it would be possible to spectrally discriminate treated and untreated leaves of lemon myrtle trees. It was assumed that typical symptoms, such as the bright, orange-yellow urediniospores would cause variation in reflectance. From a lemon myrtle plantation, spectral signatures of fungicide-treated and untreated leaves were collected using a portable field spectrometer. A third class of spectra was collected from a botanical garden (Australian Botanic Garden Mount Annan, New South Wales, Australia), where lemon myrtle leaves had not been exposed (naïve) to *A. psidii*. Reflectance spectra in their primary form and their first-order derivatives were used to train a random forest classifier resulting in an overall accuracy of 78% (kappa = 0.68) for primary spectra and 95% (kappa = 0.92) for first-order derivative-transformed spectra. A broad set of relevant discrimination features was selected. Thus, an optical sensor-based discrimination, using spectral reflectance signatures of this as yet uninvestigated pathosystem, seems technically feasible. This study provided a foundation for the development of automated, sensor-based detection and monitoring systems for myrtle rust and allowed us to focus on the selection of relevant discrimination features as well as to up-scale the detection at canopy-level.

In chapter 3, we continued to analyse the data collected for chapter 2. We were interested whether it is possible to accurately discriminate treated and untreated plants from the plantation by using a minimal number of relevant wavebands. The aim was, to develop a novel spectral disease index (SDI), the lemon myrtle-myrtle rust index (LMMR). We sampled 236 fungicide-treated (disease free) and 228 untreated (diseased) lemon myrtle leaves and used a random forest classifier to show that the LMMR discriminates those classes with an overall accuracy of 90%. Compared to three classical SVIs (PRI, MCARI, NBNDVI), commonly applied for stress detection, the LMMR clearly improved classification accuracies (58%, 67%, 60%, respectively). If the LMMR can be validated on independent datasets from similar and different host-species, it could enable land managers to reduce disease impact by earlier control. There might also be potential to collect useful data for epidemiology models. Calculating the LMMR based on hyperspectral data collected from aerial platforms (e.g. drones) would allow for rapid and high capacity screening for disease outbreaks.

For chapter 4, we were interested whether accurate detection was still possible at canopy level and if relevant features would differ between leaf- and canopy scale. We a used a multispectral imaging approach and unmanned aerial systems (UAS) to explore whether myrtle rust could be detected on a lemon myrtle plantation from the air. Multispectral aerial imagery was collected from fungicide treated and untreated tree canopies and compared to multispectral data from individual leaves from the same canopies. Spectral vegetation indices and single spectral bands were used to train a random forest classifier. The UAS-derived classification yielded far higher accuracy (95%) than the leaf-level classification (74%). Important predictors for the UAS classifier were the near-infrared (NIR) and red edge (RE) spectral band. At the leaf level NIR was no longer deemed important. Our work suggests there is clear potential for mapping myrtle rust-related stress from aerial multispectral images. Output from studies of this type could be used for pinpointing disease hotspots, for adjusting management strategies, and as input for epidemiological models.

In the final chapter of my thesis, I summarise the main findings of my research and I briefly touch on the potential implications of this work for plantation managers, plant pathologists and remote sensing scientists who aim to further advance the integration of remote sensing tools into the management of *A. psidii* for the lemon myrtle industry. Lastly, I discuss directions for future research.

References

AgriFutures, 2017. Lemon Myrtle. https://www.agrifutures.com.au/farm-diversity/lemon-myrtle/. Accessed 29 November 2018

Agrios GN, 2005. *Plant Pathology*. Burlington, MA, USA: Elsevier Academic Press.

Albetis J, Duthoit S, Guttler F *et al.*, 2017. Detection of Flavescence dorée grapevine disease using Unmanned Aerial Vehicle (UAV) multispectral imagery. *Remote Sensing* **9**, 1–20.

Alfenas AC, Zauza EA V, Assis TF, 2003. First record of Puccinia psidii on *Eucalyptus globulus* and *E. viminalis* in Brazil. *Australasian Plant Pathology* **32**, 325–326.

Apan A, Held A, Phinn S, Markley J, 2004. Detecting sugarcane "orange rust" disease using EO-1 Hyperion hyperspectral imagery. *International Journal of Remote Sensing* **25**, 489–498.

Ashourloo D, Mobasheri MR, Huete A, 2014. Evaluating the effect of different wheat rust disease symptoms on vegetation indices using hyperspectral measurements. *Remote Sensing* **6**, 5107–5123.

Barlow BA, 1986. Contributions to a Revision of Melaleuca (Myrtaceae): 1-3. *Brunonia* **9**, 163–177.

Beenken L, 2017. *Austropuccinia*: A new genus name for the myrtle rust *Puccinia psidii* placed within the redefined family sphaerophragmiaceae (Pucciniales). *Phytotaxa* **297**, 53–61.

Berthon K, Esperon-Rodriguez M, Beaumont LJ, Carnegie AJ, Leishman MR, 2018. Assessment and prioritisation of plant species at risk from myrtle rust (*Austropuccinia psidii*) under current and future climates in Australia. *Biological Conservation* **218**, 154–162.

Bhattacharya S, 2017. Deadly new wheat disease threatens Europe's crops. *Nature* **542**, 145–146.

Booth TH, Old KM, Jovanovic T, 2000. A preliminary assessment of high risk areas for *Puccinia psidii* (Eucalyptus rust) in the Neotropics and Australia. *Agriculture, Ecosystems and Environment* **82**, 295–301.

Bravo C, Moshou D, West J, McCartney A, Ramon H, 2003. Early disease detection in wheat fields using spectral reflectance. *Biosystems Engineering* **84**, 137–145.

Burgess TI, Wingfield MJ, 2017. Pathogens on the move: A 100-year global experiment with planted eucalypts. *BioScience* **67**, 14–25.

Calderón R, Montes-Borrego M, Landa BB, Navas-Cortés JA, Zarco-Tejada PJ, 2014. Detection of downy mildew of opium poppy using high-resolution multi-spectral and thermal imagery acquired with an unmanned aerial vehicle. *Precision Agriculture* **15**, 639–661.

Calderón R, Navas-Cortés JA, Zarco-Tejada PJ, 2015. Early detection and quantification of verticillium wilt in olive using hyperspectral and thermal imagery over large areas. *Remote Sensing* **7**, 5584–5610.

Campbell JB, Wynne RH, 2011. *Introduction to Remote Sensing*. New York, NY, USA: The

Guilford Press.

Candiago S, Remondino F, De Giglio M, Dubbini M, Gattelli M, 2015. Evaluating multispectral images and vegetation indices for precision farming applications from UAV images. *Remote Sensing* **7**, 4026–4047.

Cannon AM, 2011. *Myrtle Rust – Forest Industry Issues Paper*. Melbourne, VIC, Australia: Forest & Wood Products Australia Limited

Carnegie AJ, 2015. First Report of *Puccinia psidii* (Myrtle Rust) in *Eucalyptus* Plantations in Australia. *Plant Disease* **99**, 161–161.

Carnegie AJ, Kathuria A, Pegg GS, Entwistle P, Nagel M, Giblin FR, 2016. Impact of the invasive rust *Puccinia psidii* (myrtle rust) on native Myrtaceae in natural ecosystems in Australia. *Biological Invasions* **18**, 127–144.

Carnegie AJ, Lidbetter JR, Walker J *et al.*, 2010. Uredo rangelii, a taxon in the guava rust complex, newly recorded on Myrtaceae in Australia. *Australasian Plant Pathology* **39**, 463–466.

Carnegie AJ, Pegg GS, 2018. Lessons from the Incursion of Myrtle Rust in Australia. *Annual Review of Phytopathology* **56**, 457–478.

Carter GA, 1993. Responses of Leaf Spectral Reflectance to Plant Stress. *American Journal of Botany* **80**, 239.

Carter GA, Knapp DE, 2001. Leaf optical properties in higher plants: linking spectral characteristics to stress and chlorophyll concentration. *American Journal of Botany* **88**, 677–684.

De Castro HA, Krügner TL, Ideriha CHF, Cappello MSC, Marchi AB, 1983. Cross inoculation of *Eucalyptus*, *Psidium guajava* and *Syzygium jambos* with *Puccinia psidii*. *Fitopatologia Brasileira* **8**, 491–497.

Clarke M, 2012. *Australian Native Food Industry Stocktake*. Barton, ACT, Australia: Rural Industries Research and Development Corporation.

Cook LG, Morris DC, Edwards RD, Crisp MD, 2008. Reticulate evolution in the natural range of the invasive wetland tree species *Melaleuca quinquenervia*. *Molecular Phylogenetics and Evolution* **47**, 506–522.

Coutinho TA, Wingfield MJ, Alfenas AC, Crous PW, 1998. *Eucalyptus* Rust: A Disease with the Potential for Serious International Implications. *Plant Disease* **82**, 819–825.

Delalieux S, van Aardt J, Keulemans W, Schrevens E, Coppin P, 2007. Detection of biotic stress (*Venturia inaequalis*) in apple trees using hyperspectral data: Non-parametric statistical approaches and physiological implications. *European Journal of Agronomy* **27**, 130–143.

Devadas R, Lamb DW, Simpfendorfer S, Backhouse D, 2009. Evaluating ten spectral vegetation indices for identifying rust infection in individual wheat leaves. *Precision Agriculture* **10**, 459–470.

Doran J, Lea D, Bush D, 2012. *Assessing Myrtle Rust in a Lemon Myrtle Provenance Trial*. Barton, ACT, Australia: Rural Industries Research and Development Corporation.

Edwards RD, Craven LA, Crisp MD *et al.*, 2010. *Melaleuca* revisited: cpDNA and morphological data confirm that *Melaleuca* L. (Myrtaceae) is not monophyletic. *Taxon* **59**, 744–754.

Ferreira FA, 1983. Ferrugem do eucalipto. *Revista Árvore* **7**, 91–109.

Foley JA, 2005. Global Consequences of Land Use. *Science* **309**, 570–574.

Foley JA, Ramankutty N, Brauman KA *et al.*, 2011. Solutions for a cultivated planet. *Nature* **478**, 337–342.

Furtado LF, Marino CL, 2002. Eucalyptus rust management in Brazil. In: *Proceedings 2nd IUFRO Rusts of Forest Trees WP Conference*. Yangling, China, 118–124.

Gamon JA, Surfus JS, 1999. Assessing leaf pigment content and activity with a reflectometer. *New Phytologist* **143**, 105–117.

Gates DM, Keegan HJ, Schleter JC, Weidner VR, 1965. Spectral Properties of Plants. *Applied Optics* **4**, 11.

Gebbers R, Adamchuk VI, 2010. Precision Agriculture and Food Security. *Science* **327**, 828–831.

Giblin F, 2013. *Myrtle rust report: New Caledonia Assessment of myrtle rust situation in New Caledonia*. Maroochydore, QLD, Australia: University of the Sunshine Coast.

Giblin F, Carnegie AJ, 2014. *Puccinia psidii* (Myrtle Rust) – AUSTRALIAN HOST LIST version 24 September 2014.

Gitelson AA, Merzlyak MN, Chivkunova OB, 2007. Optical Properties and Nondestructive Estimation of Anthocyanin Content in Plant Leaves. *Photochemistry and Photobiology* **74**, 38–45.

Glen M, Alfenas AC, Zauza EA V, Wingfield MJ, Mohammed C, 2007. *Puccinia psidii*: A threat to the Australian environment and economy - a review. *Australasian Plant Pathology* **36**, 1–16.

Graça RN, Ross-Davis AL, Klopfenstein NB *et al.*, 2013. Rust disease of eucalypts, caused by *Puccinia psidii*, did not originate via host jump from guava in Brazil. *Molecular Ecology* **22**, 6033–6047.

Granados GM, McTaggart AR, Barnes I, Rodas CA, Roux J, Wingfield MJ, 2017. The pandemic biotype of *Austropuccinia psidii* discovered in South America. *Australasian Plant Pathology* **46**, 267–275.

Helfer S, 2014. Rust fungi and global change. *New Phytologist* **201**, 770–780.

Huete A, Didan K, Miura T, Rodriguez E., Gao X, Ferreira L., 2002. Overview of the radiometric and biophysical performance of the MODIS vegetation indices. *Remote Sensing of Environment* **83**, 195–213.

Jackson RD, 1986. Remote Sensing of Biotic and Abiotic Plant Stress. *Annual Review of Phytopathology* **24**, 265–287.

Jacquemoud S, Ustin SL, 2001. Leaf optical properties: a state of the art. *Proc. 8th International Symposium Physical Measurements & Signatures in Remote Sensing*, 223–232.

Jones JDG, Dangl JL, 2006. The plant immune system. *Nature* **444**, 323–329.

Kawanishi T, Uematsu S, Kakishima M et al., 2009. First report of rust disease on ohia and the causal fungus, *Puccinia psidii*, in Japan. Journal of General Plant Pathology **75**, 428–431.

Killgore EM, Heu R A, 2007. Ohia Rust *Puccinia psidii* Winter. *New Pest Advisory*, 4–5.

Knipling EB, 1970. Physical and Physiological Basis for the Reflectance of Visible and Near

Infrared Radiation from Vegetation. *Remote Sensing of Environment* **1**, 155–159.

Knogge W, 1996. Fungal Infection of Plants. *the Plant Cell Online* **8**, 1711–1722.

Kokaly RF, Skidmore AK, 2015. Plant phenolics and absorption features in vegetation reflectance spectra near 1.66 µm. *International Journal of Applied Earth Observation and Geoinformation* **43**, 55–83.

Kuhn M, Johnson K, 2013. *Applied Predictive Modeling*. New York, NY, USA: Springer.

Lee D, Brawner J, Pegg G, 2014. Screening *Eucalyptus cloeziana* and *E. argophloia* populations for resistance to Puccinia psidii. *Plant Disease* **99**, 71–79.

López-López M, Calderón R, González-Dugo V, Zarco-Tejada PJ, Fereres E, 2016. Early detection and quantification of almond red leaf blotch using high-resolution hyperspectral and thermal imagery. *Remote Sensing* **8**.

Mahlein, A.; Kuska, MT.; Behmann, J.; Polder, G.; Walter, A, 2018. Hyperspectral Sensors and Imaging Technologies in Phytopathology: State of the Art. *Annu. Rev. Phytopathol*. **56,** 535–558

Mahlein A-K, 2016. Plant Disease Detection by Imaging Sensors – Parallels and Specific Demands for Precision Agriculture and Plant Phenotyping. *Plant Disease* **100**, 241–251.

Mahlein AK, Rumpf T, Welke P *et al.*, 2013. Development of spectral indices for detecting and identifying plant diseases. *Remote Sensing of Environment* **128**, 21–30.

Mahlein AK, Steiner U, Dehne HW, Oerke EC, 2010. Spectral signatures of sugar beet leaves for the detection and differentiation of diseases. *Precision Agriculture* **11**, 413–431.

Maier W, McTaggart AR, Roux J, Wingfield MJ, 2016. *Phakopsora myrtacearum* sp. nov., a newly described rust (Pucciniales) on eucalypts in eastern and southern Africa. *Plant Pathology* **65**, 189–195.

Makinson B, 2014. Myrtle Rust – What ' s happening ? *Australasian Plant Conseravtion* **23**, 13–15.

Makinson RO, 2018. *Myrtle Rust reviewed: the impacts of the invasive pathogen Austropuccinia psidii on the Australian environment*. Canberra, ACT, Australia: Plant Biosecurity Cooperative Research Centre

Marlatt RB, Kimbrough JW, 1980. Rust (*Puccinia psidii*) of Allspice (*Pimenta dioica*) appears in Florida. *Proc. Fla. State Hort. Soc.* **93**, 111–111.

McCook S, Vandermeer J, 2015. The Big Rust and the Red Queen: Long-Term Perspectives on Coffee Rust Research. *Phytopathology* **105**, 1164–1173.

McTaggart AR, Roux J, Granados GM *et al.*, 2016. Rust (*Puccinia psidii*) recorded in Indonesia poses a threat to forests and forestry in South-East Asia. *Australasian Plant Pathology* **45**, 83–89.

McTaggart AR, Shuey LS, Granados GM *et al.*, 2017. Evidence that *Austropuccinia psidii* may complete its sexual life cycle on Myrtaceae. *Plant Pathology* ***67***, 729–734.

Morin L, Aveyard R, Lidbetter JR, Wilson PG, 2012. Investigating the host-range of the rust fungus *Puccinia psidii* sensu lato across tribes of the family myrtaceae present in australia. *PLoS ONE* **7** e35434.

Morin L, Talbot MJ, Glen M, 2014. Quest to elucidate the life cycle of Puccinia psidii sensu lato. *Fungal Biology* **118**, 253–263.

Moshou D, Bravo C, West J, Wahlen S, McCartney A, Ramon H, 2004. Automatic detection of “yellow rust” in wheat using reflectance measurements and neural networks. *Computers and Electronics in Agriculture* **44**, 173–188.

Mulla DJ, 2013. Twenty five years of remote sensing in precision agriculture: Key advances and remaining knowledge gaps. *Biosystems Engineering* **114**, 358–371.

Myerscough P, 1998. Ecology of Myrtaceae with special reference to the Sydney region. *Cunninghamia* ***5***, 787–807.

NSW Scientific Committee, 2017a. *Preliminary threatened species listing: Rhodamnia rubescens*. Hurstville, NSW, Australia: Office of Environment and Heritage

NSW Scientific Committee, 2017b. *Preliminary threatened species listing: Rhodomyrtus psidioides*. Hurstville, NSW, Australia: Office of Environment and Heritage

Paini DR, Sheppard AW, Cook DC, De Barro PJ, Worner SP, Thomas MB, 2016. Global threat to agriculture from invasive species. *Proceedings of the National Academy of Sciences* **113**, 7575–7579.

Palmgren MG, Edenbrandt AK, Vedel SE *et al.*, 2015. Are we ready for back-to-nature crop breeding? *Trends in Plant Science* **20**, 155–164.

Pegg GS, Brawner JT, Lee DJ, 2014a. Screening *Corymbia* populations for resistance to *Puccinia psidii*. *Plant Pathology* **63**, 425–436.

Pegg G, Carnegie A, 2018. Predicting impact of myrtle rust on broad leaved *Melaleuca* species populations in Australia. *Australasian Plant Pathology* **47**, 421–430.

Pegg GS, Giblin FR, McTaggart AR *et al.*, 2014b. *Puccinia psidii* in Queensland, Australia: Disease symptoms, distribution and impact. *Plant Pathology* **63**, 1005–1021.

Pegg G, Taylor T, Entwistle P, Guymer G, Giblin F, Carnegie A, 2017. Impact of *Austropuccinia psidii* (myrtle rust) on Myrtaceae-rich wet sclerophyll forests in south east Queensland. *PLoS ONE* **12**, e0188058.

Pérez CA, Wingfield MJ, Altier NA, Simeto S, Blanchette RA, 2011. *Puccinia psidii* infecting cultivated *Eucalyptus* and native Myrtaceae in Uruguay. *Mycological Progress* **10**, 273–282.

du Plessis E, McTaggart AR, Granados GM *et al.*, 2017. First Report of Myrtle Rust Caused by *Austropuccinia psidii* on *Rhodomyrtus tomentosa* (Myrtaceae) from Singapore. *Plant Disease* **101**, 1676–1676.

Potts BM, Sandhu KS, Wardlaw T *et al.*, 2016. Evolutionary history shapes the susceptibility of an island tree flora to an exotic pathogen. *Forest Ecology and Management* **368**, 183–193.

Raven, PH.; Evert, RF.; Eichhorn, SE, 2006. *Biologie der Pflanzen*. Berlin, Germany: De Gruyter.

Reid WV, Mooney HA, Cropper A *et al.*, 2005. *Millennium Ecosystem Assessment. Ecosystems and human well-being: synthesis*. Washington, DC, USA: Island Press

Rhoten D, Parker A, 2004. Risks and rewards of an interdiciplinary research path. *Science* **306**, 2046–2046.

Rouse JW, Hass RH, Schell JA, Deering DW, 1973. Monitoring vegetation systems in the great plains with ERTS. *Third Earth Resources Technology Satellite (ERTS) symposium* **1**, 309–317.

Roux J, Granados GM, Shuey L, Barnes I, Wingfield MJ, McTaggart AR, 2016. A unique genotype of the rust pathogen, *Puccinia psidii*, on Myrtaceae in South Africa. *Australasian Plant Pathology* **45**, 645–652.

Roux J, Greyling I, Coutinho TA, Verleur M, Wingfield MJ, 2013. The Myrtle rust pathogen, *Puccinia psidii*, discovered in Africa. *IMA Fungus* **4**, 155–159.

da S. Machado P, Alfenas AC, Alfenas RF, Mohammed CL, Glen M, 2015. Microsatellite analysis indicates that *Puccinia psidii* in Australia is mutating but not recombining. *Australasian Plant Pathology* **44**, 455–462.

Sandhu KS, Park RF, 2013. *Genetic basis of pathogenicity in Uredo rangelii*. Sydney, NSW, Australia: The University of Sydney Plant Breeding Institute

Sankaran S, Mishra A, Ehsani R, Davis C, 2010. A review of advanced techniques for detecting plant diseases. *Computers and Electronics in Agriculture* **72**, 1–13.

Sharp EL, Perry CR, Scharen AL *et al.*, 1985. Monitoring cereal rust development with a spectral radiometer. *Phytopathology* **75**, 936–939.

Sicard A, Zeilinger AR, Vanhove M *et al.*, 2018. Xylella fastidiosa: Insights into an Emerging Plant Pathogen. *Annual Review of Phytopathology* **56**, 181–202.

Soewarto J, Carriconde F, Hugot N, Bocs S, Hamelin C, Maggia L, 2017. Impact of *Austropuccinia psidii* in New Caledonia, a biodiversity hotspot. *Forest Pathology* **48**, 1–12.

Stewart JE, Ross-Davis AL, Graça RN *et al.*, 2018. Genetic diversity of the myrtle rust pathogen (*Austropuccinia psidii*) in the Americas and Hawaii: Global implications for invasive threat assessments. *Forest Pathology* **48**, 1–13.

Thenkabail P, Lyon J, Huete A, 2011. *Hyperspectral Remote Sensing Of Vegetation*. Boca Raton, FL, USA: CRC Press.

Tobias PA, Park RF, Külheim C, Guest DI, 2015. Wild-sourced *Chamelaucium uncinatum* have no resistance to *Puccinia psidii* (myrtle rust). *Australasian Plant Disease Notes* **10**, 11–13.

Vogel G, 2017. Where have all the insects gone? *Science* **356**, 576–579.

Wang E, Dong C, Park RF, Roberts TH, 2018. Carotenoid pigments in rust fungi: Extraction, separation, quantification and characterisation. *Fungal Biology Reviews* ***32**, 166–180*.

Warschefsky E, Varma Penmetsa R, Cook DR, Von Wettberg EJB, 2014. Back to the wilds: Tapping evolutionary adaptations for resilient crops through systematic hybridization with crop wild relatives. *American Journal of Botany* **101**, 1791–1800.

West JS, Bravo C, Oberti R, Lemaire D, Moshou D, McCartney HA, 2003. The potential of optical canopy measurement for targeted control of field crop diseases. *Annual Review of Phytopathology* **41**, 593–614.

Willis KJ, 2017. *State of the World's Plants Report 2017*. London, UK: Royal Botanic Gardens, Kew.

Winter G, 1884. Repertorium. *Rabenhorstii fungi europaei et extraeuropaei exsiccati cura Dr.*

G. Winter, Centuria XXXI et XXXII. Hedwigia **23**, 164–172.

Van De Wouw M, Kik C, Van Hintum T, Van Treuren R, Visser B, 2010. Genetic erosion in crops: Concept, research results and challenges. *Plant Genetic Resources: Characterisation and Utilisation* **8**, 1–15.

Zambino PJ, Nolan PA, 2011. First report of rust caused by *Puccinia psidii* on paperbark, *Melaleuca quinquenervia*, in California. *Plant Disease* **95**, 1314–1314.

Zarco-Tejada PJ, Camino C, Beck PSA et al., 2018. Previsual symptoms of *Xylella fastidiosa* infection revealed in spectral plant-trait alterations. Nature Plants **4**, 432–439.

Zhuang JY, Wei SX, Jian-yun Z, Zhuang JY, Wei SX, 2011. Additional materials for the rust flora of Hainan Province, China. *Mycosystema* **30**, 853–860.

This page is intentionally left blank.

This page is intentionally left blank.

CHAPTER II

Detecting myrtle rust (*Austropuccinia psidii*) on lemon myrtle trees using spectral signatures and machine learning

RHJ Heim • IJ Wright • HC Chang • AJ Carnegie • GS Pegg • EK Lancaster • DS Falster • J Oldeland
Published in: Plant Pathology doi: 10.1111/ppa.12830

Abstract

Hundreds of species in one of Australia's dominant plant families, the Myrtaceae, are at risk from the invasive pathogenic fungus *Austropuccinia psidii*. Since its arrival in Australia in 2010, native plant communities have been severely affected, with highly susceptible species likely to become extinct from recurring infections. While severe impact on Australian native and plantation forestry has been predicted, the lemon myrtle industry is already under threat. Commercial cultivars of lemon myrtle (*Backhousia citriodora*) are highly susceptible to *A. psidii*. Detecting and monitoring disease outbreaks is currently only possible by eye, which is costly and subject to human bias. This study aims at developing a proof-of-concept for automated, non-biased classification of healthy (naïve), fungicide-treated and diseased lemon myrtle trees by means of their spectral reflectance signatures. From a lemon myrtle plantation, spectral signatures of fungicide-treated and untreated leaves were collected using a portable field spectrometer. A third class of spectra, from naïve lemon myrtle leaves that had not been exposed to *A. psidii*, was collected from a botanical garden. Reflectance spectra in their primary form and their first-order derivatives were used to train a random forest classifier resulting in an overall accuracy of 78% (kappa = 0.68) for primary spectra and 95% (kappa = 0.92) for first-order derivative-transformed spectra. Thus, an optical sensor-based discrimination, using spectral reflectance signatures of this as yet uninvestigated pathosystem, seems technically feasible. This study provides a foundation for the development of automated, sensor-based detection and monitoring systems for myrtle rust.

Introduction

Rust fungi and other plant pathogens are affecting humans and their environment by damaging plants and their products on which we depend for clothing, housing and, most importantly, food. Outbreaks of rust fungi may result in extensive damage to agricultural and forestry crops, as seen when a new, highly virulent strain of *Puccinia graminis* destroyed tens of thousands of hectares of wheat crops in southern Europe (Bhattacharya, 2017). This study focuses on the rust fungus *Austropuccinia psidii* (Sphaerophragmiaceae, Pucciniales). In Australia, *A. psidii* causes a disease commonly known as myrtle rust and is an obligate biotroph and pathogenic organism in the highly diverse phylum Basidiomycota (Helfer, 2014). In contrast to most other rust diseases, myrtle rust has the potential to infect hundreds of different species, escalating the potential consequences of infection.

Myrtle rust has already caused damage to a multitude of species in South and Central America, its native region (Coutinho et al., 1998), and to native vegetation in various countries between the Americas and Australia (Loope, 2010). *Austropuccinia psidii* was first identified in Australia in 2010, on the central east coast of New South Wales (NSW; Carnegie et al., 2010). Subsequently, a single strain of *A. psidii* (Machado et al., 2015) has undergone a remarkable range expansion, establishing along the Australian east coast from NSW to Queensland, and with localized distributions in Victoria, Tasmania and Northern Territory (Carnegie et al., 2016; Berthon et al., 2018). Myrtle rust has since also invaded New Caledonia (Giblin, 2013), South Africa (Roux et al., 2013), Indonesia (McTaggart et al., 2016), Singapore (du Plessis et al., 2017) and, most recently, New Zealand (www.mpi.govt.nz, accessed 02 December 2017).

Although most rust pathogens are limited to infecting only a few host species (Makinson, 2014), myrtle rust infects many hundred species, meaning the potential impact on the Australian flora is very serious. The Myrtaceae is one of the dominant plant families in the Australian flora, contributing more than 2000 species (approximately 10% of the total flora), including iconic, widespread genera such as *Eucalyptus* (gum trees) and *Melaleuca* (paper barks). About half of all Australian *Myrtaceae* occur in climatic zones identified as suitable for the establishment of myrtle rust (Berthon et al., 2018). Currently, over 500 host species in 86 *Myrtaceae* genera are known worldwide, with 347 of these species occurring in Australia (Carnegie et al., 2016; Soewarto et al., 2017). Of the species studied in Australia, including those from controlled screening (Potts et al., 2016) and field-based assessments (Pegg et al., 2014; Carnegie et al., 2016), 90% have been identified as being susceptible to *A. psidii*. Several species have been identified as being highly susceptible, with severe decline in natural populations recorded. This includes the common species *Rhodamnia rubescens* and *Rhodomyrtus psidioides*, where deaths of mature stands have been reported (Carnegie et al., 2016). Both species, previously listed as 'least concern', have now been provisionally listed as 'critically endangered' in NSW. The NSW scientific committee of the Department for Environment and Heritage has acknowledged myrtle rust as constituting a major threat to the native Australian environment and the *Myrtaceae*, listing it as a 'key threatening process' (NSW Scientific Committee, 2011).

Unfortunately, the impact of myrtle rust in Australia has not been limited to native ecosystems, with industries reliant on *Myrtaceae* also affected. Loss of commercial varieties and trade restrictions, in addition to increased reliance on fungicides, have severely affected the nursery and garden industry. The young, expanding lemon myrtle industry has also been significantly impacted (Doran et al., 2012). *Backhousia citriodora* (lemon myrtle) is a small to medium-sized tree (2 to 30 m), occurring naturally in Queensland coastal forests from Brisbane to Mackay. Lemon myrtle leaves are rich in antioxidants, vitamin E, lutein (a carotenoid compound important for eye function) and calcium. Lemon myrtle has antimicrobial and antifungal properties that are superior to tea tree oil (Rural Industries Research and Development Corporation, 2012). Leaves are commercially harvested to produce lemon-flavoured herbal teas, culinary herbs or lemon-scented essential oils used for food flavouring and in personal care products. Cultivars of *B. citriodora* currently in use are moderately to highly susceptible to myrtle rust. Rust-affected leaves of *B. citriodora* are unsuitable for its main uses and the application of fungicides to control the disease is undesirable as the market demands a clean, organic product. A total farm gate value at between AU$7 million and AU$23 million is estimated for dried leaf and essential oil, respectively (Rural Industries Research and Development Corporation, 2012). Therefore, the industry’s reliance on lemon myrtle is in urgent need of rust-resistant cultivars or measures to reduce the use of fungicides. Reports of susceptibility within the eucalypts (Pegg et al., 2014; Potts et al., 2016) indicate an escalation of the problem as it suggests the potential of myrtle rust to affect the forestry industry in Australia, both native and plantation. In Brazil, commercial plantations of *Eucalyptus globulus* and *E. viminalis* have suffered reduced growth and yield loss because of myrtle rust incursions (Alfenas et al., 2003).

Myrtle rust forms purplish lesions with abundant bright, orange-yellow urediniospores on young leaves and shoots, which may die-back because of rust attack. Current field identification of these symptoms and dis- ease incidence assessments for myrtle rust and other plant pathogens are reliant on trained experts and are dependent on the experience and performance of individuals that vary considerably, leading to issues with repeatability (Mahlein, 2016). Thus, disease assessment is subject to human bias. Automated, sensor-based dis- ease detection can be performed with high reliability, sensitivity and specificity and improve the assessment of disease incidence and severity beyond the processes of visual disease detection (Mahlein, 2016). To date, no one has explored sensor-based methods that could detect these and less obvious symptoms of myrtle rust.

Currently there is increasing interest in using spectral reflectance measurements (field spectroscopy) to detect and discriminate plant pathogens in precision agriculture (Mahlein, 2016). Spectral reflectance signatures of vegetation can indicate biochemical, physiological and molecular changes caused by abiotic or biotic processes (Mahlein et al., 2010). Disease symptoms often result from such changes brought about by pathogens and can be investigated by analysing spectral reflectance signatures (Bravo et al., 2003; Delalieux et al., 2007; Mahlein et al., 2010). Mahlein et al. (2010) used reflectance spectra of sugar beet leaves to show that there was a distinctive differentiation of three sugar beet fun-gal pathogens, *Cercospora beticola* (cercospora leaf spot), *Erysiphe betae* (powdery mildew) and *Uromyces betae* (beet rust). Bravo et al. (2003) built a classification model that could discriminate wheat plants infected with *Puccinia striiformis* (yellow rust) from healthy ones with an overall accuracy of 96%. However, spectral reflectance signatures are very specific to the source of reflection (e.g. specific to the pathogen infecting a certain species or specific to the content of biochemical compounds of a leaf) and more research is required to explore the utility of these approaches for other pathosystems.

The present study builds on the fact that spectral information (including visible light) is reflected by leaf surfaces. This reflection was captured with an optical sensor and portrayed as a waveform (intensity versus wavelength). Waveforms from different plant pathogens are likely to vary in distinct sections of the light spectrum, e.g. in the visible portion (VIS, 400–700 nm), where the bright, orange-yellow urediniospores of myrtle rust would potentially cause variation in reflectance. For myrtle rust, no efforts have yet been made to investigate its specific spectral reflectance signature. Consequently, the aim of this study was to test whether it is possible to spectrally discriminate naïve, fungicide-treated and infected leaves of *B. citriodora* trees. In this study the following questions were addressed:

(i) Can the spectral response of naïve and fungicide- treated *B. citriodora* individuals be distinguished from ones displaying infection symptoms of *A. psidii* (myrtle rust)?

(ii) Amongst all predictor variables (wavebands), what are the most useful wavebands for discriminating spectral responses of these classes?

Methods

Study site

Spectral reflectance signatures of lemon myrtle leaves were measured at two locations in subtropical eastern Australia. The first site was a commercial lemon myrtle plantation in northern NSW (lat. ?28.691, long. 153.295) and the second site was the Australian Botanic Garden at Mount Annan (lat. ?34.071, long. 150.766), 800 km south of the plantation, also in NSW near Sydney. At the plantation site, the mean annual temperature is 19.4 °C and mean annual rainfall 1343 mm, while a mean annual temperature of 16.7 °C and mean annual rainfall of 792.4 mm have been recorded at the botanical garden (Australian Government Bureau of Meteorology, 2017). The plantation site was selected to take advantage of an existing experiment in which the impact of fungicide was being measured on lemon myrtle trees affected by myrtle rust. The plantation had trees that were free of active disease symptoms, having had fungicide successfully applied to them ('treated' trees), and 'untreated' trees, showing symptoms of active myrtle rust infection. Treated trees could potentially have been infected previously with myrtle rust (prior to fungicide application) and thus the leaves may have had necrotic lesions even after killing the fungus by fungicide treatment. Consequently, the botanical gar- den was chosen as an additional field site: it offered plants in a region that suffers only rare episodes of myrtle rust, and were, therefore, free from infection and corresponding symptoms (here deemed 'naïve' trees).

Trees sampled at the plantation were approx. 2 m tall and pruned regularly into a pyramid shape to get maximal sunlight and increase foliage production rates. The sampling area was composed of nine rows of trees with the treated and untreated trees separated by buffer rows (Fig. 1a). Plants at the botanical garden were not managed and varied in their habits. In general, they were approximately 2–3 times taller, produced larger, tougher leaves, and were planted in clusters instead of rows. Including these plants from a different location (and provenance, most probably) added an unknown degree of variation to the spectral reflectance measured in this study. However, it gave a valuable comparison, providing spectral signatures from the same species that were not influenced by myrtle rust.

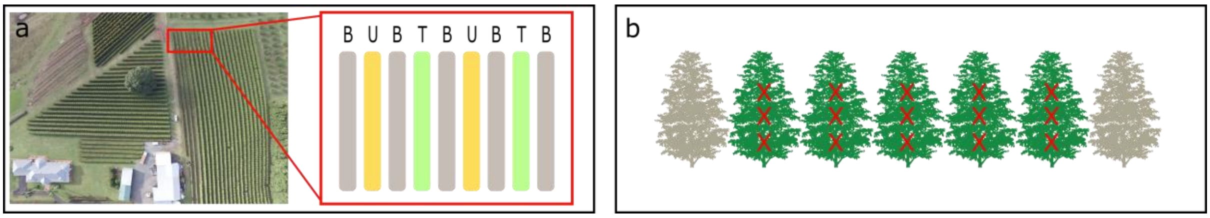

Figure 1 | Sampling design. (a) An aerial image of the plantation site; the box highlights nine rows of *Backhousia citriodora* trees that had been exposed to *Austropuccinia psidii*. Spectra were collected at three sampling points from both sides of each tree in rows that had been untreated (U) or treated (T) with fungicide, separated by buffer trees (B). (b) One side of a single row with sampling points highlighted as crosses. At each sampling point, the first two pairs of freshly expanding leaves, just large enough to apply the leaf clip accessory, were used to record the spectra. Plants growing close to management trails (grey) were not used in this study.

Spectral measurements

Spectral reflectance between 350 and 2500 nm was measured using a portable, non-imaging spectroradiometer (Spectral Evolution PSR+ 3500) with spectral resolutions of 3 nm up to 700 nm, of 8 nm up to 1500 nm, and of 6 nm up to 2100 nm. The field spectrometer was set to 15 internal repetitions, meaning that each spectrum was measured 15 times, in order to reduce measurement variability. A leaf clip holder with a 3 mm sample area, a built-in reflectance standard and a separate 5 W light source (ILM-105) was used to take measurements, while also keeping heat from the light source away from the plant tissue. Heat stress could complicate the selection of relevant wavebands by causing physiological, biochemical or molecular changes in plants that would be represented in spectral reflectance responses and mix with the stress signal caused by myrtle rust infections.

At the plantation, from each of the two untreated and treated rows of trees, leaves from five trees were selected to record spectra at three sampling points: 180, 100 and 50 cm height (Fig. 1b). Plants that appeared disturbed by close proximity to frequently used management trails were avoided. For each sampling point, one terminal shoot was selected and the first two pairs (four leaves) of newly expanding leaves, just large enough to apply the leaf clip accessory, were used to record the spectral responses. The height-stratified sampling points were chosen on both east- and west-facing sides of trees, in order to represent the spectral response of a single tree most effectively. This design resulted in 240 spectra from 240 leaves for each class and 480 spectra in total at the plantation.

Spectra at the botanical garden were collected following the same general procedure as on the plantation (i.e. height stratification; east- and west-sampling). Ten naïve plants located in the Myrtaceae beds of the garden were selected. In total, 240 spectra of 240 naïve leaves were sampled, resulting in an overall dataset of 720 spectra.

Analysis pipeline

After data collection, all analyses were conducted using the R statistical platform (R Core Team, 2016) using several add-on packages (detailed below). For transparency and reproducibility, the full analysis, including figures and tables, can be repeated using code and data archived at https://github.com/ReneHeim/ MyrtleRust-LemonMyrtle-Classification (https://doi.org/10.5281/ zenodo.1142944).

Pre-processing of spectral reflectance signatures

First, all wavelengths below 500 nm were deleted because they contained intense spectral noise. Detection and removal of out- lying spectra followed, using depth measures included in the *FUNCTIONAL DATA ANALYSIS AND UTILITIES (FDA)* package (Febrero-Bande & Oviedo de la Fuente, 2012). After the outliers had been removed the final dataset consisted of 216 observations for the naïve class, 236 for the treated class and 228 for the untreated class (from the original 240 spectra per class). Spectral resampling was used to reduce multicollinearity between predictor variables. This reduced the spectral resolution from 3–8 nm (2151 predictor variables) to a resolution of 10 nm (202 predictor variables). Spectral resampling was carried out using the *PROSPECTR* package (Stevens & Ramirez-Lopez, 2014). Finally, first-order derivatives (FOD) of each spectral signature were calculated. FOD transformations of the spectral curve are a commonly applied technique used to increase classification quality by enhancing spectral features and minimizing random noise (Demetriades-Shah et al., 1990).

Random forest classification

An ensemble machine learning method was used to assign each spectrum to one of the three classes (i.e. naïve, treated, untreated). Ensemble methods reduce variance by providing an outcome that is based on multiple independent classifiers. Here, a random forest classifier (Breiman, 2001) was used. This approach is based on multiple decision trees (Hastie et al., 2009) and is nonparametric, because high-resolution spectral data rarely meet the criteria for standard parametric tests. Several studies, including the original paper by Breiman (2001), have shown that random forest classifiers are a suitable tool for analysing spectral and other high-dimensional, multicollinear data (e.g. Immitzer et al., 2012).

For classification, the *CARET* package (Kuhn et al., 2017) was used. Two parameters are primarily responsible for the performance of a random forest classifier and must be tuned depending on the dataset to be classified. First, the number of randomly selected predictors to choose from at each split (mtry) was optimized. Secondly, the number of trees generated to gain a full ensemble (n-tree) was optimized. The dataset was split 80:20 into training and test data subsets, and a 10- fold repeated cross-validation was applied on the training data. This approach breaks the data into 10 equal-sized fractions: nine of them are used to build/train a tree, and then used to predict the values of the 10th fraction, allowing the user to estimate the training accuracy. This process was repeated 100 times and the mean accuracy over these repetitions was calculated.

By default, the accuracy of the training and validation process was evaluated using the overall accuracy (OA) as a metric. OA reflects the agreement between the reference and predicted classes and has the most direct interpretation. However, it does not provide information about the origin of an error (Kuhn & Johnson, 2013). Here, an additional metric, the kappa statistic (Cohen, 1960) is useful. Kappa can take on values between ?1 and 1; a value of 0 implies no agreement between the observed and predicted classes, while kappa of 1 indicates perfect concordance of the model prediction and the observed classes. Landis & Koch (1977) first defined the following standards for the strength of agreement: kappa of 0 = poor; kappa 0.01–0.20 = slight; 0.21–0.40 = fair; 0.41–0.60 = moderate; 0.61– 0.80 = substantial; and 0.81–1 = almost perfect. In addition to kappa and OA, two further metrics were used that can indicate class-specific errors, the producer accuracy (PA) and user accuracy (UA; Story & Congalton, 1986). PA is the number of correctly classified references for a class divided by the total number of references of that class and, thus, represents the accuracy of the classification for a specific class. UA divides the number of correct classifications (predictions) for a class by the total number of classifications (predictions) for that class. A high UA means that spectra within that class can be reliably classified as belonging to that class. UA is often termed to be a measure of reliability, which can be also interpreted as the agreement between repeated measurements within a class (Jones & Vaughan, 2010).

Finally, all three classes, naïve (216 observations), treated (236 observation) and untreated (228 observations) were classified based on 202 predictor variables (wavebands). The final model parameters were tuned to mtry = 52 and n-tree = 2000 after the best classifier was identified using the training data. Eventually, the test data (20% = 135 spectra) were used to validate the classifier, using kappa, OA, PA and UA as accuracy indices.

Waveband selection

Spectral datasets often contain thousands of predictor variables (wavebands). Using all available wavebands at a time to make a prediction is computationally intensive and problems with multicollinearity are very likely. Waveband selection techniques reduce the predictor space and provide a reduced set of wavebands that can be used in the same efficiency to predict the response variable. Here, a first set of the most important wavebands to classify naïve, untreated and treated trees was identified to provide future studies a starting point for validation or further classification tests. While including the naïve class in the waveband selection might be valuable to distinguish truly healthy trees from infected ones, the waveband selection derived only for the classes untreated and treated may be more relevant for detection systems applied on plantations as naïve plants are unlikely to occur there. Waveband selection was performed using the VSURF package in R (Genuer et al., 2015).

Results

Random forest classification

In order to investigate whether it was possible to spectrally discriminate naïve, treated and untreated lemon myrtle trees, 135 primary spectra (i.e. 20% of the data- set) were analysed. The random forest classifier internally compared the prediction to the known class information of each spectral group, achieving a substantial prediction accuracy according to the scheme of Landis & Koch (1977): kappa = 0.68, OA = 79%. The procedure was repeated using 135 FOD spectra, yielding markedly improved accuracy (kappa = 0.92, OA = 95%). According to Landis & Koch (1977) these accuracies can be considered almost perfect.

When evaluating the accuracy assessment in greater detail (Table 1) it was found that the naïve (N) and treated (T) spectral responses received good PA values (N = 79.1%, T = 87.2%) and UA values (N = 97.1%, T = 75.9%). By contrast, spectral response from untreated (U) trees received a slightly lower PA (U = 68.9%) and UA (U = 67.4%), meaning that this class-specific prediction was less accurate. For the FOD- transformed spectra, all three class-specific accuracies were excellent (UA: N = 100%, T = 90.0%, U = 95.3%; PA: N = 97.7%, T = 95.7%, U = 91.1%).

Table 1 | Assessment of classification accuracy using (a) primary spectra and (b) first-order derivative-transformed spectra. Diagonals represent correctly classified groups, off-diagonals were misclassified. The lower right cell contains the overall accuracy (no. of correct classified groups⁄total no. of groups (135)). User accuracy and producer accuracy are shown to provide class-specific accuracies. Lemon myrtle trees were in the plantation, treated and untreated with fungicide against myrtle rust, and in the botanical garden unexposed to myrtle rust (naïve).

a	Primary Spectra					
		Reference				
	#Samples	Naïve	Treated	Untreated	**Totals**	**User Accuracy**
Prediction	Naïve	34	0	1	35	97.1%
	Treated	0	41	13	54	75.9%
	Untreated	9	6	31	46	67.4%
	Totals	43	47	45	135	
	Producer Accuracy	79.1%	87.2%	68.9%		78.5%

b	First-Order Derivative Spectra					
		Reference				
	#Samples	Naïve	Treated	Untreated	**Totals**	**User Accuracy**
Prediction	Naïve	42	0	0	42	100.0%
	Treated	1	45	4	50	90.0%
	Untreated	0	2	41	43	95.3%
	Totals	43	47	45	135	
	Producer Accuracy	97.7%	95.7%	91.1%		94.8%

Important wavebands for this classification

Many of the features useful for discriminating all three classes (Table 2a, Fig. 2a, c) were within the shortwave infrared region (SWIR; 1300–2500 nm), and this was true for analyses based on primary spectra or on FOD spectra. Considering other spectral regions, the visible region (VIS; 400–700 nm) was more useful for discriminating primary spectra, and the near-infrared region (NIR; 700–1300 nm) was more useful for discriminating FOD spectra. Figure 2b, d and Table 2b highlight features that were selected when comparing spectra collected only at the plantation. By examining the NIR region (Fig. 2a) and comparing the average spectral sig- nature for naïve and treated, it can be observed that they are more similar to each other than compared to untreated.

Table 2 | Selected features for the spectra collected from myrtle trees at the plantation, treated and untreated with fungicide against myrtle rust, and from myrtle trees at the botanical garden unexposed to myrtle rust (naïve). FOD, first-order derivative; VIS, visible; NIR, near-infrared; SWIR, shortwave infrared.

		a		b	
		Primary Spectra (Naïve, Treated, Untreated)	**Derivative Spectra (Naïve, Treated, Untreated)**	**Primary Spectra (Treated, Untreated)**	**Derivative Spectra (Treated, Untreated)**
Spectral Regions	**VIS**	555, 605, 695, 715	-	545, 555, 715	555, 625
	NIR	725, 735, 755,	795, 815, 825, 915	725, 735, 745	795, 815, 845, 915
	SWIR	1405, 1415, 1425, 1435, 1895, 2025, 2035, 2085, 2095, 2115, 2145, 2165, 2175	1435, 1445, 1455, 1665, 1775, 1805, 1815, 2145, 2225, 2295	1455, 1475, 1485, 2125, 2145, 2175	1645, 1655, 2145, 2225

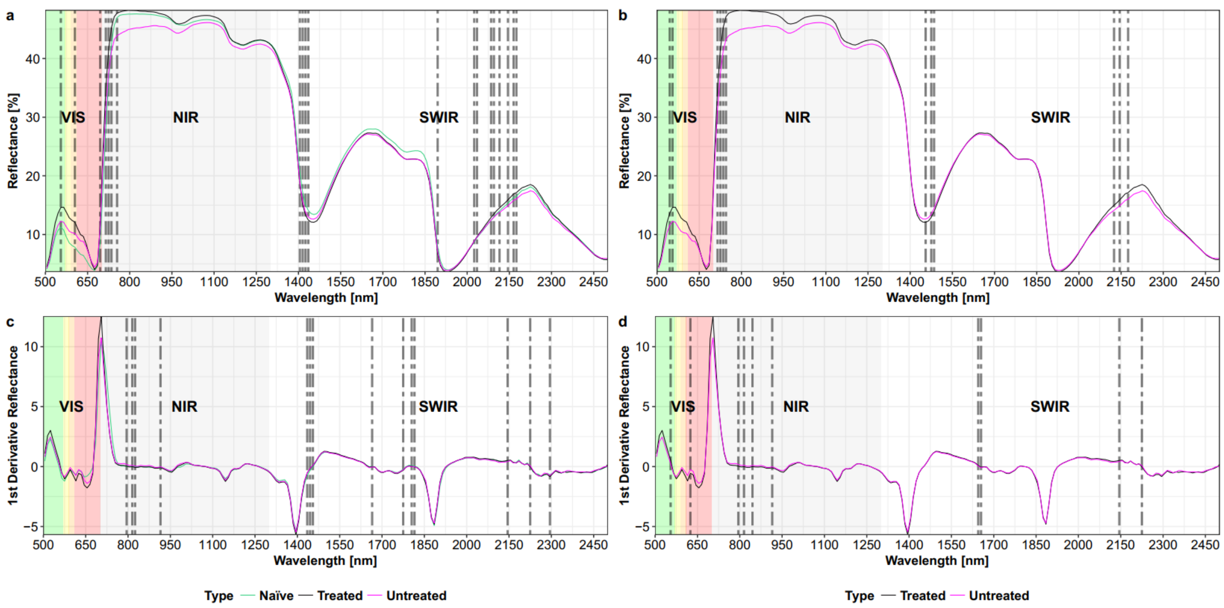

Figure 2 | Spectral signatures and selected features for spectra from lemon myrtle trees collected at the plantation and botanical garden (a, c) and at the plantation only (b, d). Trees at the plantation were either treated or untreated with fungicide to eliminate myrtle rust, whereas trees at the botanical garden were untreated but free from infection (naïve). Important wavebands (grey dashed vertical lines) are presented for primary spectra (a, b) and their first-order derivatives (c, d). All plots emphasize a traditional subsetting of the electromagnetic spectrum to better assign the features to a specific region and support interpretation of each feature. VIS, visible; NIR, near-infrared; SWIR, shortwave infrared.

Discussion

In this study, spectral signatures were compared of lemon myrtle leaves from plants that had not been exposed to *A. psidii* (naïve), from plants that were infected and thus showing myrtle rust symptoms (un- treated), and from plants that had been treated with fungicide and had no obvious symptoms of active myrtle rust (treated). Naïve trees were not available at the plantation, so trees from a botanical garden in a separate region were used. The spectral signatures of naïve trees were expected to be more similar to those from treated plants than to untreated plants, and indeed this was the case. High NIR (700–1300 nm) reflectance is generally an indicator for cellular integrity (Jensen, 2009). Thus, the similarly high NIR reflectance in naïve and treated plants in the present study suggest that *A. psidii* was not present (or at least had not caused damage) in fungicide- treated plants; if it had been present, it would have caused damage in mesophyll cells (Morin et al., 2014) and would have been detected in the NIR region. All three groups were correctly classified, either using primary spectral signatures (kappa = 0.68, OA = 79%), or, with far higher accuracy, using FOD spectra (kappa = 0.92, OA = 95%).

It was not surprising that the FOD spectra performed better than primary spectral signatures, as FOD spectra are in general better at resolving overlapping wavebands and at reducing random noise (Demetriades-Shah et al., 1990). Better performance of FOD than primary spectra was also reported by Mutanga et al. (2004) in a study focusing on biochemical indices of pasture quality in five grass species. However, this is not the case in every study. In a detailed investigation of spectral classification techniques, Ghiyamat et al. (2013) showed that FOD- based approaches showed least improvement (over primary spectra) in very complex datasets, and most improvement in less complex datasets, but also that some classification methods (e.g. Euclidean distance and Jeffreys–Matusita distance) typically performed better than others. Here, it was found that classification accuracy was increased when using a random forest classifier combined with FOD spectra. Classification accuracy using primary spectra and a random forest classifier could still be considered as substantial. Taken together with results from other studies, it seems that both the choice of classification method and the number of classes included in the classification influence whether FOD spectra improve classification accuracy.

In another step in the present study, the number of wavebands was reduced from 2151 to 202 to avoid effects of multicollinearity; nevertheless, high classification accuracies were still achieved. Therefore, it is reason- able to assume that, as in other spectral datasets, some wavebands contained redundant information (Thenkabail et al., 2011). In addition, to avoid multicollinearity, reducing the number of wavebands can have multiple positive effects, for example (i) reducing long computation times, (ii) identifying critical wavebands specific to host and pathogen, (iii) using these wavebands as input parameters to improve classifiers, or (iv) to design dis- ease-specific vegetation indices based on such a refined set of wavebands (Thenkabail et al., 2011). For the pathosystem in the present investigation (lemon myrtle–myrtle rust), a preliminary set of wavebands was identified that had higher relevance over other wavebands used in this study.

Wavebands in the visible (VIS, 400–700 nm) and near- infrared (NIR, 700–1300 nm) regions were most important for distinguishing the three infection groups. The visible domain (556–660 nm) often corresponds to necrotic or chlorotic lesions, and a reduction in chlorophyll activity, while the red-edge (685–715 nm) can be used to detect general symptoms of plant stress (Delalieux et al., 2007). Some wavebands in the shortwave infrared region (SWIR; 1300–2500 nm) were also found to be important. Variation in this region has been linked to changes in water content caused by air humidity or water loss from lesions (Delalieux et al., 2007). In the present study, many lesions were observed on untreated (infected) leaves, very few, and probably old, on treated leaves, and none on naïve leaves. The few lesions found on the naïve leaves were probably caused by other biotic or abiotic factors. These observations provide a possible explanation why the waveband selection resulted in wavebands within the SWIR regions. Consequently, results of this study echoed those of Delalieux et al. (2007), not only in the high classification accuracies (80%) but also in finding similar wavebands important for plant disease detection.

The refined set of wavebands listed in the present study are a first indication of which wavebands might be unique for this pathosystem but, without further refinement, they cannot be confidently distinguished from general indicators of stress caused by fungal pathogens.

There is increasing demand in precision agriculture for differentiation between pathogen-related effects and other stress-inducing factors (Mahlein, 2016). For example, it may be necessary to refine spectral sets of data down to some level where single wavebands can be considered unique for the system under investigation. Amongst the important regions found in the present study, that could be related to those found by Delalieux et al. (2007), the wavebands 545, 555, 625, 745, 755 and 845 nm were also considered by Bravo et al. (2003) to be important for successfully classifying spectral signatures from healthy and yellow rust (*P. striiformis*) infected wheat plants. Bravo et al. (2003) were limited to using wavebands between 460 and 900 nm but could still achieve classification accuracies of 96% using four wavebands only (543, 630, 750 and 861 nm). As yellow rust is a closely related family to A. psidii and the wave- bands found in the present investigation are in close proximity to those found by Bravo et al. (2003), it seems reasonable to suggest that some of the selected wave- bands might be unique for the lemon myrtle–myrtle rust pathosystem. Further investigation would be needed to confirm or disprove this suggestion.

The successful discrimination between spectral signatures is only the first step towards using spectral approaches to detect and monitor myrtle rust in the lemon myrtle industry. A promising next step would be the development of a disease-specific vegetation index (Mahlein et al., 2013). Such indices allow land managers a straightforward disease assessment by indicating, for example, the level of infection. In theory, a disease- specific spectral index for lemon myrtle–myrtle rust pathosystem could be developed by refining the provided set of wavebands. Sensor systems based on those specifications could be built and used in a plantation setting, mounted on terrestrial or aerial vehicles, to detect infection hotspots and enable targeted fungicide application. This would reduce the costs spent on fungicides, the human-caused interassessor bias and also damage caused by fungicides on vegetation in close proximity to the crop of interest.

Austropuccinia psidii, has not previously been subject to investigations using spectral sensor systems. The results of the present study represent a proof-of-concept for incorporating a spectral approach into a precision farming tool used for the lemon myrtle industry as well as other industries. The establishment of spectral libraries of specific plant–pathogen interactions could enable land managers to detect pathogens before symptoms are visible to the naked eye, accurately track the spread of infection, objectively quantify disease severity and differentiate pathogen-related effects from other stress- inducing factors.

Acknowledgements

The authors thank Gary Mazzorana from Australian Rainforest Products for access to his plantation, and the Australian Botanic Garden at Mount Annan for access to their gardens. Anne-Katrin Mahlein, Pablo J. Zarco-Tejada and Andrew Allen gave invaluable advice on various aspects of this study. R.H.J.H. was supported by a Macquarie University Research Excellence Scholarship. Special thanks are given to Michelle Leishman for suggesting the application of a spectral approach to investigating myrtle rust. The authors declare no conflict of interest.

References

Alfenas AC, Zauza EAV, Assis TF, 2003. First record of *Puccinia psidii* on *Eucalyptus globulus* and *E. viminalis* in Brazil. *Australasian Plant Pathology* **32**, 325–6.

Australian Government Bureau of Meteorology, 2017. Climate data online. [http://www.bom.gov.au/climate/data/index.shtml?bookmark= 200]. Accessed 17 August 2017.

Berthon K, Esperon-Rodrigues M, Beaumont L, Carnegie AJ, Leishman L, 2018. Assessment and prioritisation of plant species at risk from myrtle rust (*Austropuccinia psidii*) under current and future climates in Australia. *Biological Conservation* 218, 247–53.

Bhattacharya S, 2017. Deadly new wheat disease threatens Europe's crops. *Nature* **542**, 145–6.

Bravo C, Moshou D, West J, McCartney A, Ramon H, 2003. Early disease detection in wheat fields using spectral reflectance. *Biosystems Engineering* **84**, 137–45.

Breiman L, 2001. Random forests. *Machine Learning* **45**,5–32.

Carnegie AJ, Lidbetter JR, Walker J et al., 2010. *Uredo rangelii*, a taxon in the guava rust complex, newly recorded on Myrtaceae in Australia. *Australasian Plant Pathology* **39**, 463–6.

Carnegie AJ, Kathuria A, Pegg GS, Entwistle P, Nagel M, Giblin FR, 2016. Impact of the invasive rust *Puccinia psidii* (myrtle rust) on native Myrtaceae in natural ecosystems in Australia. *Biological Invasions* **18**, 127–44.

Cohen J, 1960. A coefficient of agreement for nominal scales. *Educational and Psychological Measurement* **20**,37–46.

Coutinho TA, Wingfield MJ, Alfenas AC, Crous PW, 1998. Eucalyptus rust: a disease with the potential for serious international implications. *Plant Disease* **82**, 819–825.

Delalieux S, van Aardt J, Keulemans W, Coppin P, 2007. Detection of biotic stress (*Venturia inaequalis*) in apple trees using hyperspectral data: non-parametric statistical approaches and physiological implications. *European Journal of Agronomy* **27**, 130–43.

Demetriades-Shah TH, Steven MD, Clark JA, 1990. High resolution derivative spectra in remote sensing. *Remote Sensing of Environment* **33**,55–64.

Doran J, Lea D, Bush D, 2012. *Assessing Myrtle Rust in a Lemon Myrtle Provenance Trial*. Barton, ACT, Australia: Rural Industries Research and Development Corporation.

Febrero-Bande M, Oviedo de la Fuente M, 2012. Statistical computing in functional data analysis: The R package FDA.USC. *Journal of Statistical Software* **51**,1–28.

Genuer R, Poggi J-M, Tuleau-Malot C, 2015. VSURF: An R package for variable selection using random forests. *The R Journal* **7**,19–33.

Ghiyamat A, Shafri HZM, Amouzad Mahdiraji G, Shariff ARM, Mansor S, 2013. Hyperspectral discrimination of tree species with different classifications using single- and multiple-endmember. *International Journal of Applied Earth Observation and Geoinformation* **23**,177–91.

Giblin F, 2013. *Myrtle rust report: New Caledonia Assessment of myrtle rust situation in New Caledonia*. Maroochydore, QLD, Australia: University of the Sunshine Coast.

Hastie T, Tibshirani R, Friedman J, 2009. *The Elements of Statistical Learning: Data Mining, Inference, and Prediction*. Berlin, Germany: Springer Science & Business Media.

Helfer S, 2014. Rust fungi and global change. *New Phytologist* **201**, 770–780.

Immitzer M, Atzberger C, Koukal T, 2012. Tree species classification with random forest using very high spatial resolution 8-band Worldview-2 satellite data. *Remote Sensing* **4**, 2661–2693.

Jensen JR, 2009. *Remote Sensing of the Environment: An Earth Resource Perspective*. New Delhi, India: Pearson Education India.

Jones HG, Vaughan RA, 2010. *Remote Sensing of Vegetation: Principles, Techniques, and Applications*. Oxford, UK: Oxford University Press.

Kuhn M, Johnson K, 2013. *Applied Predictive Modelling*. New York, NY, USA: Springer.

Kuhn M, Wing J, Weston S et al., 2017. CARET: Classification and regression training. R package version 6.0-76. [https://CRAN.R-projec t.org/package=caret.]. Accessed 9 January 2018.

Landis JR, Koch GG, 1977. The measurement of observer agreement for categorical data. *Biometrics* **33**, 159–174.

Loope L, 2010. *A Summary of Information on the Rust Puccinia psidii Winter (Guava Rust) with Emphasis on Means to Prevent Introduction of Additional Strains to Hawaii. Open-File Report 2010–1082*. Reston, Virginia, USA: US Geological Survey.

Machado P, Alfenas AC, Alfenas RF, Mohammed CL, Glen M, 2015. Microsatellite analysis indicates that *Puccinia psidii* in Australia is mutating but not recombining. *Australasian Plant Pathology* **44**, 455–462.

Mahlein AK, 2016. Plant disease detection by imaging sensors – parallels and specific demands for precision agriculture and plant phenotyping. *Plant Disease* **100**, 241–251.

Mahlein AK, Steiner U, Dehne H-W, Oerke E-C, 2010. Spectral signatures of sugar beet leaves for the detection and differentiation of diseases. *Precision Agriculture* **11**, 413–431.

Mahlein AK, Rumpf T, Welke P et al., 2013. Development of spectral indices for detecting and identifying plant diseases. *Remote Sensing of Environment* **128**, 21–30.

Makinson B, 2014. Myrtle rust – what's happening? *Australasian Plant Conservation* **23**,13–15.

McTaggart AR, Roux J, Granados GM et al., 2016. Rust (*Puccinia psidii*) recorded in Indonesia poses a threat to forests and forestry in South-East Asia. *Australasian Plant Pathology* **45**, 83–89.

Morin L, Talbot MJ, Glen M, 2014. Quest to elucidate the life cycle of *Puccinia psidii* sensu lato. *Fungal Biology* **118**, 253–263.

Mutanga O, Skidmore A, Prins HH, 2004. Predicting in situ pasture quality in the Kruger National Park, South Africa, using continuum- removed absorption features. *Remote Sensing of Environment* **89**, 393–408.

NSW Scientific Committee, 2011. *Introduction and Establishment of Exotic Rust Fungi of the Order Pucciniales Pathogenic on Plants of the Family Myrtaceae – Key Threatening Process Listing*. Sydney, NSW, Australia: Office of Environment and Heritage.

Pegg GS, Brawner JT, Lee DJ, 2014. Screening *Corymbia* populations for resistance to *Puccinia psidii*. *Plant Pathology* **63**, 425–436.

du Plessis E, McTaggart AR, Granados GM et al., 2017. First report of myrtle rust caused by *Austropuccinia psidii* on *Rhodomyrtus tomentosa* (Myrtaceae) from Singapore. *Plant Disease* **101**, 1676.

Potts BM, Sandhu KS, Wardlaw T et al., 2016. Evolutionary history shapes the susceptibility of an island tree flora to an exotic pathogen. *Forest Ecology and Management* **368**, 183–193.

R Core Team, 2016. *R: A Language and Environment for Statistical Computing*. Vienna, Austria: R Foundation for Statistical Computing.

Roux J, Greyling I, Coutinho TA, Verleur M, Wingfield MJ, 2013. The myrtle rust pathogen, *Puccinia psidii*, discovered in Africa. *IMA Fungus* **4**, 155–159.

Rural Industries Research and Development Corporation, 2012. *Lemon Myrtle.* RIRDC Publication No. 12/066. Canberra, ACT, Australia: Australian Native Food Industry Stocktake, RIRDC.

Soewarto J, Carriconde F, Hugot N, Bocs S, Hamelin C, Maggia L, 2017. Impact of *Austropuccinia psidii* in New Caledonia, a biodiversity hotspot. *Forest Pathology* **48**, e12402.

Stevens A, Ramirez-Lopez L, 2014. An introduction to the PROSPECTR package. R Package Vignette, Report No. 3, R Package version 0.1. [https://cran.r-project.org/web/packages/prospectr/vignettes/ prospectr-intro.pdf.] Accessed 9 January 2018.

Story M, Congalton R, 1986. Accuracy assessment – a user's perspective. *Photogrammetric Engineering and Remote Sensing* **52**, 397–399.

Thenkabail PS, Lyon GJ, Huete A, 2011. *Hyperspectral Remote Sensing of Vegetation*. Boca Raton, FL, USA: CRC Press.

This page is intentionally left blank.

This page is intentionally left blank.

CHAPTER III

Developing a spectral disease index for myrtle rust (*Austropuccinia psidii*)

RHJ Heim • IJ Wright • AP Allen, I Geedicke • J. Oldeland
Published in: *Plant Pathology* doi: pending

Abstract

Since 2010 Australian ecosystems and managed landscapes have been severely threatened by the invasive fungal pathogen, Austropuccinia psidii. Detecting and monitoring disease outbreaks is currently only possible by human assessors, which is slow and labour intensive. Over the last 25 years, spectral vegetation indices (SVIs) have been designed to assess variation in biochemical or biophysical traits of vegetation. However, diagnosis of individual diseases based on classical SVIs is currently not possible since they lack disease specificity. We develop a novel spectral disease index (SDI), the lemon myrtle-myrtle rust index (LMMR). The index was designed from hyperspectral leaf-clip data collected at a lemon myrtle plantation in New South Wales, Australia. We sampled 236 fungicide-treated (disease free) and 228 untreated (diseased) lemon myrtle leaves and used a random forest classifier to show that the LMMR discriminates those classes with an overall accuracy of 90%. Compared to three classical SVIs (PRI, MCARI, NBNDVI), commonly applied for stress detection, the LMMR clearly improved classification accuracies (58%, 67%, 60%, respectively). If the LMMR can be validated on independent datasets from similar and different host-species, it could enable land managers to reduce disease impact by earlier control. There also might be potential to collect useful data for epidemiology models. Calculating the LMMR based on hyperspectral data collected from aerial platforms (e.g. drones) would allow for rapid and high capacity screening for disease outbreaks.

Introduction

Plant pathogens, such as rust fungi, play a versatile role in ecology and economy. They affect community dynamics and diversification through co-evolution with their host plants (Helfer, 2014) but also cause extensive damage to agricultural and forestry crops. This was recently demonstrated by a new, highly virulent strain of *Puccinia graminis,* a rust fungus, that destroyed tens of thousands of hectares of wheat crops in southern Europe (Bhattacharya, 2017). Here we focus on the rust fungus *Austropuccinia psidii* (Sphaerophragmiaceae, Pucciniales), an obligate biotrophic plant pathogen in the highly diverse phylum Basidiomycota (Beenken, 2017). In Australia, *A. psidii* is invasive and causes a disease, commonly known as "myrtle rust" that exclusively affects one of Australia's dominant plant families, the Myrtaceae (Carnegie & Pegg, 2018). In contrast to other rust diseases, which are mostly restricted to few host species, myrtle rust infects hundreds of species, escalating the potential consequences for Australia's natural landscapes (Carnegie & Pegg, 2018). Australian native species have already been severely damaged by myrtle rust in the wild (Carnegie & Pegg, 2018).

Industries that rely on species within the Myrtaceae, such as the nursery and garden industry, have also been affected by myrtle rust through losses of commercial varieties, trade restrictions, and increased dependency on fungicides (Carnegie & Pegg, 2018). In Australia, the expanding lemon myrtle (*Backhousia citriodora*) industry has been particularly affected, as cultivars of *B. citriodora* currently in use are moderately to highly susceptible to myrtle rust (Doran *et al.*, 2012). Leaves of lemon myrtle are commercially harvested to produce lemon-flavoured herbal teas, culinary herbs, and lemon-scented essential oils used for food flavouring and personal care products (Clarke, 2012). The farm gate value of this market has been estimated to be between 7-23 million AUD annually (Clarke, 2012). Rust-affected leaves of *B. citriodora* are unsuitable for use and cause yield losses up to 70%. The application of fungicides to control the disease is undesirable as the market demands a clean, organic product (Carnegie & Pegg, 2018). Therefore, the industries reliant on lemon myrtle are in urgent need of rust-resistant cultivars or measures to reduce the use of fungicides.

The detection of myrtle rust symptoms and those of other pathogens has traditionally relied on human, visual assessment. However, human assessment is somewhat subjective such as the assessor’s individual experience and the visual cues humans use, vary through time within individuals (Bock *et al.*, 2010). Automated methods using optical remote sensing have the potential to detect diseases with greater sensitivity, specificity and reliability than what is possible by humans using visual estimation (Mahlein, 2016).

Over the last 30 years, the field of ‘precision agriculture’ adopted optical remote sensing to optimize all production-related materials such as fertilizers and agro-chemicals (Mulla, 2013). A sub-field in precision agriculture is efficient disease detection and management. Acquiring disease-related spectral data is information-intense and often requires a reduction to the most relevant wavebands to reflect the pathosystem under investigation (Stafford, 2000). In many cases, the visual region (VIS, 400 nm – 700 nm) has been found most useful for indicating visible disease symptoms (e.g., discolorations), while the near-infrared region (NIR, 700 nm – 1300 nm) has indicated changes in structural leaf traits (Jacquemoud & Ustin, 2001; Mulla, 2013). Parallel to the progress in precision agriculture, spectral vegetation indices (SVIs) have been developed to simplify the prediction of biochemical, structural or physiological changes in plants. For instance, the photochemical reflectance index (PRI) was developed as an indicator for the efficiency of carbon fixation using photosynthetic radiation (Gamon *et al.*, 1997). Ashourloo et al. (2014) evaluated the effect of wheat rust symptoms on a set of SVIs (e.g. NDVI, NBNDVI and PRI) and they were found to be effective when disease severity was high while being less effective in discriminating different symptoms. Mahlein and colleagues (2013) already stated a year earlier that SVIs would not be suitable for disease detection as they were originally designed for other purposes. Therefore, they developed spectral disease indices (SDIs) that could successfully discriminate among different sugar beet diseases.

The primary aim of the presented study was to develop a SDI for myrtle rust detection on lemon myrtle plants (*Backhousia citriodora*). We base our analyses on data recorded on a myrtle rust infested plantation, also used in a previous study (Heim *et al.*, 2018). In that previous work we showed that fungicide treated and untreated *B. citriodora* leaves could be classified with high accuracy based on a broad set of 202 wavebands (i.e. predictor variables). In the presented study, we first refined these 202 wavebands to provide the minimum number of wavebands required to accurately classify the two classes (treated/untreated). Next, by using the refined wavebands, we designed the SDI. Finally, we compared the classification accuracy of our SDI to that of three SVIs widely used in plant disease detection. An additional aim was to provide the first coded framework presented in the *R* statistical programming environment (R Core Team, 2017) for developing SDIs.

Methods

Data collection

Leaf spectral data were collected on a lemon myrtle (*Backhousia citriodora*) plantation in northern New South Wales, Australia (28.6911090 S, 153.295480 E). For more information refer to Heim et al. (2018). A proportion of trees had been treated with fungicide to control *A. psidii,* while a proportion was untreated and thus diseased. Measurements were made on leaves affected by *A. psidii* (untreated leaves; Fig. 1 B, C, D) and on leaves that had been treated with fungicides and therefore showed negligible signs of *A. psidii* infection (Fig. 1 A). Leaves from untreated trees had varying levels of disease, including small purple spots through to large necrotic lesions and yellow pustules. Leaves from treated trees showed mostly no signs of *A. psidii* infection, although some had small purple spots, likely due to infection occurring prior to fungicide application, with fungicide that have been shown effective and halting the infection process (Horwood *et al.*, 2013). We exclude the influence of other biotic agents as no other serious pathogen on lemon myrtle was known prior to *A. psidii* (Dr Angus Carnegie and Gary Mazzorana, pers. comm.). Spectral reflectance signatures between 350 nm and 2500 nm were recorded with a portable non-imaging spectroradiometer (Spectral Evolution PSR+ 3500) with a spectral resolution of 3 nm steps between 450 nm and 700 nm, 8 nm steps between 700 nm and 1500 nm and 6 nm steps between 1500 nm and 2100 nm. Measurements were made from the adaxial leaf surface using a leaf clip holder with a 3-mm sample area, a built-in reflectance standard and a separate 5-watt light source (ILM-105; please see supp. material for illumination spectrum). We measured 236 fungicide-treated and 228 untreated lemon myrtle leaf samples, with three leaves sampled per tree (n=464). Further details on sampling design were given by Heim et al*.* (2018).

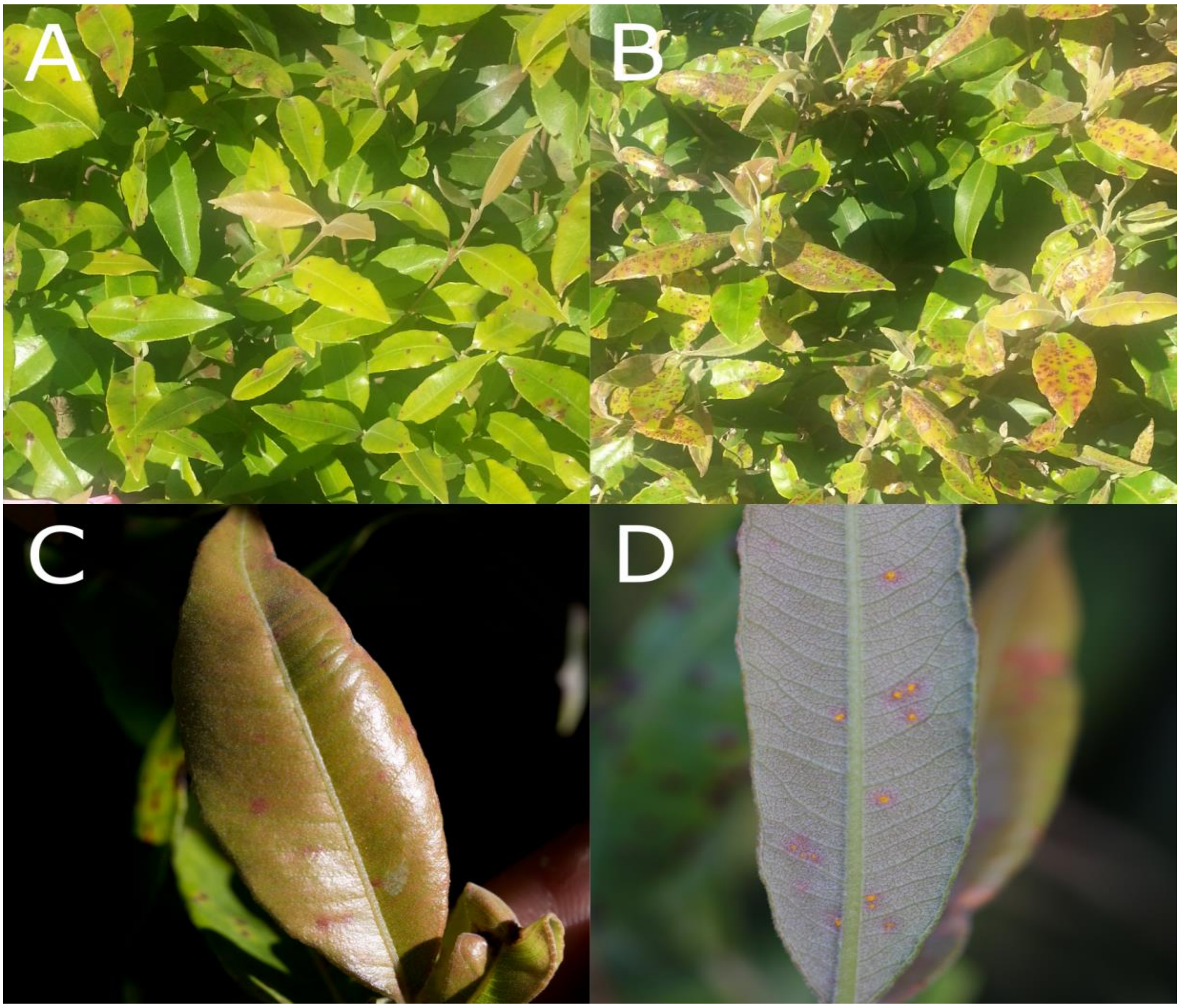

Figure 1 | Fungicide treated (A) and untreated (B, C, D) *Backhousia citriodora* leaves that have been assessed at a lemon myrtle plantation in New South Wales, Australia. Fungicide treated trees were free of active disease but could show stray, necrotic lesions or purple spots, likely due to infection occurring prior to fungicide application. Leaves that were not treated, were largely covered with dark necrotic lesions, purple lesions and yellow spores (D) as A. psidii was not contained (B). Images: Ina Geedicke

Data preparation

The original dataset (Heim et al., 2018) contained 2151 spectral wavebands (i.e. predictor variables), thus more predictor variables than observations, a situation referred to as 'high dimensionality' (Hastie *et al.*, 2009). High-dimensional data can contain unknown groups of highly correlated predictors (Genuer *et al.*, 2015). Correlated predictor variables may lead to inaccurate selection of relevant wavebands. To counter this, we used spectral resampling. This reduced the original spectral resolution of 3 nm – 8 nm (2151 wavebands) to a resolution of 10 nm (202 wavebands; Heim et al., 2018). The spectral data used in this study is no longer high-dimensional (Mahlein *et al.*, 2013) and still contains 464 spectral reflectance profiles, including 236 fungicide-treated and 228 untreated lemon myrtle leaves.

All analyses were conducted using the R statistical platform (R Core Team, 2017). The full analysis (Fig. 2) can be reproduced using code and data archived at https://reneheim.github.io/RustIndex/ (doi to be provided on acceptance). The provided code has potential to serve as a framework to develop SDIs for other host-pathogen combinations.

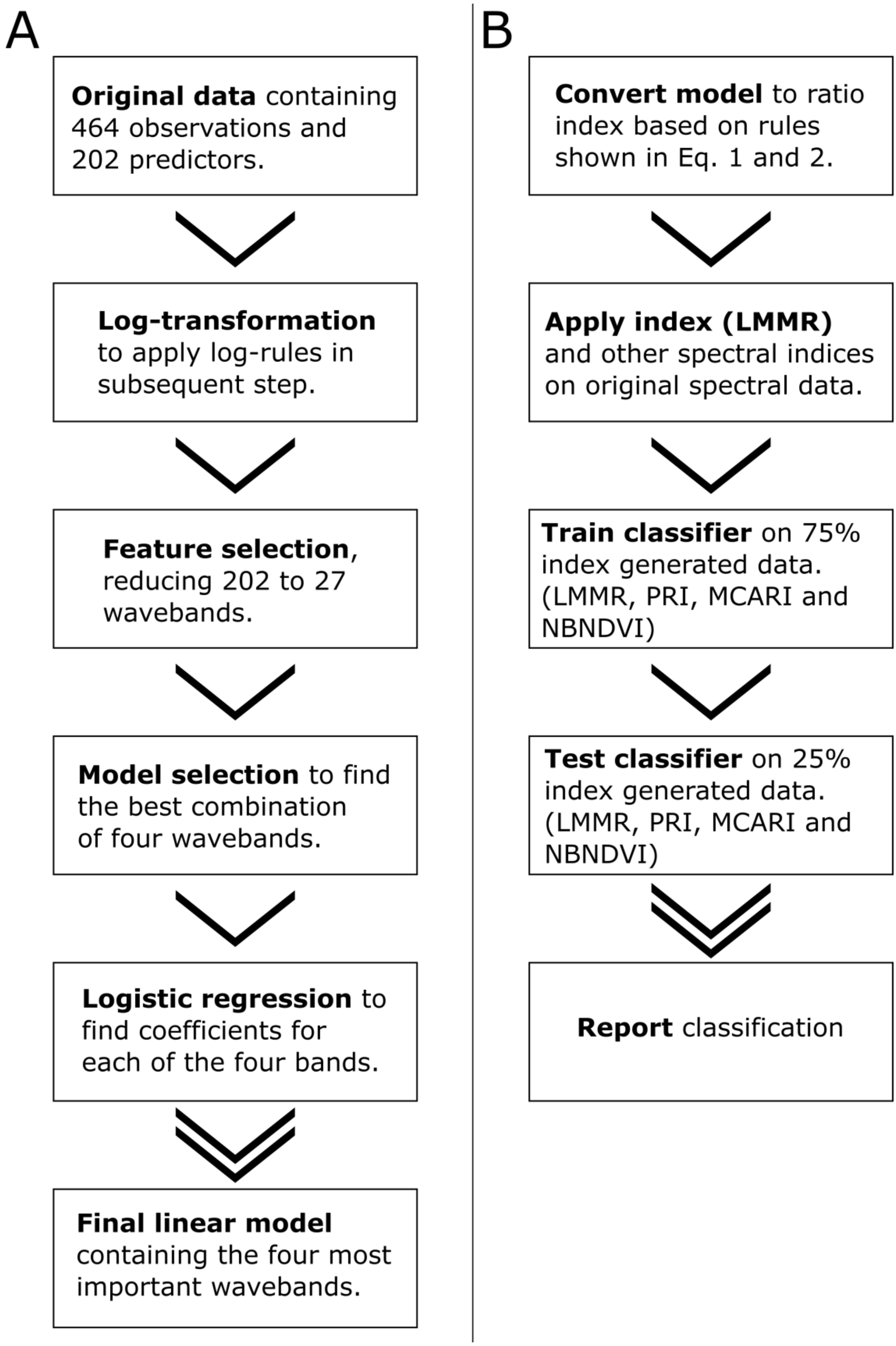

Figure 2 | Workflow summarizing each step from original raw data to the final classification report. A) This section produces the linear, parsimonious model including the four most relevant wavebands and their coefficients. B) This section takes the parsimonious model from A) which is transformed and simplified to yield the new spectral index specific to the pathosystem lemon myrtle/myrtle rust (LMMR). The performance of the LMMR, to discriminate treated and untreated lemon myrtle trees, is compared against common spectral vegetation indices PRI, MCARI and NBNDVI.

Raw data to linear model

Spectral vegetation indices commonly use two to four wavebands, and ratios thereof (Mahlein et al., 2013). Similarly, we decided to reduce our 202 wavebands to four wavebands, allowing us to design an easily interpretable index in the form of SVIs like the NBNDVI (Eqn 7; Thenkabail *et al.*, 2000).

To create ratio indices from linear models, as we attempted to do, we log-transformed the original reflectance data yielding logged reflectance values (i.e., log(B1)). By introducing a log-term into a linear equation, the following basic algebra rules (Eqn 1 and 2) apply and ratios and products of reflectance adhere to:

Eqn 1

$$\log(B1^a * B2^b) = a * \log(B1) + b * \log(B2)$$

Eqn 2

$$\log(\frac{B1^a}{B2^b}) = a * \log(B1) - b * \log(B2)$$

Before these rules became relevant, we applied a random-forest-based feature selection on our original data (following Fig. 2A), repeating it ten times to account for variability in the selection process. This resulted in a set of 27 wavebands which retained predictive power while avoiding redundancy. Here, the R package *'VSURF'* (Genuer et al., 2015) was used, as it is suitable for regular and high-dimensional data. This was necessary because the computational effort of a direct exhaustive model selection, as applied in the following, would have been too high and time-consuming using 202 predictor variables. This refined set of twelve wavebands was submitted as a candidate set of predictor variables to an exhaustive model search using a binominal generalized linear model. This allowed us to identify a linear model containing the four most relevant wavebands to discriminate our binary response (treated and untreated). The best model was indicated by the small-sample-corrected Akaike Information Criterion (AIC_c).

At this stage, we had to include an intermediate step to compute the coefficients for our best model as wavelength (parameters) were provided without the corresponding numerical coefficients. By submitting the linear combination of the best four wavebands (e.g., Response~1+Band545+Band555+Band1505+Band2195) from the previous step to another binominal generalized linear model, we yielded the required model coefficients (Eqn 3).

Linear model to classification report

The best four parameters including their coefficients from the above described binominal generalized linear model characterized the predicted probability, *p*, that a given leaf was infected (Eqn 3). As mentioned in the beginning, the model (Eqn 3) contains log-transformed reflectance values to make use of the algebraic rules (Eqn 1 and 2).

Eqn 3

$$\log\left(\frac{p}{1-p}\right) = 18.39 + 75.38 * \log(B545) - 78.81 * \log(B555) + 45.99 * \log(B1505) - 46.83 * \log(B2195)$$

Wavelengths 545 nm and 555 nm straddle the VIS spectrum; 1485 nm and 2195 nm are both in the short-wavelength infrared (SWIR) spectrum. In our model (Eqn 3) the coefficients for log(*B545*) and log(*B555*) are of approximately equal magnitude and opposite in sign, as are the coefficients for log(*B1505*) and log(*B2195*). This observation also indicates that both pairs of variables can be treated as ratios for the construction of our specific disease index and is further supported by overlapping 95% confidence intervals found during the analysis (95% CI B545 [57.01, 96.09], B555 [99.93, 60.08], B1505 [37.32, 56.03], B2195 [57.07, 38.05]). The magnitudes of the coefficients for log(*B545*) and log(*B555*) are approximately 1.66-times greater than those for log(*B1505*) and log(*B2195*). Thus, to transpose Equation 3 into the form of a ratio SDI, giving our Lemon Myrtle –Myrtle Rust index (LMMR; Eqn 6), we applied the following steps (see also Fig. 2):

1. Summarise coefficients of approximately equal magnitude and opposite in sign.

Eqn 4

$$\log(\frac{p}{1-p}) = 18.39 + 76.50 * \log(\frac{B545}{B555}) + 46.50 * \log(\frac{B1505}{B2195})$$

2. Drop constant coefficient (18.387 = const.) and transpose further ($\frac{76.5}{46.5} \approx \frac{5}{3}$).

Eqn 5

$$\log(\frac{p}{1-p}) = \frac{5}{3} * \log\left(\frac{B545}{B555}\right) + \log(\frac{B1505}{B2195})$$

3. Take exponential of both sides.

Eqn 6

$$\frac{p}{1-p} = (\frac{B545}{B555})^{\frac{5}{3}} * \frac{B1505}{B2195} = LMMR$$

To assess the performance of our LMMR (Eqn 6) we compared its accuracy to discriminate untreated and treated lemon myrtle leaves to the accuracy of spectral vegetation indices commonly applied to detect plant pathogens (Ashourloo et al., 2014; Mahlein et al., 2013). We selected these indices according to the biological processes they indicate and whether these processes could be linked with physiological changes caused by myrtle rust. For example, urediniospores of rust fungi contain carotenoids and melanin-like pigments, hence their brown-orange-yellow colour (Mahlein et al., 2013). Changes in plant pigments can be detected, amongst others, by applying either the photochemical reflectance index (PRI; Eqn 7; Gamon *et al.*, 1997) or the modified chlorophyll absorption in reflectance index (MCARI; Eqn 8; Daughtry, 2000). Also, the structural integrity of the mesophyll cells is reduced when hyphae of *A. psidii* enter this cell layer (Morin *et al.*, 2014). Processes that interfere with the cellular integrity, and therefore cause stress, are usually reflected in the near-infrared region (Peñuelas & Filella, 1998). Therefore, the narrow-band normalized difference vegetation index (NBNDVI; Eqn 9, Thenkabail *et al.*, 2000), could mirror this variation as it measures the ratio between the near-infrared and visual region.

Eqn 7

$$PRI = \frac{B531 - B570}{B531 + B570}$$

Eqn 8

$$MCARI = \left((B700 - B670) - 0.2 * (B700 - B550)\right) * \left(\frac{B700}{B670}\right)$$

Eqn 9

$$NBNDVI = \frac{B850 - B680}{B850 + B680}$$

We calculated values for each index from our original reflectance data and yielded a new dataset (n=464) containing two response classes (treated and untreated) and four predictor variables (PRI, MCARI, NBNDVI and LMMR). This data was randomly split (75/25) into a training set (n=348) and a test set (n=116). As the LMMR was developed on the log-scale, it should only receive log-transformed data when compared to other indices.

A logistic regression classifier was used to evaluate which index was the most accurate predictor variable for our classification problem. To increase model accuracy data were resampled (drawing random samples with replacement) using the '.632+ bootstrap' method (Efron & Tibshirani, 1997); this approach estimates prediction error with less variability than cross-validation (Efron and Tibshirani,1997). The training models of all four indices were used to predict the probability, using a threshold of 0.5, that a leaf/tree in the test data was either fungicide treated or untreated. The test dataset was not seen by the classifier before and could therefore be used to validate the models. To evaluate the prediction performance, we produced an error matrix containing the following metrics: overall accuracy (OA), producer accuracy (PA) and user accuracy (UA).

By default, the accuracy of the training and testing process was evaluated using OA as a metric. OA reflects the agreement between the reference and predicted classes and has the most direct interpretation. However, it does not provide information about the origin of an error (Kuhn & Johnson, 2013). Here, PA and UA can indicate class-specific errors (Congalton & Green, 2009). PA is the number of correctly classified references for a class divided by the total number of references of that class and, thus, represents the accuracy of the classification for a specific class. UA divides the number of correct classifications (predictions) for a class by the total number of classifications (predictions) for that class. A high UA means that spectra within that class can be reliably classified as belonging to that class. User accuracy is often termed to be a measure of reliability, which can be also interpreted as the agreement between repeated measurements within a class.

Results

We selected the four most import spectral wavebands, 545 nm, 555 nm, 1505 nm and 2195 nm, (Fig. 3E - vertical, dashed lines) from a dataset originally containing 202 wavebands for each spectral signature. The binominal generalized linear model containing these wavebands as parameters was more successful in predicting whether a lemon myrtle tree was treated with fungicides or untreated than models containing other wavebands between 500 nm and 2500 nm. While the wavebands at 545 nm and 555 nm are situated in the visual region (VIS 400 to 700 nm) of the electromagnetic spectrum, the wavebands at 1505 nm and 2195 nm can be found in the short-wave infrared region (SWIR 1300 to 2500 nm). Based on these wavebands, we derived a new disease-specific spectral index, the LMMR (Eqn 6)

LMMR classification performance

The training process of the classifier was assessed graphically (Figs. 3A-D). The PRI and the MCARI (Figs. 3A, 3B) could discriminate between treated (red circles) and untreated (blue triangles) lemon myrtle trees only marginally (OA; PRI=66.7%, MCARI=66.3%). The NBNDVI (Fig. 3C) does not improve disease detection over random guessing (OA; NBNDVI=52.9%). By contrast, the LMMR (Fig. 3D) could clearly discriminate treated and untreated trees in the training process (OA; LMMR=86.5%).

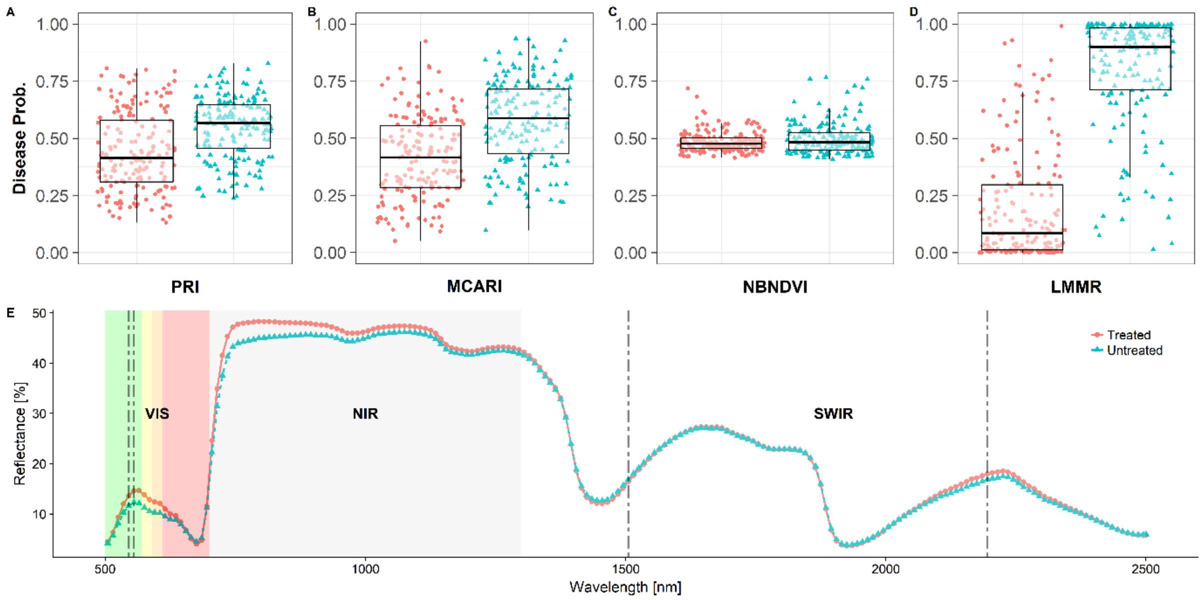

Figure 3 | A-D displays the potential of the applied classifier to discriminate treated (red-circle) and untreated (blue-triangle) lemon myrtle leaves (*Backhousia citriodora*) after the training process. Plot E is showing a classical sub-division of the electromagnetic spectrum (VIS, NIR, SWIR) and the locations of the four most important wavebands to successfully discriminate the spectral signatures.

We isolated 25% of our data before running the training procedure so as to validate the classifier on data not yet seen by the classifier. For the validation, LMMR substantially outperformed other indices in predicting the disease. The LMMR classified untreated and treated trees with an overall accuracy of 90% (Table 1 A-D – lower right cells). Other indices ranged from OA 58% to 67%. Evaluating producer accuracies (PA) and user accuracies (UA), yielded the same overall trend. The MCARI had similar UA (Treated=68%, Untreated=66%) and PA (Treated=66%, Untreated=68%). Also, the UA for both indices (Table 1 A and C), the PRI (Treated=58%, Untreated=58%) and the NBNDVI (Treated=59%, Untreated=63%) are balanced. For the PA, the probability that a certain class found on the plantation is classified as such, it seems that treated trees can be detected slightly better (PRI - Treated=63%, Untreated=53%, NBNDVI - Treated=75%, Untreated=46%). Overall, the LMMR delivers high user accuracies (Treated=89%, Untreated=91%) and high producer accuracies (PA) for both classes (Treated=92%, Untreated=88%).

Table 1 | Accuracy assessment for the logistic regression classification using validation data (116 observations) that was isolated before the training classifier was trained. Classification was performed using the index values derived by applying the indices PRI (A), MCARI (B), NBNDVI (C) and LMMR (D) on spectral reflectance data from fungicide treated (TR) and untreated (UN) lemon myrtle trees. Accuracy can be evaluated comparing the overall accuracy in every lower right corner of each table and user (UA) and producer accuracies (PA). The error matrix is also showing class totals (TOTAL) for the reference columns and prediction rows. The number of correctly classified trees is highlighted in each grey shaded cell.

A) PRI		Reference			UA	**B) MCARI**		Reference			UA
		TR	UN	TOTAL				TR	UN	TOTAL	
Pred	TR	37	27	**64**	58%	Pred	TR	39	18	**57**	68%
	UN	22	30	**52**	58%		UN	20	39	**59**	66%
	TOTAL	**59**	**57**	**116**			TOTAL	**59**	**57**	**116**	
PA		63%	53%		58%	PA		66%	68%		67%
C) NBNDVI		Reference			UA	**D) LMMR**		Reference			UA
		TR	UN	TOTAL				TR	UN	TOTAL	
Pred	TR	44	31	**75**	59%	Pred	TR	54	7	**61**	89%
	UN	15	26	**41**	63%		UN	5	50	**55**	91%
	TOTAL	**59**	**57**	**116**			TOTAL	**59**	**57**	**116**	
PA		75%	46%		60%	PA		92%	88%		90%

Discussion

In this study, we derived a new potential spectral disease index (SDI) that allowed us to detect symptoms caused by the invasive, fungal pathogen *Austropuccinia psidii* on lemon myrtle trees (*Backhousia citriodora*). The LMMR (lemon myrtle – myrtle rust) index discriminated between fungicide treated and untreated lemon myrtle plants with notably higher accuracy (90%) than classical spectral vegetation indices (SVIs; 58%-67%).

The increased classification accuracy was achieved by selecting the four most relevant wavebands from initially 202 wavebands. They are specific to our pathosystem and were able to perform better than indices developed for other situations. We aimed at dropping as many wavebands as possible while sustaining substantial prediction accuracies and were guided by the common principle to use three-band indices at the leaf-scale and four band indices at canopy-scale (Thenkabail *et al.*, 2000).

The waveband selection process resulted in two wavebands (545 nm, 555 nm) with high predictive power for myrtle rust disease in the visible (VIS) region of the electromagnetic spectrum, and two wavebands (1505 nm and 2195 nm) in the short-wave-infrared (SWIR) region. Variation in reflectance in the VIS region between treated and untreated leaves is mainly caused by changing contents of leaf pigments, while reflectance variation in the SWIR region is often influenced by the composition of leaf chemicals and water content (Jacquemoud and Ustin, 2001).

In this study, we found variation in spectral reflectance around 550 nm and it is known that between 510 nm and 550 nm spectral variation is closely related to the total carotenoid pigment content of leaves (Gitelson *et al.*, 2002). Carotenoids are presumably the pigments giving the yellow colour to urediniospores of some rusts (Wang, 2018). On *B. citriodora*, we found yellow pigmented pustules on the adaxial (Figure 4 A-C) and abaxial (Figure 4 D-F) leaf surfaces of infected leaves. It is likely that the same pigments also occur within the leaves, as during the infection and penetration process of *A. psidii*, the orange-yellow pigmented contents are transferred into the leaf by the infection hyphae (Hunt, 1968).

There are no studies describing the exact biochemical composition of *A. psidii* pigments (Dr Robert Park pers. comm.).

Figure 4 | Lemon myrtle (*Backhousia citriodora*) leaves as they were assessed at the plantation in New South Wales, Australia. Images A-C are showing the adaxial leaf surface with yellow urediniospores (*Austropuccinia psidii*) present. Images D-F are showing yellow urediniospores on the abaxial leaf surface. Red discolorations around lesions are visible from both sides. Image G-shows lemon myrtle trees how they occurred on the plantation. Images H-I are showing reddish young leaves with various hue intensities.

We also observed red discolorations around lesions caused by *A. psidii* (Fig. 4 A-F). Anthocyanins are the basis for most orange, pink, red, magenta, purple, blue and blue-black colours in plants (Davies, 2004) and might be responsible for the red colouring around lesions as they are often found at later stages of an infection (Glen *et al.*, 2007). Anthocyanins are water-soluble vacuolar pigments of higher plants that are abundant in juvenile and senescing plants and are represented by a spectral reflectance peak around 550 nm (Gitelson *et al.*, 2007). Thus, anthocyanins might be responsible for the observed spectral shift around 550 nm.

That said, we observed red discolorations on young leaves (Fig. 4 G-I) of *B. citriodora* plants, and this might be regarded as a confounding factor. However, red young leaves were present on treated as well as on untreated plants. As the spectral feature, linked to anthocyanin content, was still selected it should represent a difference in pigment content. We are also aware, that both carotenoids and anthocyanins absorb light between 500 nm and 550 nm (Ustin *et al.*, 2009). Nearby wavebands are usually highly correlated, and these have been selected although we applied methods designed to avoid choosing correlated bands. Overlapping signals often resulted in inconsistencies in separating and quantifying different pigments (Ustin et al., 2009). However, as the wavebands at 545 nm and 555 nm were chosen consistently in our study, this may indicate that carotenoids, as well as anthocyanins are both independently important for indicating the presence of *A. psidii* urediniospores.

For the two important wavebands at 1505 nm and 2195 nm found in our study, we assume that these might be caused by lack of water, caused by necrotic lesions occurring on leaves during *A. psidii* infection (Glen *et al.*, 2007). Within the SWIR region (1300 nm – 2500 nm), light is primarily absorbed by water in a fresh leaf, but also by dry matter. Therefore, this region is linked to changes in water content (Peñuelas & Filella, 1998). It has been shown that water loss in leaves can be caused by the destruction of the leaf cuticle (Lindenthal *et al.*, 2005) which, in our case, was damaged by many necrotic lesions on untreated leaves (Fig. 1B). Leaves from fungicide treated trees did have some evidence of *A. psidii* infection (purple spots), likely due to infection occurring prior to fungicide application. However, the fungicide used (Bayfidan, Amistar, copper oxychloride) has been shown to work effectively as an eradicant (i.e. kill the rust) (Horwood et al. 2013) such that these purple spots did not develop further into yellow pustules and necrotic spots as they did on untreated trees. Furthermore, prior to myrtle rust, there were no other significant biotic agents that caused damage to lemon myrtle trees (Gary Mazzorana, Australian Rainforest Products, pers. comm.). Of course, it needs further testing whether the LMMR index can specifically detect myrtle rust against other stress causing agents. However, differentiation among diseases using optical sensors has already been proven feasible for sugar beet pathogens (Mahlein *et al.*, 2013).

Conclusion

We presented a newly developed spectral disease index (SDI) which performs better (90% OA) than common spectral vegetation indices (SVIs, 58%-67% OA). By publishing the code of our analysis, we provide a framework to generate new SDIs for other pathosystems. While further testing and validation for the LMMR is required, the concept of specific disease indices is a promising tool in plant disease detection (Mahlein et al. 2013). Our study was conducted in a plantation setting where leaves on untreated trees had varying levels of severity of *A. psidii*, from small purple spots through to necrotic lesions. Thus, the LMMR index is specific to physiological and phenotypic changes caused by *A. psidii.* Confounding stress causing agents could be excluded during our study as effective fungicides were applied and no stress causing agent prior to *A. psidii* was known. Future research could focus on the development of specific disease indices for certain infection stages (e.g. early). Additionally, it would be interesting to test the LMMR index on infected lemon myrtle plants at different locations and against other abiotic and biotic stress causing agents. Moreover, it should be tested if the index correlates with disease severity. Similar goals for the development of specific disease indices were already postulated (Mahlein 2016). For the lemon myrtle industry, that seeks to meet organic standards to be able to compete economically (Doran et al., 2012), a validated LMMR could enable land managers to assess high areas of their arable land and make decisions on fungicide applications.

Acknowledgements

The authors thank Gary Mazzorana from Australian Rainforest Products for access to his plantation, Dr Gerhard Muche for invaluable advice on the mathematical development of the LMMR and Dr Daniel S. Falster for his input on the reproducible publication of our code. Special thanks to Drs Anne-Katrin Mahlein, Robert Park and Angus Carnegie for providing invaluable feedback on the plant pathological aspects of the manuscript. R.H.J.H. was supported by a Macquarie University Research Excellence Scholarship. The authors declare no conflict of interest.

References

Ashourloo D, Mobasheri MR, Huete A, 2014. Evaluating the effect of different wheat rust disease symptoms on vegetation indices using hyperspectral measurements. *Remote Sensing* **6**, 5107–5123.

Beenken L, 2017. *Austropuccinia*: A new genus name for the myrtle rust puccinia psidii placed within the redefined family sphaerophragmiaceae (Pucciniales). *Phytotaxa* **297**, 53–61.

Bhattacharya S, 2017. Deadly new wheat disease threatens Europe's crops. *Nature* **542**, 145–146.

Bock CH, Poole GH, Parker PE, Gottwald TR, 2010. Plant disease severity estimated visually, by digital photography and image analysis, and by hyperspectral imaging. *Critical Reviews in Plant Sciences* **29**, 59–107.

Carnegie A, Pegg G, 2018. Lessons from the Incursion of Myrtle Rust in Australia. *Annual Review of Phytopathology* **56**, 1–22.

Clarke M, 2012. *Australian Native Food Industry Stocktake*. Barton, ACT, Australia: Rural Industries Research and Development Corporation.

Congalton R, Green K, 2009. *Assessing the Accuracy of Remotely Sensed Data, Principles and Practices*. Boca Raton, FL, USA: CRC Press

Daughtry C, 2000. Estimating Corn Leaf Chlorophyll Concentration from Leaf and Canopy Reflectance. *Remote Sensing of Environment* **74**, 229–239.

Davies K, 2004. *Plant Pigments and their Manipulation*. Oxford, UK: Blackwell.

Doran J, Lea D, Bush D. 2012. *Assessing myrtle rust in a lemon myrtle provenance trial*. Barton, ACT, Australia: Rural Industries Research and Development Corporation

Efron B, Tibshirani R, 1997. Improvements on Cross-Validation: The 0.632+ Bootstrap Method. *Journal of the American Statistical Association* **92**, 548–560.

Gamon JA, Serrano L, Surfus JS, 1997. The photochemical reflectance index: An optical indicator of photosynthetic radiation use efficiency across species, functional types, and nutrient levels. *Oecologia* **112**, 492–501.

Genuer R, Poggi J-M, Tuleau-Malot C, 2015. VSURF: An R Package for Variable Selection Using Random Forests. *The R Journal* **7**, 19–33.

Gitelson A, Gritz Y, Merzlyak M, 2003. Relationships between leaf chlorophyll content and spectral reflectance and algorithms for non-destructive chlorophyll assessment in higher plant leaves. *Journal of Plant Physiology* **160**, 271–282.

Gitelson AA, Merzlyak MN, Chivkunova OB, 2007. Optical Properties and Nondestructive Estimation of Anthocyanin Content in Plant Leaves. *Photochemistry and Photobiology* **74**, 38–45.

Gitelson AA, Zur Y, Chivkunova OB, Merzlyak MN, 2002. Assessing Carotenoid Content in Plant Leaves with Reflectance Spectroscopy. *Photochemistry and Photobiology* **75**, 272.

Glen M, Alfenas AC, Zauza EA V, Wingfield MJ, Mohammed C, 2007. *Puccinia psidii*: A threat to the Australian environment and economy - A review. *Australasian Plant Pathology* **36**, 1–16.

Hastie T, Tibshirani R, Friedman J, 2009. The Elements of Statistical Learning Data Mining, Inference, and Prediction. New York, NY, USA: Springer

Heim RHJ, Wright IJ, Chang H-C et al., 2018. Detecting myrtle rust (*Austropuccinia psidii*) on lemon myrtle trees using spectral signatures and machine learning. *Plant Pathology* **67**, 1114–1121.

Helfer S, 2014. Rust fungi and global change. New Phytologist **201**, 770–780.

Horwood M, Carnegie AJ, Park RF. 2013. *Gathering efficacy data to indentify the most effective chemicals for controlling myrtle rust (Uredo rangelii)*. Canberra, ACT, Australia: Plant Health Australia

Hunt P, 1968. Cuticular penetration by germinating uredospores. *Transactions of the British Mycological Society* **51**, 103-112.

Jacquemoud S, Ustin SL, 2001. Leaf optical properties: a state of the art. *Proc. 8th International Symposium Physical Measurements & Signatures in Remote Sensing*. Aussois, FRANCE: CNES, 223–232.

Kuhn M, Johnson K, 2013. *Applied Predictive Modeling*. New York, NY, USA: Springer

Lindenthal M, Steiner U, Dehne H-W, Oerke E-C, 2005. Effect of Downy Mildew Development on Transpiration of Cucumber Leaves Visualized by Digital Infrared Thermography. *Phytopathology* **95**, 233–240.

Mahlein A-K, 2016. Plant Disease Detection by Imaging Sensors – Parallels and Specific Demands for Precision Agriculture and Plant Phenotyping. *Plant Disease* **100**, 241–251.

Mahlein AK, Rumpf T, Welke P et al., 2013. Development of spectral indices for detecting and identifying plant diseases. *Remote Sensing of Environment* **128**, 21–30.

Morin L, Talbot MJ, Glen M, 2014. Quest to elucidate the life cycle of *Puccinia psidii* sensu lato. *Fungal Biology* **118**, 253–263.

Mulla DJ, 2013. Twenty five years of remote sensing in precision agriculture: Key advances and remaining knowledge gaps. *Biosystems Engineering* **114**, 358–371.

Peñuelas J, Filella L, 1998. Visible and near-infrared reflectance techniques for diagnosing plant physiological status. *Trends in Plant Science* **3**, 151–156.

R Core Team (2017). R: A language and environment for statistical computing. Foundation for Statistical Computing, Vienna, Austria. URL https://www.R-project.org/.

Stafford J V., 2000. Implementing precision agriculture in the 21st century. *Journal of Agricultural and Engineering Research* **76**, 267–275.

Thenkabail PS, Smith RB, De Pauw E, 2000. Hyperspectral vegetation indices and their relationships with agricultural crop characteristics. *Remote Sensing of Environment* **71**, 158–182.

Ustin SL, Gitelson AA, Jacquemoud S et al., 2009. Retrieval of foliar information about plant pigment systems from high resolution spectroscopy. *Remote Sensing of Environment* **113**, 67–77.

This page is intentionally left blank.

CHAPTER IV

Multispectral, aerial disease detection for myrtle rust (*Austropuccinia psidii*) on a lemon myrtle plantation

RHJ Heim • IJ Wright • P Scarth • AJ Carnegie • D Taylor • J Oldeland
Under review

Abstract

Disease management in agriculture often assumes that pathogens are spread homogeneously across crops. In practice, pathogens can manifest in patches. Currently, disease detection is predominantly carried out by human assessors, which can be slow and expensive. A remote sensing approach holds promise. Current satellite sensors are not suitable to spatially resolve individual plants or lack temporal resolution to monitor pathogenesis. Here, we used multispectral imaging and unmanned aerial systems (UAS) to explore whether myrtle rust (*Austropuccinia psidii*) could be detected on a lemon myrtle (*Backhousia citriodora*) plantation. Multispectral aerial imagery was collected from fungicide treated (to control myrtle rust) and untreated tree canopies and compared to multispectral data from individual leaves from the same canopies. Spectral vegetation indices and single spectral bands were used to train a random forest classifier. The UAS-derived classification yielded higher accuracy (95%) than the leaf-level classification (74%). Important predictors for the UAS classifier were the near-infrared (NIR) and red edge (RE) spectral band. At the leaf level NIR was no longer deemed important. Our work suggests potential for mapping myrtle rust-related symptoms from aerial multispectral images. Similar studies could focus on pinpointing disease hotspots to adjust management strategies and to feed epidemiological models.

Introduction

Sustaining human food demands in a world with a global population growing toward 10 billion has been identified as a major challenge (Foley *et al.*, 2011; Crist *et al.*, 2017). The implementation of technologies to increase food supply through intensification rather than expansion is regarded as a sensible approach to tackle this challenge (Crist *et al.*, 2017). Precision agriculture comprises a set of technologies that combines sensors and information systems to inform management decisions for optimizing farm inputs by accounting for variability and uncertainties within agricultural systems (Gebbers & Adamchuk, 2010). Satellite imagery is often used to study variations in crop and soil conditions, however, the availability, limited resolution and sometimes prohibitive costs of satellite imagery limits its universal application in precision agriculture. Unmanned aerial systems (UAS, also known as drones) are now commercially available to anyone and can be equipped with a wide range of sensors (e.g. thermal or spectral). Thus, they offer a cost-effective alternative to satellite systems while providing a higher spatial and temporal resolution (Zhang & Kovacs, 2012; Mulla, 2013).

In agriculture, UAS have been used for estimating leaf area index, chlorophyll content and water stress (Berni *et al.*, 2009). Various other applications were reviewed by Zhang and Kovacs (Zhang & Kovacs, 2012) and Mulla (Mulla, 2013). One of these applications is sensor-guided disease detection (West *et al.*, 2003). Plant diseases can cause tremendous damage to agricultural production as has been shown recently when a new strain of wheat rust destroyed tens of thousands of hectares of crops in Italy (Bhattacharya, 2017). Traditional disease management practices often assume that pathogens are spread homogeneously over cultivation areas, potentially leading to untargeted and wasteful application of fungicides and other crop management measures (Mahlein, 2016). By contrast, site- and problem-specific use of pesticides is likely to reduce amounts required for application and therefore reduce costs and ecological impact in agricultural crop production systems (Gebbers & Adamchuk, 2010). To detect disease hotspots, sensors with a spatial resolution of more than 1 m (e.g. satellite mounted sensors) are hardly suitable and often proximal sensor platforms are preferred as they allow for high (>10 cm) spatial resolution (Oerke *et al.*, 2014). Nowadays, the same high spatial resolution can be achieved by camera systems mounted on UAVs (Dash *et al.*, 2017) and compared to proximal sensors, UAV systems allow for disease screening at high capacity and frequency (Zhang & Kovacs, 2012). As an example, Calderón et al. (Calderón *et al.*, 2014) acquired airborne thermal and multi-spectral imagery using an UAS to detect downy mildew (caused by *Peronospora arborescens* (Berk.)) on opium poppy (*Papaver somniferum* L.). The following spectral regions were useful to detect infections: the visible (VIS, 400–700 nm) and red-edge (670–750 nm) spectral region, due to the necrotic and chlorotic lesions caused by chlorophyll degradation; the near-infrared region (800 nm) due to changes in canopy density and leaf area; and the thermal-infrared region because of the changes in the transpiration rate that affect canopy temperature. It was further demonstrated that canopy temperature and the green/red ratio (R550/R670) were related to physiological stress caused by downy mildew infection.

The rust fungus *Austropuccinia psidii*, known as myrtle rust, is now regarded as a globally invasive pathogen that has been established in Australia since 2010 (Carnegie & Pegg, 2018). A. psidii infects growing shoots, fruits and flowers, resulting in leaf and shoot distortion, dieback and tree mortality in severe cases (Glen *et al.*, 2007; Carnegie *et al.*, 2016). Infection of young foliage results in discoloration (chlorosis and reddening), development of yellow uredinia (pustules) and ultimately necrosis (Glen *et al.*, 2007). In contrast to other rust diseases, which are mostly restricted to few host species, myrtle rust has the potential to infect hundreds of different hosts, escalating the potential consequences for Australia’s natural landscapes (Berthon *et al.*, 2018) where it specializes exclusively on one of Australia’s dominant plant families, the Myrtaceae. Industries that rely on species within the Myrtaceae, such as the nursery and garden industry, have also been affected by myrtle rust through losses of commercial varieties, trade restrictions, and increased dependency on fungicides (Carnegie & Pegg, 2018). In Australia, the expanding lemon myrtle (*Backhousia citriodora*) industry has been particularly affected (Carnegie & Pegg, 2018). Leaves of lemon myrtle are commercially harvested to produce lemon-flavored herbal teas, culinary herbs, and lemon-scented essential oils used for food flavoring and personal care products. The farm gate value of this market has been estimated to be 5.3 - 17.5 million USD annually (Clarke, 2012). Cultivars of *B. citriodora* that are currently in use are moderately to highly susceptible to myrtle rust. Rust-affected leaves of *B. citriodora* are unsuitable for use, and the application of fungicides to control the disease is undesirable as the market demands a clean, organic product (Doran *et al.*, 2012). Therefore, industries reliant on lemon myrtle are in urgent need of rust-resistant cultivars or measures to reduce the use of fungicides.

In a previous study (Heim *et al.*, 2018), we showed that it is feasible to use ground-based, narrow-band hyperspectral sensors to discriminate fungicide treated and untreated lemon myrtle leaves with high accuracy (95%). In the present study, we deployed an UAV carrying a broad-band multispectral sensor. We aimed to test (1) if it would be possible to accurately discriminate fungicide-treated and untreated plants at canopy-level. Because we were interested in whether a multispectral sensor would be sufficient at leaf-level to accurately discriminate our tree classes, we then compared (2) the classification performance of multispectral data at leaf-level to multispectral data at canopy-level. The leaf-level multispectral data were derived by down-sampling the hyperspectral data from our previous study (Heim *et al.*, 2018). Finally, it has been shown to be important to select for wavebands specific to the pathosystem for accurately detecting a disease (Mahlein *et al.*, 2013). Thus, (3) we tested if the important wavebands, derived from multispectral data, would differ between canopy- and leaf-level. To answer the last question, we considered four vegetation indices in addition to the five spectral bands provided by the multispectral sensor to explore if vegetation indices behave differently as pure spectral bands.

Methods

Study site and spectral data

Spectral data of lemon myrtle trees were collected at canopy- and leaf-level on a commercial lemon myrtle (*Backhousia citriodora*) plantation in northern New South Wales, subtropical eastern Australia (latitude -28.691055, longitude 153.295510). Mean annual temperature is 19.4 °C and mean annual rainfall 1343 mm. Leaf-level spectral signatures were collected in a previous study (Heim *et al.*, 2018) using a PSR+ 3500 hand-held (Spectral Evolution, Lawrence, MA, U.S.) spectrometer. At the plantation, we took advantage of an existing experiment in which the impact of fungicide was being assessed on lemon myrtle trees affected by myrtle rust (Heim *et al.*, 2018). We recorded spectral data from trees that were free of active disease, having had fungicide successfully applied to them ("treated"), and trees showing symptoms of active myrtle rust infection ("untreated"). Leaves from treated trees showed mostly no signs of *A. psidii* infection, although some had small purple spots, likely due to infection occurring prior to fungicide application, with fungicide that have been shown effective and halting the infection process (Horwood *et al.*, 2013). We exclude the influence of other biotic agents as no other serious pathogen on lemon myrtle was known prior to *A. psidii* (Manager Gary Mazzorana, pers. comm.). The experimental design consisted of two treated and two untreated rows of trees, separated by rows of trees designated as "buffer" trees to avoid accidental treatment of trees intended to be untreated (Figure 1). Plants that appeared disturbed by proximity to frequently used management trails were avoided. Each row had five trees, and on each tree, we recorded four leaf spectral signatures of four leaves at 180, 100 and 50 cm height. Leaves were selected from a single terminal shoot and the first two pairs (four leaves) of newly expanding leaves were used to record the spectral responses. The height-stratified sampling points were chosen on both east- and west-facing sides of trees, in order to represent the spectral response of a single tree most effectively. We sampled 240 spectra from the 240 selected leaves for each class resulting in a total of 480 spectra. After removing outlier spectra, a total of 236 treated leaves (from 79 trees) and 228 untreated leaves (from 76 trees) were included in the analysis. Further details of sample design and hand-held sensor specifications were reported by Heim *et al.* (2018) (Heim *et al.*, 2018).

Aerial imagery of the experimental site was captured in the same year as spectra collection (05.06.2016 – 3 pm). Daily temperatures were between 14.5°C and 22.5°C, daily global solar exposure was 16.4 MJ/m^2 with a scattered cloud cover (~30%). A five-band multispectral camera (B=475±20 nm, G=560±20 nm, R=668±10 nm, NIR=840±40 nm and RE=717±10 nm; RedEdge 3, MicaSense, Inc., Seattle, WA, U.S.) was mounted on a consumer-grade Inspire-1 quadcopter (DJI Inc., Shenzhen, China). The camera had a focal length of 5.5 mm and captured images at a resolution of 1280 x 960 and a pixel size of 3.75 x 3.75 µm. Images were captured with a forward overlap (e.g. overlap between photos along the same flight line) of 70%, a lateral overlap (overlap between photos on adjacent flight lines) of 80%, a flight speed of 3 m/s (10.8 km/h) and a flight altitude of 40 m above ground on average. Considering the tree height (~180 cm), the mentioned settings achieved a ground sampling distance of approx. 2.78 cm per pixel.

Image processing

Aerial images were processed in Agisoft PhotoScan Professional (Version: 1.4.2 build 6205, 64 bit). Spectral reflectance for each band was calibrated and normalized using images and the according correction factors of a white reference panel (RP02-1543031-SC). Images were aligned by matching tie points across all adjacent images using “high accuracy” settings. Such tie points are reference points that can be clearly identified by the software in two or more images and used to reconstruct the entire scene. Subsequently, images were optimized by fitting the reconstruction uncertainty and the projection accuracy. High reconstruction uncertainty is often caused by noisy points reconstructed from nearby images. The projection accuracy was used to filter out projected points that were below an error threshold of three. The reprojection error determines the distance between reconstructed projection and the original projection and was reduced to 0.35 by removing bad points due to pixel residual error. Image post-processing was guided by recommendations of the United States Geological Survey scientific agency (USGS National UAS Project Office, 2017). Then, a dense point cloud was generated and cropped to the extent of our sample area (Figure 1). Further, the dense point cloud was categorized in tree-points-only (T) and tree-ground-points (TG). Therefore, we tuned the ground point classification tool in Agisoft PhotoScan Professional. The categorization was done to remove all areas classified as being “ground”, yielding an image only displaying the relevant lemon myrtle trees. This image was useful to apply our classification model and create a risk map (see results). Without the categorization, non-relevant ground points would have been included in the prediction model. Eventually, both dense point clouds (TG and T) were exported as orthophotos (e.g. an ortho-rectified image is free of distortion and shows a uniform scale over its entire surface).

Our radiometric calibration was not optimal as we had to fly under sporadically cloudy conditions. Therefore, our aerial multispectral data is not suitable for temporal variation analysis or comparisons between sensors (Wang & Myint, 2015). However, in our study we only compare classification accuracies based on self-contained datasets and therefore the relative relationships between treated and untreated spectra should not be affected.

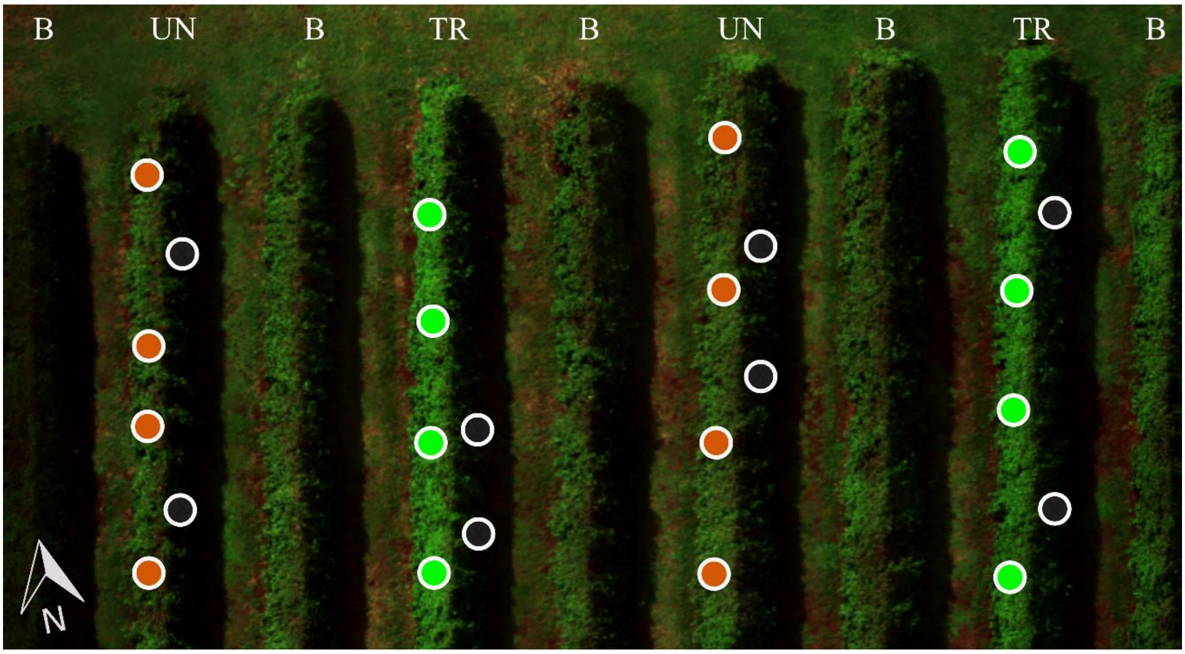

Figure 1 | Bird's eye view of the experimental setup. For each of the three classes (TR=treated, UN=untreated, SHD=shadow) eight equally sized polygons were drawn and representatively distributed across the lemon myrtle trees. In our analysis, these circular areas were used to sample pixels from each class. These pixel samples were used to train our random forest classification model. UN=brown/orange, TR=green, SHD=black.

Data preparation

To yield sample data to train our classification model, we used the open-source software QGIS (version 3.4.1) (QGIS Development Team, 2009) to draw circular shaped polygons as pixel sample areas onto the TG orthophoto (Figure 1). We created eight sample areas for each class (shadow=SHD, treated=TR, untreated=UN). The class "SHD" was specified to discriminate areas where trees were overcast by shadows. Shadow areas (east-facing tree sides, Figure 1) are likely to confound a classification between treated and untreated trees as they were much darker than sample areas from sunlit canopies. Pixel samples were extracted for each class and polygon using the 'raster' package (Hijmans, 2017) within the R environment (version 3.4.3) (R Core Team, 2017). The full analysis can be reproduced by re-running our stored data and code (https://github.com/ReneHeim/MR_Drone).

The pixel data extraction process yielded an initial spectral dataset at canopy (C) level (Figure 2) containing 14438 observations, 9 predictor variables (see below) and a response column containing the classes (SHD, TR, UN). We ran a random forest classification on these data to explore whether it would be possible to discriminate treated and untreated myrtle rust trees at canopy-level. To answer the question whether the classification performance of multispectral data at canopy level would differ from multispectral data collected at leaf level, we had to compare the initial dataset (C, Figure 2) to data recorded at leaf-level. We derived the leaf-level dataset by down-sampling the hyperspectral leaf-clip spectra from our previous study (Heim *et al.*, 2018) to the band specifications of the MicaSense RedEdge camera used in the presented study. This leaf-level (L) dataset (Figure 2) contained 464 observations, 9 predictor variables and two classes (TR and UN) as response variables. Because the leaf level dataset was recorded using a leaf-clip accessory the SHD-class was not existing as the active illumination source did not cast shadows. We dropped the SHD-class from our initial canopy dataset (C) and derived a third dataset at canopy level without shadows (C-S, Figure 2) containing 9628 observations, 9 predictor variables and two classes (TR and UN) as response variables. Thereby, we could fairly compare classification results of data at leaf level (L) and at canopy level (C-S).

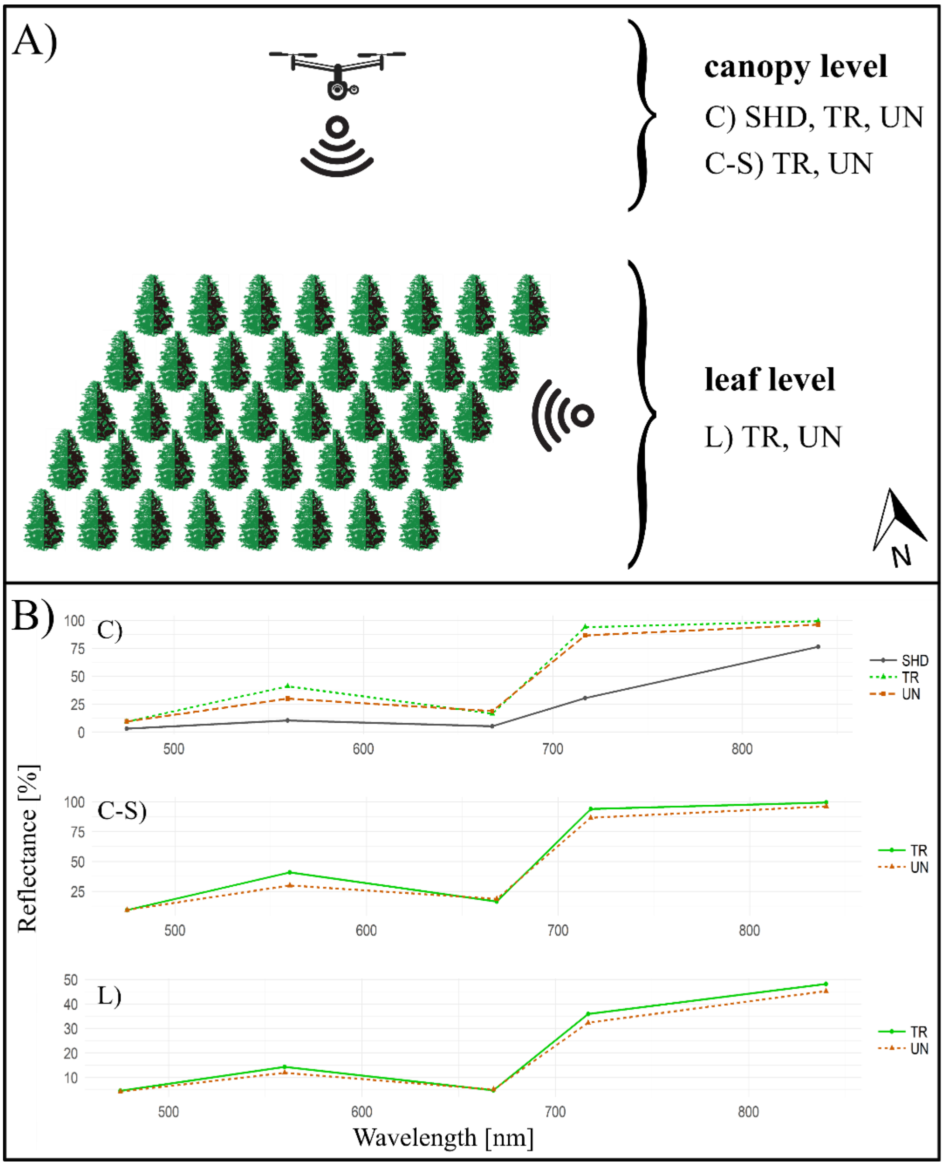

Figure 2 | Overview of dataset modifications that were applied to answer our research questions (A) and the according multispectral signatures (B). We collected multispectral data at canopy level (C) to run an overall classification of all present classes (TR=treated, UN=untreated, SHD=shadow). Hyperspectral leaf level data was down-sampled to match the specifications of our multispectral sensor. This yielded a second dataset at leaf level (L) which was compared to a third canopy dataset (C-S) created by dropping the SHD-class from data (C).

Each dataset contained 9 predictor variables. These were five spectral bands native to the MicaSense RedEdge camera (B, G, R, RE, NIR) and four vegetation indices (Table 1) that we added according to variation in biophysical and physiological parameters, likely to be caused by infection by *A. psidii*. Red discoloration (Figure 3C/D) has been observed during *A. psidii* infection (Glen *et al.*, 2007), and we assume that this is caused by anthocyanin pigments which are responsible for most red and purple discolorations in plants (Davies, 2004). Therefore, we used the anthocyanin reflectance index (ARI, (Gitelson *et al.*, 2007)).

Also, chlorotic lesions have been observed during A. psidii infection (Lee *et al.*, 2014), and as chlorophyll breakdown and reduction in photosynthesis rate has been associated with other biotrophic pathogens and especially rusts (Walters & McRoberts, 2006), we assumed that chlorophyll content and regulation were also affected. Therefore, we calculated the Red/Green ratio, a simple ratio index that has been applied by Calderon (Calderón *et al.*, 2014) to detect downy mildew in poppy seed and has been found to be related to changes in chlorophyll content. Yellow/orange pigments in *A. psidii* urediniospores (Figure 3C/D) have been speculated to provide UV protection and to resist desiccation (Ramsfield *et al.*, 2010). As carotenoids are known to provide UV protection and being present in other rusts (Wang *et al.*, 2018), we also assume changes in carotenoid content caused by *A. psidii*. We thus applied the structure insensitive pigment index (SIPI, (Penuelas *et al.*, 1995)) which is known to be related to changes in carotenoid content. Regarding biophysical parameters, it is known that *A. psidii* hyphae enter the mesophyll layer (Morin *et al.*, 2014), therefore it is likely that mesophyll cell integrity is lowered. Hyphae entering mesophyll cells is likely to cause plant stress, therefore we selected the NDVI. The NDVI (Rouse *et al.*, 1973) has been used in numerous studies to detect stress in vegetation (Calderón *et al.*, 2014; Di Gennaro *et al.*, 2016; Dash *et al.*, 2017).

Figure 3 | The sampled lemon myrtle trees (A) are grown in rows on the plantation. Trees without fungicide treatment can show various symptoms depending on the phase of pathogenesis. The upper right image (B) shows treated mature leaves that are not actively infected and thus show only old necrotic lesions caused by infections when those leaves were still young. Examples of active infections are found in image C and D where yellow urediniospores cause symptoms on untreated younger leaves. Surrounding those infections sites, red halos can be observed. (Source: Ina Geedicke)

Table 1| Spectral vegetation indices included as predictor variables in our classification models.

Spectral Vegetation Index (SVI)	**SVI Abbrev.**	**Formula**	**Reference**
Normalized Difference Vegetation Index	NDVI	$NDVI = \frac{NIR - R}{NIR + R}$	(Rouse *et al.*, 1973)
Structure Insensitive Pigment Index	SIPI	$SIPI = \frac{NIR - B}{NIR - R}$	(Penuelas *et al.*, 1995)
Anthocyanin Reflectance Index	ARI	$ARI = \frac{1}{G} - \frac{1}{RE}$	(Gitelson *et al.*, 2007)
Red/Green Simple Ratio Index	R/G	$RG_{Index} = \frac{R}{G}$	(Calderón *et al.*, 2014)

Random forest classification

We used a non-parametric random forest classifier (Breiman, 2001) to produce classification models for all three datasets (C, C-S, L). This approach reduces classification variance by evaluating accuracy across multiple independent decision trees (Hastie *et al.*, 2009). Random forests and their variable importance measures have been extensively exploited in different scenarios and can successfully handle multicollinear data of high dimensionality. Also, they are less sensitive to overfitting and do not require as high quality training samples as other streamline machine learning classifiers (Belgiu & Drăgu, 2016). This is due to the large number of decision trees produced and by randomly selecting a subset of training samples and a subset of variables for splitting at each tree node (Belgiu & Drăgu, 2016). For our models, we first optimized the chosen number of randomly selected predictors at each split (mtry) by iterating over a sequence of ascending mtry-values and selected mtry=5 (C), mtry=6 (C-S) and mtry=7 (L). Secondly, the number of trees generated to gain a full ensemble (n-tree) was optimized. All three datasets were initially split 75:25 into training (C=10380 obs., C-S=7222 obs., L=348 obs.) and test data (C=3608 obs., C-S=2406 obs., L=116 obs.). Each of the three models was trained by drawing 100 bootstrap samples from the training data. For each bootstrap sample, an individual and independent decision tree was constructed. Then, from each bootstrap sample, another subsample (out-of-bag sample) was set aside. The out-of-bag sample is passed down each of the 100 decision trees to estimate an unbiased training classification error. To assess the importance of each contributing variable for each tree we applied a random-forest-based feature selection (Genuer *et al.*, 2015) for each dataset. The method is suitable for regular, high-dimensional and correlated data (Genuer *et al.*, 2010).

Accuracy assessment

We quantified the accuracy of the classification using three metrics: overall accuracy (OA, producer accuracy (PA) and user accuracy (UA). While, OA reflects the agreement between reference and predicted classes and has the most direct interpretation, PA and UA (Story & Congalton, 1986) are class-specific accuracy measures. PA is the number of correctly classified references for a class divided by the total number of references of that class and, thus, represents the accuracy of the classification for a specific class. UA divides the number of correct classifications (predictions) for a class by the total number of classifications (predictions) for that class. A high UA means that spectra within that class can be reliably classified as belonging to that class. UA is often termed to be a measure of reliability, which can be also interpreted as the agreement between repeated measurements within a class.

Results

Canopy data classification

The random forest classification, discriminating between fungicide treated and untreated lemon myrtle trees, resulted in an overall accuracy of test data of 95%. Considering the class “Shadow” (Table 2) from the perspective of the person who sampled the reference data, 1202 pixels were extracted from trees and were labelled as such (Table 2 – Reference, columns). The classifier slightly disagreed with our observation and suggested that 16 shaded pixels should have been labelled as “Treated” and 27 as “Untreated” (PA= 96.4%, columns). When changing this to the perspective of the classifier (Table 2 – Prediction, rows), the model predicted 1198 pixels as being the class “Shadow”. However, from those pixels we initially labelled 16 belonging to the class “Treated” and 23 to the class “Untreated”. In 96.7% of cases our labels confirmed the prediction for that class (User Accuracy). When evaluating the remaining classes, the agreement between our labels and the classifier’s predictions was high from both perspectives.

To emphasize the high accuracy of the prediction, we applied our model to an aerial image of the experimental site to predict whether a pixel could be classified as being a shadow or a treated or untreated lemon myrtle tree. Thus, we created a map, using the orthophoto where all ground pixels were removed (T, see chapter 2.2), that could be used to pinpoint areas of potential incidence of myrtle rust (Figure 4).

Table 2 | Classification metrics for the dataset C (canopy, all classes). The lower right cell contains the overall accuracy (95.0%). Class specific accuracies can be found in the lower marginal row (producer accuracy, PA) and outer right marginal column (user accuracy, UA). Values shown in diagonal cells contain correctly classified pixel samples for each class and the total number of pixel samples (3608).

Data C		Reference				
		Shadow	Treated	Untreated	Total	UA
Prediction	Shadow	**1159**	16	23	1198	96.7%
	Treated	16	**1135**	45	1196	94.9%
	Untreated	27	52	**1135**	1214	93.5%
	Total	1202	1203	1203	**3608**	
	PA	96.4%	94.3%	94.3%		**95.0%**

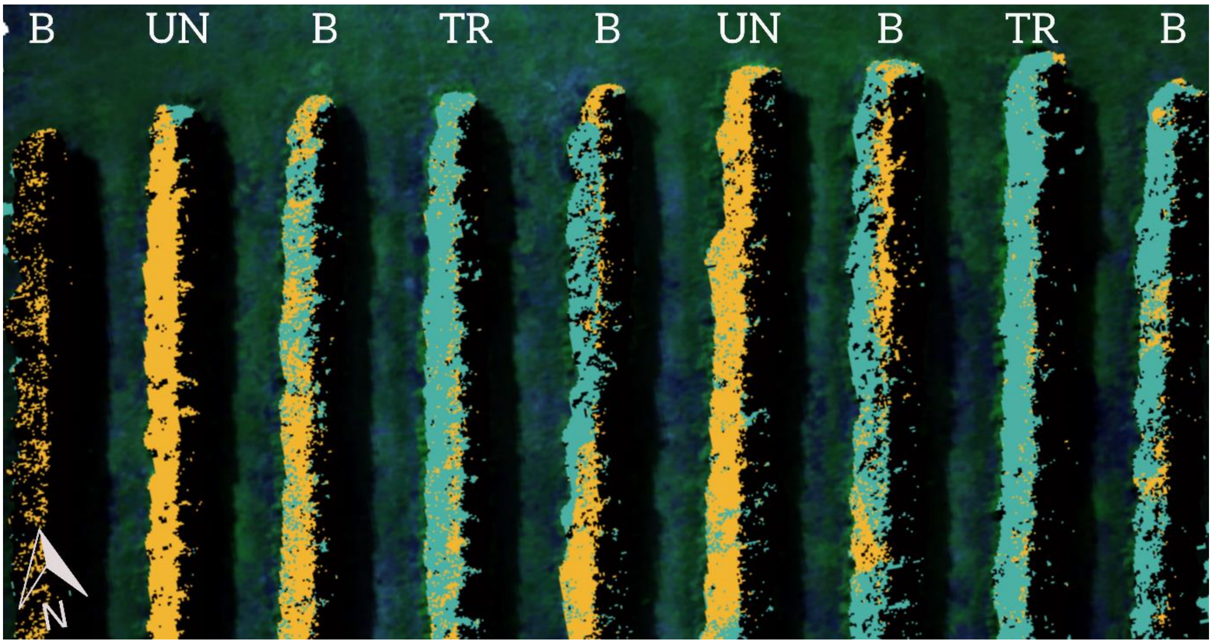

Figure 4 | Experimental site from an aerial view. Each fungicide treated (TR) row of trees was separated by a buffer row (B) from untreated (UN) trees. Buffer rows were interspersed to avoid unintentional fungicide treatment of untreated trees. All trees have been colored according to the predictions of our classification model. Treated rows are expected to be healthy (green) and were mostly predicted as such. Rows without fungicide treatment are likely to be infected (orange) and were also predicted with high accuracy. East-facing shadows (black; compare Figure 1) were added to the prediction to avoid confusion between shadows of treated trees and untreated trees. Shadows were also predicted with high accuracy.

Comparing canopy and leaf-level classification

Whether it would be more accurate to classify treated and untreated trees by using a multispectral camera at the canopy level (40 m above ground) or by using the same type of sensor at leaf-level can be evaluated by comparing their respective overall accuracies (Tables 3 and 4). At leaf level, treated and untreated trees were discriminated with an accuracy of 74.1% (Table 4). By contrast, at canopy level, the tree classes were discriminated with an OA of 96.2% (Table 3). Note that this canopy-level classification is almost the same as before (Table 2) except the shadow-class was dropped to facilitate a fair comparison of canopy- and leaf-level data. As the leaf data were collected in a previous study with a field-spectrometer, including an active illumination source, no shadow-class could be recorded. A classification at leaf level, using the multispectral data derived by spectral resampling of hyperspectral leaf-clip data, is less accurate then using the same sensor at canopy level. This is also reflected by PA and UA for both classes. At the leaf level (Table 4) PA and UA range between 72.9% and 75.4%. However, at the canopy level they range between 96% and 96.4% (Table 3).

Table 3 | Classification metrics for the dataset B (aerial, shadow class dropped). The lower right cell contains the overall accuracy (96.2%). Class specific accuracies can be found in the lower marginal row (producer accuracy, PA) and outer right marginal column (user accuracy, UA). Values shown in diagonal cells contain correctly classified pixel samples for each class and the total number of pixel samples (2406).

Data C-S		Reference			
		Treated	Untreated	Total	UA
Prediction	Treated	**1155**	43	1198	96.4%
	Untreated	48	**1160**	1208	96.0%
	Total	1203	1203	**2406**	
	PA	96.0%	96.4%		**96.2%**

Table 4 | Classification metrics for the dataset C (leaf, no shadows when recording leaf spectra). The lower right cell contains the overall accuracy (74.1%). Class specific accuracies can be found in the lower marginal row (producer accuracy, PA) and outer right marginal column (user accuracy, UA). Values shown in diagonal cells contain correctly classified spectral reflectance signatures for each class and the total number of spectra (116).

Data L		Reference			
		Treated	Untreated	Total	UA
Prediction	Treated	**43**	14	57	75.4%
	Untreated	16	**43**	59	72.9%
	Total	59	57	**116**	
	PA	72.9%	75.4%		**74.1%**

Important variables at canopy and leaf-level

In addition to comparing accuracy metrics between canopy- and leaf-level we aimed to assess the importance of the spectral bands (blue=B, green=G, red=R, red-edge=RE and near-infrared=NIR) and the vegetation indices (NDVI, SIPI, ARI, R/G) for the classification at both levels and for all datasets (C, C-S and L). The importance is given in absolute values, as provided by the selection algorithm, and as normalized, relative values between 0 and 1 (Table 5). Overall, at canopy level (Table 5, C and C-S), the NIR and RE have a high relevance for the classification. The RE loses importance (Table 5, C-S, Rank 4) when no shadows are present. At leaf-level (Table 5, L) the NIR is less important (Rank 6) while the NDVI (Rank 3) and the G (Rank 2) band were more relevant. Specifically, for dataset C (canopy, treated, untreated, shadow), the RE (717±10 nm, Rank 1) and the NIR (840±40 nm, Rank 2) were most important. The G band (560±20 nm, Rank 6) band, was among the least important predictors to discriminate treated, untreated and shadow overcast trees. The most important index, the R/G simple ratio ranked on 4th place. For dataset C-S (canopy without shadow class) the NIR band was most important. The RE lost importance (Table 5, C-S, Rank 4 instead of 1). For spectral indices, the R/G ratio was most important (Table 5, C-S, Rank 2) while the SIPI, had very low influence on the classification (Table 5, C-S, Rank 9). The NDVI ranked sixth. For leaf level data (Table 5, L), most relevant predictors were the RE band and the G band. The NDVI had a higher relevance compared to data collected at canopy level (Table 5, L, Rank 3). Interestingly, the R/G index was most important for canopy data without shadows (Table 5, C-S, Rank 2), lost importance when shadows were included (Table 5, C, Rank 4) and had no relevance at leaf-level (Table 5, L, Rank 8).

Table 5 | Important predictors for each classified dataset (C, C-S, L). The absolute and relative importance is provided. The first row indicates the overall rank for each predictor.

	Rank	1	2	3	4	5	6	7	8	9
Data C	**Band**	**RE**	**NIR**	**R**	**R/G**	**ARI**	**G**	**NDVI**	**B**	**SIPI**
	Abs. Imp.	0.3	0.26	0.13	0.13	0.11	0.09	0.08	0.07	0.04
	Rel. Imp.	1	0.85	0.36	0.34	0.26	0.21	0.17	0.13	0
Data C-S	**Band**	**NIR**	**R/G**	**ARI**	**RE**	**G**	**NDVI**	**B**	**R**	**SIPI**
	Abs. Imp.	0.23	0.16	0.07	0.06	0.05	0.04	0.03	0.03	0.02
	Rel. Imp.	1	0.67	0.23	0.19	0.14	0.1	0.07	0.06	0
Data L	**Band**	**RE**	**G**	**NDVI**	**B**	**R**	**NIR**	**SIPI**	**R/G**	**ARI**
	Abs. Imp.	0.1	0.06	0.05	0.04	0.03	0.02	0	0	0
	Rel. Imp.	1	0.63	0.52	0.41	0.34	0.19	0	0	0

Discussion

In recent years the rust fungus *Austropuccinia psidii* has caused tremendous damage globally and also in Australia, where it is threatening plant industries and native vegetation (Carnegie & Pegg, 2018). In 2017, *A. psidii* was detected in New Zealand. Industries in Australia and New Zealand are now severely threatened (Government, 2018; Carnegie & Pegg, 2018). While the extent of damage in Australia was already projected (Berthon *et al.*, 2018), it can be assumed that all Myrtaceae species in New Zealand are at risk and the impacts could be devastating (Lambert *et al.*, 2018). A rapid measure to detect and monitor the impact of *A. psidii* on arable land could make it possible to optimize management strategies.

Given this context, the primary goal of this study was to explore whether it would be possible to spectrally discriminate lemon myrtle trees on a plantation at canopy-level. At this level, detection and monitoring could be carried out by UASs to facilitate a rapid and versatile surveillance strategy. Instead of using an expensive hyperspectral sensor, we used an affordable lightweight (150 g) UAS-borne multispectral sensor with a coarser spectral resolution and successfully classified treated, untreated and shaded trees with an accuracy of 95%.

Depending on the time when aerial images are captured, trees can be partially overcast by shadows. If this is the case, a classifier should be able to discriminate healthy, infected and shaded trees. The inclusion of shadows can be reduced by capturing the data at noon when the sun is at its zenith. When we removed data derived from shadows from our classification, we were still able to discriminate treated and untreated trees with an accuracy of 96.2%. As multispectral sensors are more affordable than hyperspectral sensors, we investigated whether we could also achieve accurate classification results at leaf-level when using a multispectral sensor. Thus, we simulated multispectral leaf spectra by down-sampling the leaf spectral signatures captured for our previous study (Heim *et al.*, 2018). The classification accuracy for down-sampled leaf spectra was reduced to 74%. A likely explanation is the coarser spectral resolution of the multispectral sensor. The hyperspectral sensor in Heim et al. (2018) could capture spectral variation in 2 nm intervals, resulting in hundreds of bands that may vary depending on physiological and phenotypic changes caused by myrtle rust. However, the multispectral sensor in this study utilizes only five broad spectral bands (blue 475±20 nm, green 560±20 nm, red 668±10 nm, red-edge 717±10 nm and near-infrared 840±40 nm). While multispectral sensors are cheaper than hyperspectral sensors, their less detailed spectral signature is more likely to be related to general stress symptoms caused by *A. psidii*.

Another feasible framework to detect *A. psidii* was recently published by Sandino et al. (Sandino *et al.*, 2018) for paperbark tea trees (*Melaleuca quinquenervia*), similarly using treated and untreated trees. They used a hyperspectral camera at 20 m above the ground, resulting in a ground sample distances of 4.7 cm/pixel. Healthy paperbark trees were detected at rates of 97.24% and affected trees at 94.72%. Sandino et al. (Sandino *et al.*, 2018) emphasized that future studies should focus on monitoring disease progression and link specific biophysiological parameters with spectral responses caused by infection through *A. psidii*. Such an inclusion of biophysiological parameters was considered by Asner et al. (Asner *et al.*, 2018). They linked leaf chemical parameters with spectral reflectance signatures at leaf and canopy level of *Metrosideros polymorpha* to develop a monitoring approach for Rapid Ohia Death (ROD). They found that close to 80% of ROD-infected plants underwent marked decreases in foliar concentrations of chlorophyll, water and non-structural carbohydrates, which collectively resulted in strong consistent changes in leaf spectral reflectance in the visible (400–700 nm) and shortwave-infrared (1300–2500 nm) wavelength regions. Leaf-level results were replicated at the canopy level using airborne laser-guided imaging spectroscopy, with quantitative spectral separability of normal green-leaf canopies from suspected ROD-infected brown-leaf canopies in the visible and shortwave-infrared spectrum.

We selected relevant wavebands for each of our classifications and found spectral bands (RE, NIR) and spectral vegetation indices (ARI, NDVI and R/G) that contain more discriminatory power than others. At canopy level, the NIR and RE were important spectral regions for the classification of treated and myrtle rust infected trees. Also, a simple ratio index, the red/green ratio, seems to be useful. In a study by Calderon et al. (Calderón *et al.*, 2014), the red/green ratio was applied on canopy multispectral data for the detection of physiological stress in opium poppy infected with downy mildew (Calderón *et al.*, 2014). However, in our study the red/green ratio lost importance at canopy level when shadows were part of the classification. The red/green ratio had low relevance at leaf level. Further, the green and blue band, SIPI and NDVI were also less important at canopy level. These results show what was already suggested by Mahlein et al. (Mahlein *et al.*, 2010), namely that the variation of single predictors is too high to use them for comparisons between pathosystems and detect specific diseases. The application and development of specific disease indices can be recommended (Mahlein *et al.*, 2013). While the NIR and RE are important predictors, they are unlikely to be specific for myrtle rust as they have been found to be an important predictor for various other diseases (Delalieux *et al.*, 2007; Mahlein *et al.*, 2010; AL-Saddik *et al.*, 2017).

The MicaSense RedEdge camera, which was used in our study, covers a spectral range between 455 nm and 880 nm. With its five bands it only covers broad sections within that range (Figure 5 - blue, green, red, violet and black peak). For instance, the RE and NIR band ranges between 707 nm and 727 nm and from 800 nm to 880 nm, respectively. In our previous study, when using a hyperspectral sensor with very narrow bands, we selected 735 nm, 755 nm as being important wavebands to detect myrtle rust symptoms at leaf level. If these would be the only important bands for a specific disease, they could not have been detected by a multispectral camera with the above-mentioned band specifications. A similar downside of the MicaSense RedEdge camera is, that it does not cover the SWIR (short-wave-infrared) region. However, studies that used hyperspectral sensors, found this region to be important for the detection of their pathogen under investigation (Delalieux *et al.*, 2009; Asner *et al.*, 2018; Heim *et al.*, 2018). As plant diseases often affect the integrity of the leaf cuticle, the plant´s transpiration rate and water content is affected (Yeats & Rose, 2013). Fluctuations in plant water is usually reflected though the SWIR (Seelig *et al.*, 2008). It can be suggested that including the SWIR region could be beneficial for specific disease detection.

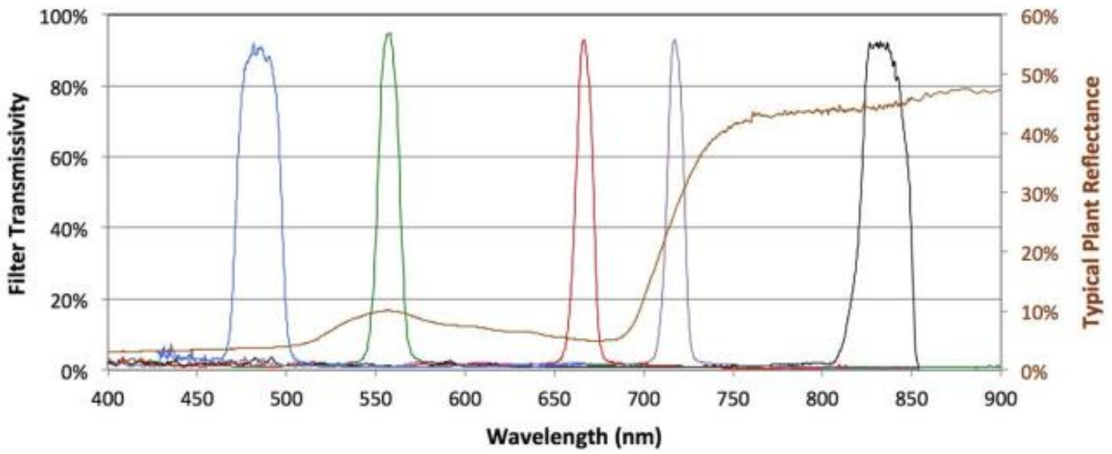

Figure 5 | Spectral range and bandwidth of the applied multispectral camera (Source: MicaSense RedEdge™ 3 Multispectral Camera User Manual Rev 06 – October 2015)

Conclusion

By using an unmanned aerial system (UAS) and a multispectral camera, we were able to discriminate fungicide treated and untreated lemon myrtle trees at canopy-level with high accuracy (95%). These results corroborate those of other studies that aimed to classify diseased and healthy vegetation using UAS and multispectral sensor systems. An ultimate goal in plant disease detection is to detect a pathogen while its symptoms are still imperceptible to visual screening, measuring disease severity, discriminating biotic and abiotic stress and differentiation among disease. As we performed our experiment on a plantation, we can assume that the land manager maintains optimal growth conditions for the plants and that they were not subject to any relevant stress causing agents other than *A. psidii*. There were no other pests and disease issues in lemon myrtle plantations, supporting our assumptions that the spectral stress indicators we identified are associated with myrtle rust. Our study also selected relevant multispectral wavebands and spectral vegetation indices for an accurate classification at leaf- and canopy level.

While the red-edge (RE) and near-infrared (NIR) band were important predictors at both levels, we also found that the relevance of other predictors can change depending on the level. As RE and NIR are known to be generally good predictors for stress detection in plants it seems likely that our selected variables are not specific for myrtle rust and only useful when other stresses can be avoided by suitable management strategies as was the case in our experimental setting. We recommend the use of hyperspectral sensors for future studies in the realm of plant disease detection as they reflect physiological and structural changes caused by pathogens on a finer spectral scale than multispectral sensors. Also, the inclusion of thermal, fluorescence and plant biochemical/physiological parameters (via canopy reflectance models) can be recommended as such measures could be linked with a specific disease response. However, the fact that our selected predictor variables varied between leaf- and canopy- level classification for a multispectral sensor, also allows us to conclude that this variation might occur for other optical sensor systems. Therefore, future studies should design their experiments according to standards that allow for across scale and pathosystem comparison.

Acknowledgements

The authors thank Gary Mazzorana from Australian Rainforest Products for access to his plantation. We also thank Emily Lancaster for access to her experimental setup. R.H.J.H. was supported by the Macquarie University Research Excellence Scholarship.

References

AL-Saddik H, Simon J-CC, Cointault F, 2017. Development of Spectral Disease Indices for ‘Flavescence Dorée’ Grapevine Disease Identification. *Sensors* **17**, 2772.

Asner GP, Martin RE, Keith LM *et al.*, 2018. A spectral mapping signature for the Rapid Ohia Death (ROD) pathogen in Hawaiian forests. *Remote Sensing* **10,** 404.

Belgiu M, Drăgu L, 2016. Random forest in remote sensing: A review of applications and future directions. *ISPRS Journal of Photogrammetry and Remote Sensing* **114**, 24–31.

Berni JAJ, Zarco-Tejada PJ, Suárez L, Fereres E, Suarez L, Fereres E, 2009. Thermal and narrowband multispectral remote sensing for vegetation monitoring from an unmanned aerial vehicle. *IEEE Transactions on Geoscience and Remote Sensing* **47**, 722–738.

Berthon K, Esperon-Rodriguez M, Beaumont LJ, Carnegie AJ, Leishman MR, 2018. Assessment and prioritisation of plant species at risk from myrtle rust (*Austropuccinia psidii*) under current and future climates in Australia. *Biological Conservation* **218**, 154–162.

Bhattacharya S, 2017. Deadly new wheat disease threatens Europe’s crops. *Nature* **542**, 145–146.

Breiman L, 2001. Random Forests. *Machine Learning* **45**, 5–32.

Calderón R, Montes-Borrego M, Landa BB, Navas-Cortés JA, Zarco-Tejada PJ, 2014. Detection of downy mildew of opium poppy using high-resolution multi-spectral and thermal imagery acquired with an unmanned aerial vehicle. *Precision Agriculture* **15**, 639–661.

Carnegie AJ, Kathuria A, Pegg GS, Entwistle P, Nagel M, Giblin FR, 2016. Impact of the invasive rust *Puccinia psidii* (myrtle rust) on native Myrtaceae in natural ecosystems in Australia. *Biological Invasions* **18**, 127–144.

Carnegie AJ, Pegg GS, 2018. Lessons from the Incursion of Myrtle Rust in Australia. *Annual Review of Phytopathology* **56**, 457–478.

Clarke M, 2012. *Australian Native Food Industry Stocktake*. Barton, ACT, Australia: Rural Industries Research and Development Corporation.

Crist E, Mora C, Engelman R, 2017. The interaction of human population, food production, and biodiversity protection. *Science* **356**, 260–264.

Dash JP, Watt MS, Pearse GD, Heaphy M, Dungey HS, 2017. Assessing very high resolution UAV imagery for monitoring forest health during a simulated disease outbreak. *ISPRS Journal of Photogrammetry and Remote Sensing* **131**, 1–14.

Davies K, 2004. *Plant Pigments and their Manipulation*. Oxford, UK: Blackwell.

Delalieux S, van Aardt J, Keulemans W, Schrevens E, Coppin P, 2007. Detection of biotic stress (*Venturia inaequalis*) in apple trees using hyperspectral data: Non-parametric statistical approaches and physiological implications. *European Journal of Agronomy* **27**, 130–143.

Delalieux S, Somers B, Verstraeten WW, van Aardt JAN, Keulemans W, Coppin P, 2009. Hyperspectral indices to diagnose leaf biotic stress of apple plants, considering leaf phenology. *International Journal of Remote Sensing* **30**, 1887–1912.

Doran J, Lea D, Bush D, 2012. *Assessing Myrtle Rust in a Lemon Myrtle Provenance Trial*. Barton, ACT, Australia: Rural Industries Research and Development Corporation.

Foley JA, Ramankutty N, Brauman KA *et al.*, 2011. Solutions for a cultivated planet. *Nature* **478**, 337–342.

Gebbers R, Adamchuk VI, 2010. Precision Agriculture and Food Security. *Science* **327**, 828–831.

Di Gennaro SF, Battiston E, Di Marco S, Facini O, Matese A, 2016. Unmanned Aerial Vehicle (UAV)-based remote sensing to monitor grapevine leaf stripe disease within a vineyard affected by esca complex. *Phytopathologia Mediterranea* **55**, 262–275.

Genuer R, Poggi J, Tuleau-Malot C, 2010. Variable selection using random forests. *Pattern Recognition Letters* **31**, 2225–2236.

Genuer R, Poggi J-M, Tuleau-Malot C, 2015. VSURF: An R Package for Variable Selection Using Random Forests. *The R Journal* **7**, 19–33.

Gitelson AA, Merzlyak MN, Chivkunova OB, 2007. Optical Properties and Nondestructive Estimation of Anthocyanin Content in Plant Leaves. *Photochemistry and Photobiology* **74**, 38–45.

Glen M, Alfenas AC, Zauza EA V, Wingfield MJ, Mohammed C, 2007. *Puccinia psidii*: A threat to the Australian environment and economy - A review. *Australasian Plant Pathology* **36**, 1–16.

Government NZ, 2018. Protection and response: myrtle rust. *Biosecurity New Zealand: Tiakitanga Putaiao Aotearoa*.

Hastie T, Tibshirani R, Friedman J, 2009. *The Elements of Statistical Learning*. New York, NY: Springer New York.

Heim RHJ, Wright IJ, Chang H-C *et al.*, 2018. Detecting myrtle rust (*Austropuccinia psidii*) on lemon myrtle trees using spectral signatures and machine learning. *Plant Pathology* **67**, 1114–1121.

Hijmans RJ, 2017. raster: Geographic Data Analysis and Modeling.

Horwood M, Carnegie A, Park R, 2013. *Gathering efficacy data to indentify the most effective chemicals for controlling myrtle rust (Uredo rangelii)*. Sydney, NSW, Australia.

Lambert S, Waipara N, Black A, Mark-Shadbolt M, Wood W, 2018. Indigenous Biosecurity: Māori Responses to Kauri Dieback and Myrtle Rust in Aotearoa New Zealand. In: *The Human Dimensions of Forest and Tree Health*. Cham: Springer International Publishing, 109–137.

Lee D, Brawner J, Pegg G, 2014. Screening Eucalyptus cloeziana and E. argophloia populations for resistance to Puccinia psidii. *Plant Disease* **99**, 71–79.

Mahlein A-K, 2016. Plant Disease Detection by Imaging Sensors – Parallels and Specific

Demands for Precision Agriculture and Plant Phenotyping. *Plant Disease* **100**, 241–251.

Mahlein AK, Rumpf T, Welke P *et al.*, 2013. Development of spectral indices for detecting and identifying plant diseases. *Remote Sensing of Environment* **128**, 21–30.

Mahlein AK, Steiner U, Dehne HW, Oerke EC, 2010. Spectral signatures of sugar beet leaves for the detection and differentiation of diseases. *Precision Agriculture* **11**, 413–431.

Morin L, Talbot MJ, Glen M, 2014. Quest to elucidate the life cycle of Puccinia psidii sensu lato. *Fungal Biology* **118**, 253–263.

Mulla DJ, 2013. Twenty five years of remote sensing in precision agriculture: Key advances and remaining knowledge gaps. *Biosystems Engineering* **114**, 358–371.

Oerke E-C, Mahlein A-K, Steiner U, 2014. *Detection and Diagnostics of Plant Pathogens* (ML Gullino, PJM Bonants, Eds,). Dordrecht: Springer Netherlands.

Penuelas J, Baret F, Filella I, 1995. Semi-empirical indices to assess carotenoids/chlorophyll a ratio from leaf spectral reflectance. *Photosynthetica* **31**, 221–230.

QGIS Development Team, 2009. QGIS Geographic Information System.

R Core Team, 2017. R: A Language and Environment for Statistical Computing.

Ramsfield T, Dick M, Bulman L, Ganley R, 2010. Briefing Document on Myrtle Rust , a Member of the Guava Rust Complex , and the Risk To New Zealand. , 16 p.

Rouse JW, Hass RH, Schell JA, Deering DW, 1973. Monitoring vegetation systems in the great plains with ERTS. *Third Earth Resources Technology Satellite (ERTS) symposium* **1**, 309–317.

Sandino J, Pegg G, Gonzalez F, Smith G, 2018. Aerial mapping of forests affected by pathogens using UAVs, hyperspectral sensors, and artificial intelligence. *Sensors (Switzerland)* **18**, 1–17.

Seelig HD, Hoehn A, Stodieck LS, Klaus DM, Adams WW, Emery WJ, 2008. The assessment of leaf water content using leaf reflectance ratios in the visible, near-, and short-wave-infrared. *International Journal of Remote Sensing* **29**, 3701–3713.

Story M, Congalton RG, 1986. Accuracy assessment: a user’s perspective. *Photogrammetric Engineering & Remote Sensing* **52**, 397–399.

USGS National UAS Project Office, 2017. *Unmanned Aircraft Systems Data Post-Processing*. Lakewood, CO, USA: U.S. Geological Survey (USGS) National Unmanned Aircraft Systems (UAS) Project Office (NUPO).

Walters DR, McRoberts N, 2006. Plants and biotrophs: a pivotal role for cytokinins? *Trends in Plant Science* **11**, 581–586.

Wang E, Dong C, Park RF, Roberts TH, 2018. Carotenoid pigments in rust fungi: Extraction, separation, quantification and characterisation. *Fungal Biology Reviews*.

Wang C, Myint SW, 2015. A Simplified Empirical Line Method of Radiometric Calibration for Small Unmanned Aircraft Systems-Based Remote Sensing. *IEEE Journal of Selected*

Topics in Applied Earth Observations and Remote Sensing **8**, 1876–1885.

West JS, Bravo C, Oberti R, Lemaire D, Moshou D, McCartney HA, 2003. The potential of optical canopy measurement for targeted control of field crop diseases. *Annual Review of Phytopathology* **41**, 593–614.

Yeats TH, Rose JKC, 2013. The Formation and Function of Plant Cuticles. *Plant Physiology* **163**, 5–20.

Zhang C, Kovacs JM, 2012. The application of small unmanned aerial systems for precision agriculture: A review. *Precision Agriculture* **13**, 693–712.

This page is intentionally left blank.

This page is intentionally left blank.

CHAPTER V

General discussion of developing a remote sensing framework for myrtle rust (*Austropuccina psidii*) detection on lemon myrtle (*Backhousia citriodora*)

RHJ Heim

General Discussion

Key results

This thesis showed that sensor-guided detection of *A. psidii* is generally possible at leaf-scale and remotely, at canopy scale. The first data chapter focused on leaf-scale experiments and showed that raw spectral signatures of fungicide treated (healthy) and untreated (diseased) lemon myrtle trees (*Backhousia citriodora*) can be discriminated with an overall accuracy (OA) of 78%. By converting the raw spectra, consisting of more than 200 wavebands, into their first-order derivatives, classification accuracies were improved to 95%. In the second data chapter it was demonstrated that not the entire array of 200 wavebands is necessary to accurately discriminate treated and untreated trees. Hyperspectral signature dimensionality was reduced by selecting relevant wavebands for accurate classification. By using four wavebands only, it was possible to build a disease-specific spectral disease index (SDI), the LMMR (lemon myrtle-myrtle rust) index. The LMMR performed better than conventional spectral vegetation indices (SVIs) used for stress detection, discriminating between treated and untreated trees with an overall accuracy of 90%. Conventional SVIs used in this thesis achieved accuracies of only 58%, 67% and 60%, respectively. Finally, results of the third data chapter showed that fungicide-treated and untreated trees could also be accurately discriminated (95%) at canopy-scale. Data for this study were collected by deploying a multispectral imaging sensor mounted on an unmanned aerial system. As the spectral and spatial resolution of aerial multispectral sensors is inferior to those of hyperspectral sensors applied directly at the leaf surface, and because the classification results were as accurate as found in the first data chapter (95% OA), it raised the question of whether hyperspectral sensors are necessary to accurately identify pathogen-related disease symptoms. To explore this question, the third data chapter also included the simulation of multispectral data at leaf-scale. This allowed me to explore spectral differences between leaf- and canopy-scale. I found that relevant wavebands to accurately classify selected tree classes were different at leaf-scale compared to canopy-scale.

My overall conclusion is that optical sensors have clear potential for myrtle rust detection. I could show this by using a hyperspectral and a multispectral sensor applied at leaf- and canopy-scale. Additionally, I developed a novel disease-specific vegetation index by selecting relevant spectral wavebands for the investigated pathosystem. There are practical uses for such research but also various limitations, as expanded on below.

Discriminating *A. psidii* from other stress causing agents

This thesis explored the potential for ground-based and aerial optical sensors to detect *A. psidii* in a commercial plantation setting. To avoid confounding sensor signals, the presence of other stress causing agents was minimised as much as possible. Fungicides used on the plantation to control myrtle rust (e.g. triadimenol, azoxystrobin, tebuconazole) have been shown to work effectively as both an eradicant and a protectant for myrtle rust (Horwood *et al.*, 2013). Furthermore, prior to myrtle rust, there were no other significant biotic agents that caused damage to lemon myrtle trees (Plant Health Australia, 2017) suggesting that treated plants were not affected by other biotic stressors. Furthermore, examination of leaves in this study, including by lemon myrtle experts and myrtle rust experts, indicated no other damaging agents present. However, to further strengthen the specificity of the spectral signatures recorded in this thesis, I could have investigated the possible link between the physiological changes caused exclusively by *A. psidii*. For example, I could have explored the production of specific biochemical compounds or quantified the presence of pathogen-related pigments during infection. While this approach seems not applicable to discriminate hundreds of different stress sources, it could be used on a plantation where only a limited number of stress-causing agents might be present at any point in time.

For *A. psidii*, it might be useful to look at the biochemical composition of urediniospores that land on leaf surfaces and start infecting their host. Carotenoids are presumably the pigments giving the yellow colour to urediniospores of some rusts (Wang *et al.*, 2018). For *B. citriodora,* the host plant in this thesis, we found yellow pigmented pustules associated with A. psidii on the adaxial and abaxial leaf surfaces of infected leaves (data chapter 2). It is likely that the same pigments also occur within the leaves, as during the infection and penetration process of *A. psidii* the orange-yellow pigmented contents are transferred into the leaf by the infection hyphae (Hunt, 1968). However, there are no studies describing the exact biochemical composition of *A. psidii* pigments (Robert Park, University of Sydney, pers. comm.). Also, secondary metabolites, such as terpenes, might be of interest as they have been found at higher levels in relation to infection with *A. psidii* (Hsieh, 2018). Individual terpenes and groups of terpenes were also successfully predicted from hyperspectral data in *Eucalyptus grandis* (Naidoo *et al.*, 2018) and within *Eucalyptus polybractea* (Kainer, Windley, Kulheim, unpublished, pers. comm.).

Another promising approach to discriminate among diseases is the development of disease-specific indices, as conducted here in data chapter two. The use of SVIs is a common method to analyse and detect changes in plant physiology and biochemistry. Usually consisting of only a few relevant wavebands, these indices were designed to respond to different plant parameters, such as pigment content (Ustin *et al.*, 2009), leaf area (Broge & Leblanc, 2001) or leaf water content (Penuelas *et al.*, 1993). As these physiological changes are caused in some combination by plant pathogens, SVIs can be used to potentially detect plant diseases (Hatfield *et al.*, 2008). However, it has been criticized that common SVIs lack disease specificity (Mahlein *et al.*, 2013). Therefore, Mahlein *et al.* (2013) optimized SDIs and tested their ability to detect and classify healthy and diseased sugar beet leaves infected with Cercospora leaf spot, sugar beet rust and powdery mildew. They found that their SDIs could discriminate their classes with high accuracies (89%, 92%, 87%, 85%, respectively). These findings are in line with those of our data chapter 2 as we were able to develop a new SDI, the LMMR, that could discriminate between treated and untreated trees with an overall accuracy of 90%. Conventional SVIs, such as the PRI, MCARI and NBNDVI, achieved accuracies of only 58%, 67% and 60%, respectively.

To summarize, it is crucial to understand the biology of a pathosystem to create meaningful links between sensor systems and pathological processes. For the development of SDIs, it is especially important to link selected wavebands to those pathological processes that occurred while the data was being recorded. Thus, we can reinforce the relationship of the specificity of a recorded signal to a certain pathosystem. Due to the change of symptoms during pathogenesis it would be valuable to also link pathogen-related alteration in *A. psidii* hosts and other pathosystems to specific points in time. If the aim would be to detect a disease before obvious symptoms appear (Zarco-Tejada *et al.*, 2018) it would be necessary to know about subtle changes in host plants that could be detected with a sensor.

Early (pre-visual) detection of plant diseases

In this thesis I took advantage of an existing experiment where the impact of fungicide was being measured on lemon myrtle trees affected by myrtle rust (Lancaster *et al.*, in preparation). As described in data chapter 2, in that experiment the trees in the plantation were either classified as 'untreated', or 'treated'. The 'untreated' trees showed symptoms of active myrtle rust infection, whereas the 'treated' trees were free of active disease symptoms following a fungicide treatment. Treated trees could potentially have been infected previously with myrtle rust (prior to fungicide application) and thus the leaves may have had some necrotic lesions due to old infections. Hence, the recorded reflectance signatures only captured a single and arbitrary stage during pathogenesis of *A. psidii.* However, stress responses like those caused by pathogens undergo multiple phases (Selye, 1936; Lichtenthaler, 1998). After pathogen infection two possible stress responses can occur: a positive, adaptive stress triggered by low levels of a stressor (eustress), and a negative stress caused by high levels of a stressor (distress). After the plant recovers from eustress, a resistance phase may occur, which is dominated by adjustment of metabolism to cope with the stressor (Wojtaszek, 1997). Distress and long-term exposure to a stress-causing agent can subsequently result in an exhaustion phase, leading to plant death (Kilian *et al.*, 2007). Thus, detecting stress at a single time point does not capture the full extent of the readjustment of plant metabolism. The understanding of stress responses is vital to explore whether the origin of stress is biotic or abiotic (Jansen & Potters, 2017) and then create meaningful links between those responses and spectral features at certain points in time. Without such information it will be difficult to find a useful application for remote sensing techniques in disease detection and precision agriculture.

A potential measure to detect disease at specific phases during pathogenesis is the fusion of sensor systems (Martinelli *et al.*, 2015). For instance, by adding thermal sensors it would be possible to capture temperature changes caused by variances in transpiration during early infection (Oerke *et al.*, 2011; Mahlein, 2016; Zarco-Tejada *et al.*, 2018). The leaf temperature shows a close correlation to the plant transpiration (Jones, 2002). The epidermal layer (cuticle and stomata), the outermost barrier of a leaf, is partially responsible for the regulation of leaf transpiration and the uncontrolled loss of water (Riederer & Schreiber, 2001). Many foliar pathogens, such as leaf spots or rusts like *A. psidii*, modify the leaf cuticle and therefore cause unintentional transpiration (Oerke *et al.*, 2011; Mahlein, 2016). Other pathogens affect transpiration rates differently. For instance, root pathogens (e.g., *Rhizoctonia solani* or *Pythium* spp.) or systemic infections (e.g., *Fusarium* spp.) often influence the transpiration rate by altering plant vascular tissue and therefore the water flow of entire plants or plant organs (Mahlein, 2016).

Pathogen-related plant water stress could also be detected by solar-induced chlorophyll fluorescence emission (Zarco-Tejada *et al.*, 2012, 2018). Chlorophyll fluorescence is associated with photosynthesis and other physiological processes (Krause & Weis, 1984) and can be detected passively at leaf to canopy level (Rascher *et al.*, 2009) using high-resolution spectrometers and the Fraunhofer Line Depth (FLD) principle (Plascyk, 1975; Malenovský *et al.*, 2009). Direct or indirect recording of plant fluorescence signals has been applied successfully for plant fungal pathogens (Konanz *et al.*, 2014).

Finally, plant architecture and plant biomass can provide important information about the health status or the presence of a disease (Paulus *et al.*, 2014). Both parameters can be changed when pathogens cause deviations from natural growth. Some of the symptoms of *A. psidii* are defoliation and leaf distortion (Coutinho *et al.*, 1998). Laser scanning devices have been used in an agricultural context to capture plant architecture traits and biomass (Paulus et al., 2014) and could be deployed to detect *A. psidii* incidence. Unfortunately, leaf distortion and defoliation are not early symptoms, occurring later in the disease cycle (Coutinho *et al.*, 1998). Therefore, their detection could only be useful as a decision support system for management at later disease stages. However, the successful combination of different sensor systems for disease detection has recently been shown in a study by Zarco-Tejada *et al*. (2018). They successfully combined remotely deployed hyperspectral and thermal sensors to carry out the first intensive multiyear study of more than 7,000 olive trees, infected with *X. fastidiosa*, across 15 orchards. By modelling fluorescence emissions of individual tress, they successfully identified *X. fastidiosa* as the stress-causing pathogen and detection of infection was even possible pre-visually.

Symptoms of *Xylella fastidiosa* are usually browning of leaves and yellowing of leaf veins (i.e. leaf scorch) and only appear several weeks after successful inoculation (Chatterjee *et al.*, 2008). During this pre-visual phase management options are limited and a detection early during this life-cycle stage would allow to react on the disease more swiftly (Zarco-Tejada *et al.*, 2018). For myrtle rust and its causal agent *A. psidii*, initial symptoms become already visible two to four days after a host has been infected with urediniospores (Coutinho *et al.*, 1998). Thus, for early detection, the stress response of an infected host needs to be detected within the first four days. There is reasonable doubt that remote sensing techniques for the detection of fast-spreading foliar fungal disease, such as rusts, can provide a means for better management because foliar fungal diseases often disperse rapidly through the air (Cooke *et al.*, 2006). Only highly reliable detection of infection hotspots would potentially convince a manager to conduct curative treatment locally, if curative agrochemicals are available. However, the decision to apply remote sensing techniques as a decision support tool must be made by managers on an individual basis which requires close collaboration with land managers to develop applicable systems. Often, preventive agrochemicals against foliar fungal diseases are inexpensive and managers will apply them over the entire crop area to avoid the risk of secondary infections. In some cases, it might be possible to use sensor systems for remote screening of infection hotspots. For instance, after heavy rainfall events remote sensing techniques could be applied to locate areas where additional fungicide treatment might be necessary as the rain has washed off earlier applied agrochemicals. These locally untreated spots would enable a pathogen to infect its host and the host response could then be detected. Another case, specific to the lemon myrtle industry and other crop sectors that demand an organic product and try to avoid any agrochemical treatments (Carnegie & Pegg, 2018), the incentive to explore possibilities for the incorporation of remote sensing detection and the avoidance of agrochemicals might be higher. In cases where pathogen dispersion rates are low, mostly due to the mode of spread (e.g. wind, soil, rain) and propagule type (e.g. spore size, weight, shape), remote sensing techniques can generally be regarded as a useful detection tool. In those cases, it can take several months for hosts to develop symptoms which in turn increases response time for management (Pablo Zarco-Tejada and Rocio Calderón-Madrid, pers. comm.). Unfortunately, this is not the case for myrtle rust. However, sensor guided detection could be an option for fast-spreading pathogens like *A. psidii* as the estimation of disease severity might lead to dosage adjustment of agrochemicals.

Quantifying disease severity

In the lemon myrtle plantation used for the work in this thesis, the assessed leaves showed symptoms of various disease severity. The disease severity was influenced, amongst other factors, by leaf age, microclimate, proximity of neighbouring plants and inoculum load. While we aimed to provide a general concept for myrtle rust detection, an additional step could have been to assess the trees for its disease severity, e.g. either by random sampling of leaves or by calculating the Crown Damage Index (Stone *et al.*, 2003), after taking their spectral signature. Such an additional sampling would have allowed us to evaluate whether individual trees varied in susceptibility. Studies have shown that *A. psidii* causes a disease pattern with substantial variability in host-susceptibility within species across provenances (Morin *et al.*, 2012; Sandhu & Park, 2013; Pegg *et al.*, 2018). For example, Pegg et al. (2018) examined variability in susceptibility to *A. psidii* within populations of *M. quinquenervia*, *M. leucadendra* and *M. viridiflora* and identified wide variation in susceptibility between the three species, among provenances within these species, as well as within provenances (i.e., between individual trees). Sensor-guided severity assessment of symptoms can be useful in first locating susceptible individuals and secondly in determining disease-resistant genotypes. The tremendously negative impact of *A. psidii* on important natural plant communities in Australia (Carnegie *et al.*, 2016; Pegg *et al.*, 2017) might make it imperative to select resistant individuals across susceptible species for plant breeding programs, at least in a commercial context (Pegg *et al.*, 2014). However, this wide variability in host-susceptibility to *A. psidii* makes it complicated to design a structured screening process for resistance. Plant breeding processes can be aimed at finding resistant genotypes, therefore a large number of those genotypes need to be tested for disease- and abiotic stress resistance, potential yield, biomass quality, and many other secondary traits (Fiorani & Schurr, 2013). During resistance screening processes, researchers are interested in subtle defence reactions that are crucial for the ability of plants to prevent pathogen invasion across all scales, from cell cultures to single plant organs to entire fields (Granier & Vile, 2014). Using optical sensors in plant phenotyping is a fast-developing research field that combines plant biology, sensor technology, and automation engineering while gaining increasing importance owing to the need to accelerate progress in plant breeding (Fiorani & Schurr, 2013). It is centred around the assessment of appearance and performance of a plant genotype under distinct environmental conditions (Granier & Vile, 2014). Especially the need for high-throughput screening methods due to the high number of repeated genotype measurements in plant phenotyping makes this field very suitable for the use of optical sensor (Granier & Vile, 2014; Mahlein, 2016). In the case of *A. psidii* and the highly variation of host-susceptibility, sensor-guided phenotyping approaches could be applied to screen for resistant genotypes across all vulnerable species within the Myrtaceae. Currently, experts are using disease scales and screen for resistant genotypes by using the naked eye. This approach could be optimized by using fast, objective and automated sensor systems.

Conclusion

By using a hyperspectral sensor at leaf-level and a multispectral sensor at canopy-level, this thesis took an across-scale approach to show that optical remote sensing is a suitable tool for the detection of *A. psidii* in a managed landscape. This was done successfully with classification accuracies of 95% at both levels. These findings contribute to the emerging field of sensor-guided disease detection in precision agriculture by providing relevant discrimination features in the VIS, NIR and SWIR spectral region of the pathosystem lemon myrtle (*Backhousia citriodora*) and myrtle rust (*Austropuccinia psidii*). Further, we developed a coded framework to design our innovative spectral disease index. This coded framework might enable other researchers to design SDIs for their pathosystem of interest. The presented findings provide a foundation for future research on myrtle rust detection using remote sensing techniques. Extensions could be experiments on sensor-guided disease severity and resistance screening on vulnerable *A. psidii* hosts, spectral discrimination of *A. psidii* against other biotic and abiotic host responses and the pre-visual detection of *A. psidii* symptoms.

Applications for myrtle rust detection using the presented technologies are manifold. A task of high priority is to prevent the arrival of new strains in countries with vulnerable host-species. Biosecurity detection protocols at international borders could be equipped with spectral sensors to screen potentially infected plant material. The nursery industry (including growing for forestry, essential oils, landscaping and ornamental retail supply chains) would be a suitable field of application as plants are grown in a homogenous manner. Depending on the size of a nursery or other enterprises it would be possible to use hyperspectral sensors at leaf level to screen for *A. psidii*. These sensors are superior to multispectral sensors, especially at leaf-level, as they provide more spectral information. Therefore, they are more likely to reveal complex plant-pathogen interactions at early stages of infection. Infected plants at nurseries could be discarded to prevent further spread through transport, or fungicides applied at an early stage to reduce damage to affected plants and spread of inoculum to other plants. Eventually, the large-scale screening of managed forests could be supported by spectral sensor systems. Spectral information collected from airplanes, helicopters or drones can guide human assessors to infection hotspots (e.g. in *Eucalyptus* plantation forestry) to estimate spore load for the integration into epidemiology models and the prediction of further spread.

For future research and applications, it is imperative to create meaningful links between spectral signatures and structural, physiological and biochemical alterations in hosts. Because experimental setups in plant phenotyping are often better to control, it is likely that progress will be made here first before systems can be adopted for the field. For a successful trajectory of sensor-guided disease detection, it will be indispensable to involve complementary research fields, such as plant pathology, sensor engineering, informatics, and machine learning. Thirty years ago, Jackson (1986) suggested that: *"…continued research at all levels, ground, aircraft, and satellite, should build the foundation for a future global stress-detection system that would be readily available to all.*" It seems that these conclusions are still valid. As new technologies are available now, we should focus on clear communication and common research goals in this interdisciplinary field to overcome the discussed major challenges.

References

Broge N., Leblanc E, 2001. Comparing prediction power and stability of broadband and hyperspectral vegetation indices for estimation of green leaf area index and canopy chlorophyll density. *Remote Sensing of Environment* **76**, 156–172.

Carnegie AJ, Kathuria A, Pegg GS, Entwistle P, Nagel M, Giblin FR, 2016. Impact of the invasive rust Puccinia psidii (myrtle rust) on native Myrtaceae in natural ecosystems in Australia. *Biological Invasions* **18**, 127–144.

Carnegie AJ, Pegg GS, 2018. Lessons from the Incursion of Myrtle Rust in Australia. *Annual Review of Phytopathology* **56**, 457–478.

Chatterjee S, Almeida RPP, Lindow S, 2008. Living in two Worlds: The Plant and Insect Lifestyles of *Xylella fastidiosa*. *Annual Review of Phytopathology* **46**, 243–271.

Cooke BM, Gareth Jones D, Kaye B, 2006. *The Epidemiology of Plant Diseases*. Dordrecht, The Netherlands: Springer.

Coutinho TA, Wingfield MJ, Alfenas AC, Crous PW, 1998. *Eucalyptus* Rust: A Disease with the Potential for Serious International Implications. *Plant Disease* **82**, 819–825.

Fiorani F, Schurr U, 2013. Future Scenarios for Plant Phenotyping. *Annual Review of Plant Biology* **64**, 267–291.

Granier C, Vile D, 2014. Phenotyping and beyond: Modelling the relationships between traits. *Current Opinion in Plant Biology* **18**, 96–102.

Hatfield JL, Gitelson AA, Schepers JS, Walthall CL, 2008. Application of spectral remote sensing for agronomic decisions. *Agronomy Journal* **100**, 117–131.

Heim RHJ, Wright IJ, Chang H-C *et al.*, 2018. Detecting myrtle rust (Austropuccinia psidii) on lemon myrtle trees using spectral signatures and machine learning. *Plant Pathology* **67**, 1114–1121.

Horwood M, Carnegie A, Park R, 2013. *Gathering efficacy data to indentify the most effective chemicals for controlling myrtle rust (Uredo rangelii)*. Sydney, NSW, Australia.

Hsieh JF, 2018. Molecular and Chemical Mechanisms of Defence against Myrtle Rust in Australian Myrtaceae. The Australian National University.

Hunt P, 1968. Cuticular penetration by germinating uredospores. *Transactions of the British Mycological Society* **51**, 103-112.

Jansen MAK, Potters G, 2017. Stress: The Way of Life. In: Shabala S: *Plant Stress Physiology*. Oxfordshire, UK: CABI

Jones HG, 2002. Use of infrared thermography for monitoring stomatal closure in the field: application to grapevine. *Journal of Experimental Botany* **53**, 2249–2260.

Kilian J, Whitehead D, Horak J *et al.*, 2007. The AtGenExpress global stress expression data set: Protocols, evaluation and model data analysis of UV-B light, drought and cold stress responses. *Plant Journal* **50**, 347–363.

Konanz S, Kocsányi L, Buschmann C, 2014. Advanced Multi-Color Fluorescence Imaging System for Detection of Biotic and Abiotic Stresses in Leaves. *Agriculture* **4**, 79–95.

Krause GH, Weis E, 1984. Chlorophyll fluorescence as a tool in plant physiology - II. Interpretation of fluorescence signals. *Photosynthesis Research* **5**, 139–157.

Lichtenthaler HK, 1998. The stress concept in plants: an introduction. *Annals of the New York Academy of Sciences* **851**, 187–198.

Mahlein A-K, 2016. Plant Disease Detection by Imaging Sensors – Parallels and Specific Demands for Precision Agriculture and Plant Phenotyping. *Plant Disease* **100**, 241–251.

Mahlein AK, Rumpf T, Welke P *et al.*, 2013. Development of spectral indices for detecting and identifying plant diseases. *Remote Sensing of Environment* **128**, 21–30.

Malenovský Z, Mishra KB, Zemek F, Rascher U, Nedbal L, 2009. Scientific and technical challenges in remote sensing of plant canopy reflectance and fluorescence. *Journal of Experimental Botany* **60**, 2987–3004.

Martinelli F, Scalenghe R, Davino S *et al.*, 2015. Advanced methods of plant disease detection. A review. *Agronomy for Sustainable Development* **35**, 1–25.

Morin L, Aveyard R, Lidbetter JR, Wilson PG, 2012. Investigating the host-range of the rust fungus puccinia psidii sensu lato across tribes of the family myrtaceae present in australia. *PLoS ONE* **7**, e35434.

Naidoo S, Christie N, Acosta JJ *et al.*, 2018. Terpenes associated with resistance against the gall wasp, Leptocybe invasa, in Eucalyptus grandis. *Plant Cell and Environment* **41**, 1840–1851.

Oerke EC, Fröhling P, Steiner U, 2011. Thermographic assessment of scab disease on apple leaves. *Precision Agriculture* **12**, 699–715.

Paulus S, Behmann J, Mahlein AK, Plümer L, Kuhlmann H, 2014. Low-cost 3D systems: Suitable tools for plant phenotyping. *Sensors (Switzerland)* **14**, 3001–3018.

Pegg GS, Brawner JT, Lee DJ, 2014. Screening *Corymbia* populations for resistance to *Puccinia psidii*. *Plant Pathology* **63**, 425–436.

Pegg GS, Lee DJ, Carnegie AJ, 2018. Predicting impact of *Austropuccinia psidii* on populations of broad-leaved *Melaleuca* species in Australia. *Australasian Plant Pathology* **47**, 421–430.

Pegg G, Taylor T, Entwistle P, Guymer G, Giblin F, Carnegie A, 2017. Impact of *Austropuccinia psidii* (myrtle rust) on *Myrtaceae*-rich wet sclerophyll forests in south east Queensland. *PLOS ONE* **12**, e0188058.

Penuelas J, Filella I, Biel C, Serrano L, Save R, 1993. The reflectance at the 950-970 nm region as an indicator of plant water status. *International Journal of Remote Sensing* **14**, 1887–1905.

Plant Health Australia, 2017. Plant Health Australia. http://www.planthealthaustralia.com.au/. Accessed 30 November 2018

Plascyk JA, 1975. The MK II Fraunhofer line discriminator (FLD-II) for airborne and orbital remote sensing of solar-stimulated luminescence. *Optical Engineering* **14**, 144339.

Rascher U, Agati G, Alonso L *et al.*, 2009. CEFLES2: The remote sensing component to quantify photosynthetic efficiency from the leaf to the region by measuring sun-induced fluorescence in the oxygen absorption bands. *Biogeosciences* **6**, 1181–1198.

Riederer M, Schreiber L, 2001. Protecting against water loss: analysis of the barrier properties of plant cuticles. *Journal of Experimental Botany* **52**, 2023–2032.

Sandhu KS, Park RF, 2013. *Genetic basis of pathogenicity in Uredo rangelii*. Sydney, NSW, Australia.

Selye H, 1936. A syndrome produced by diverse nocuous agents. *Nature* **138**, 32.

Stone C, Matsuki M, Carnegie A, 2003. *Pest and disease assessment in young eucalypt plantations: field manual for using the Crown Damage Index*. Canberra, ACT, Australia.

Ustin SL, Gitelson AA, Jacquemoud S *et al.*, 2009. Retrieval of foliar information about plant pigment systems from high resolution spectroscopy. *Remote Sensing of Environment* **113**, 67–77.

Wang E, Dong C, Park RF, Roberts TH, 2018. Carotenoid pigments in rust fungi: Extraction, separation, quantification and characterisation. *Fungal Biology Reviews* **32**, 166–180.

Wojtaszek P, 1997. Oxidative burst: an early plant response to pathogen infection. *The Biochemical Journal* **322**, 681–92.

Zarco-Tejada PJ, Camino C, Beck PSA *et al.*, 2018. Previsual symptoms of *Xylella fastidiosa* infection revealed in spectral plant-trait alterations. *Nature Plants* **4**, 432–439.

Zarco-Tejada PJ, González-Dugo V, Berni JAJ, 2012. Fluorescence, temperature and narrow-band indices acquired from a UAV platform for water stress detection using a micro-hyperspectral imager and a thermal camera. *Remote Sensing of Environment* **117**, 322–337.

This page is intentionally left blank.

DECLARATION

Certificate of Originality

English: I hereby declare that the contents of this thesis entitled “Developing a remote sensing framework for myrtle rust (*Austropuccina psidii*) detection on lemon myrtle (*Backhousia citriodora*)” are a record of my own original work, except where other contributors are named. In detail, my contributions and those of others are listed in the below statement.

German: Hiermit erkläre ich an Eides statt, dass ich die vorliegende Dissertationsschrift selbst verfasst und keine anderen als die angegebenen Quellen verwendet habe. Mein Anteil an Konzeption, Durchführung und Berichtsabfassung, sowie die Beiträge Anderer sind im „Contribution Statement“ im Einzelnen dargelegt.

René Hans-Jürgen Heim

Hamburg, December 2018

Contribution Statement

Chapter 1 | General Introduction

Conceptualization, René Hans-Jürgen Heim (RHJH); Investigation, RHJH; Writing – Original Draft Preparation, RHJH; Writing – Review & Editing, Jens Oldeland (JO), Ian Wright (IW), RHJH, Angus Carnegie (AC); Visualization, RHJH

Chapter 2 | Detecting myrtle rust (*Austropuccinia psidii*) on lemon myrtle trees using spectral signatures and machine learning

Conceptualization, JO, IW and RHJH; Methodology, JO and RHJH ; Formal Analysis, RHJH; Investigation, RHJH; Resources, RHJH, Michael Chang (MC), Geoff Pegg (GP), Emily Lancaster (EL); Data Curation, RHJH and Daniel Falster (DF); Writing – Original Draft Preparation, RHJH; Writing – Review & Editing, JO, IW, RHJH, GP, AC, DF, EL; Visualization, RHJH; Supervision, JO, IW, MC and AC ; Project Administration, RHJH; Funding Acquisition, RHJH

Chapter 3 | Developing a spectral disease index for myrtle rust (*Austropuccinia psidii*)

Conceptualization, JO, IW and RHJH; Methodology, Andrew Allen (AA), Ina Geedicke (IG), JO and RHJH ; Formal Analysis, RHJH; Investigation, IG and RHJH; Resources, RHJH; Data Curation, RHJH; Writing – Original Draft Preparation, RHJH; Writing – Review & Editing, AA, IG, JO, IW, RHJH; Visualization, RHJH; Supervision, JO and IW ; Project Administration, RHJH; Funding Acquisition, RHJH

Chapter 4 | Multispectral, aerial disease detection for myrtle rust (*Austropuccinia psidii*) on a lemon myrtle plantation

Conceptualization, JO, IW and RHJH; Methodology, JO, IW and RHJH ; Formal Analysis, RHJH; Investigation, RHJH; Resources, RHJH, Dominique Taylor (DT); Data Curation, RHJH; Writing – Original Draft Preparation, RHJH; Writing – Review & Editing, JO, IW, RHJH, Peter Scarth (PS), AC and DT; Visualization, RHJH; Supervision, JO, IW and AC ; Project Administration, RHJH; Funding Acquisition, RHJH

Chapter 5 | General Discussion

Conceptualization, René Hans-Jürgen Heim (RHJH); Investigation, RHJH; Writing – Original Draft Preparation, RHJH; Writing – Review & Editing, Jens Oldeland (JO), Ian Wright (IW), RHJH, Angus Carnegie (AC); Visualization, RHJH